Liquidity Stress Testing in Asset Management
Part 1. Modeling the Liability Liquidity Risk[*]

Thierry Roncalli
Quantitative Research
Amundi Asset Management, Paris
thierry.roncalli@amundi.com

Fatma Karray-Meziou
Risk Management
Amundi Asset Management, Paris
fatma.karraymeziou@amundi.com

François Pan
Risk Management
Amundi Asset Management, Paris
francois.pan@amundi.com

Margaux Regnault
Quantitative Research
Amundi Asset Management, Paris
margaux.regnault@amundi.com

December 2020

Abstract

This article is part of a comprehensive research project on liquidity risk in asset management, which can be divided into three dimensions. The first dimension covers liability liquidity risk (or funding liquidity) modeling, the second dimension focuses on asset liquidity risk (or market liquidity) modeling, and the third dimension considers asset-liability liquidity risk management (or asset-liability matching). The purpose of this research is to propose a methodological and practical framework in order to perform liquidity stress testing programs, which comply with regulatory guidelines (ESMA, 2019) and are useful for fund managers. The review of the academic literature and professional research studies shows that there is a lack of standardized and analytical models. The aim of this research project is then to fill the gap with the goal to develop mathematical and statistical approaches, and provide appropriate answers.

In this first part that focuses on liability liquidity risk modeling, we propose several statistical models for estimating redemption shocks. The historical approach must be complemented by an analytical approach based on zero-inflated models if we want to understand the true parameters that influence the redemption shocks. Moreover, we must also distinguish aggregate population models and individual-based models if we want to develop behavioral approaches. Once these different statistical models are calibrated, the second big issue is the risk measure to assess normal and stressed redemption shocks. Finally, the last issue is to develop a factor model that can translate stress scenarios on market risk factors into stress scenarios on fund liabilities.

Keywords: liquidity, stress testing, liability, redemption rate, redemption frequency, redemption severity, zero-inflated beta model, copula.

JEL classification: C02, G32.

---

1   Introduction

Liquidity stress testing in asset management is a complex topic because it is related to three dimensions — liquidity risk, asset management and stress testing, whose linkages have been little studied and are hard to capture. First, liquidity is certainly the risk that is the most difficult to model with the systemic risk. If we consider market, credit, operational and counterparty risks, there is a huge amount of academic literature on these topics in terms of models, statistical inference and analysis. In terms of liquidity risk, the number of practical studies and applied approaches is limited. Even though a great deal of research has been completed on this subject, much of it is overly focused on descriptive analyses of liquidity, or its impact on systemic risk, or policy rules for financial regulation. Moreover, this research generally focuses on the banking sector (Grillet-Aubert, 2018). For instance, the liquidity coverage ratio (LCR) and the net stable funding ratio (NSFR) of the Basel III regulatory framework are of no help when measuring the liquidity risk in asset management. In fact, the concept of liquidity risk in asset management is not well defined. More generally, it is a recent subject and we must admit that the tools and models used in asset management are very much lagging those developed in the banking sector. This is why the culture of asset-liability management (ALM) is poor in investment management, both on the side of asset managers and asset owners. Therefore, if we add the third dimension, stress testing, we obtain an unknown and obscure topic, because the combination of liquidity risk and stress testing applied to asset management is a new and difficult task.

This is not the first time that the regulatory environment has sped up the development of a risk management framework. Previous occurrences include the case of market risk with the Amendment of the first Basel Accord (BCBS, 1996), credit risk with the second consultative paper on Basel II (BCBS, 2001), credit valuation adjustment with the publication of the Basel III Accord (BCBS, 2010), interest rate risk in the banking book with the IRRBB guidelines (BCBS, 2016), etc. However, the measurement of these risks had already benefited from the existence of analytical models developed by academics and professionals. One exception was operational risk, since banks started from a blank page when asked to measure it (BCBS, 1999). Asset managers now face a similar situation at this moment. Between 2015 and 2018, the US Securities and Exchange Commission established several rules governing liquidity management (SEC, 2015, 2016, 2018a,b). In particular, Rule 22e-4 requires investment funds to classify their positions in one of four liquidity buckets (highly liquid investments, moderately liquid investments, less liquid investments and illiquid investments), establish a liquid investment minimum, and develop policies and procedures on redemptions in kind. From September 2020, European asset managers must also comply with new guidelines on liquidity stress testing (LST) published by the European Securities and Markets Authority (ESMA, 2019). These different regulations are rooted in the agenda proposed by the Financial Stability Board to monitor and manage systemic risk of non-bank non-insurer systemically important financial institutions (FSB, 2010). Even if the original works of the FSB were biased, the idea that the asset management industry can contribute to systemic risk has gained ground and is now widely accepted. Indeed, FSB (2015) confused systemic risk and systematic market risk (Roncalli and Weisang, 2015a). However, Roncalli and Weisang (2015b) showed that "*the liquidation channel is the main component of systemic risk to which the asset management industry contributes*". In this context, liquidity is the major risk posed by the asset management industry that regulators must control. But liquidity risk is not only a concern for regulators. It must also be a priority for asset managers. The crisis of money market funds in the fourth quarter of 2008 demonstrated the fragility of some fund managers (Schmidt *et al.*, 2016). Market liquidity deteriorated in March and April 2020, triggering a liquidity shock on some investment funds

and strategies. However, aside from the 2008 Global Financial Crisis and 2020 coronavirus pandemic, which have put all asset managers under pressure, the last ten years have demonstrated that liquidity is also an individual risk for fund managers. It was especially true during episodes of flash crash[1], where fund managers reacted differently. In a similar way, idiosyncratic liquidity events may affect asset managers at the individual level (Thompson, 2019). Following some high-profile fund suspensions in mid-2019, asset managers received requests from asset owners to describe their liquidity policies and conduct a liquidity review of their portfolios. Therefore, we notice that liquidity is increasingly becoming a priority for asset managers for three main reasons, because it is a reputational risk, they are challenged by asset owners and it can be a vulnerability factor for financial performance.

However, even though liquidity stress testing in asset management has become one of the hot topics in finance, it has attracted few academics and professionals, implying that the research on this subject is not as dynamic as one might expect. In fact, it is at the same stage as operational risk was in the early 2000s, when there was no academic research on this topic. And it is also at the stage of ALM banking risk, where the most significant contributions have come from professionals. Since liquidity stress testing in asset management is an asset-liability management exercise, modeling progress mainly comes from professionals, because the subject is so specific, requires business expertise and must be underpinned by industry-level data. This is obviously an enormous hurdle for academics, and this explains the lack of modeling and scientific approach that asset managers encounter when they want to develop a liquidity stress testing framework. Therefore, the objective of this research is twofold. First, the idea is to provide a mathematical and statistical formalization to professionals in order to go beyond expert qualitative judgement. Second, the aim is to assist academics in understanding this topic. This is important, because academic research generally boosts the development of analytical models, which are essential for implementing liquidity stress testing programs in asset management.

Liquidity stress testing in asset management involves so many dimensions that we have decided to split this research into three parts:

1. liability liquidity risk modeling;

2. asset liquidity risk modeling;

3. asset-liability liquidity risk management.

Indeed, managing liquidity risk consists of three steps. First, we have to model the liability liquidity of the investment fund, especially the redemption shocks. By construction, this step must incorporate client behavior. Second, we have to develop a liquidity model for assets. For that, we must specify a transaction cost model beyond the traditional bid-ask spread measure. In particular, the model must incorporate two dimensions: price impact and trading limits. These first two steps make the distinction between funding liquidity and market liquidity. As noticed by Brunnermeier and Pedersen (2009), these two types of liquidity may be correlated. However, we suppose that they are independent at this level of analysis. While the first step gives the liquidity amount of the investment fund that can be required by the investors, the second step gives the liquidity amount of the investment fund that can be available in the market. Therefore, the third step corresponds to the asset-liability management in terms of liquidity, that is the matching process between required liquidity and available liquidity. This implies defining the part of the redemption shock that can be managed by asset liquidation and the associated liquidity costs. It also implies

---

[1]For instance, during the US stock market flash crash (May 6, 2010), the US Treasury flash crash (October 15, 2014), the US ETF flash crash (August 24, 2015), etc.

defining the liquidity tools that can be put in place in order to manage the non-covered part of the redemption shock or the liquidation shortfall. For instance, a liquidity buffer is an example of one of these tools, but this is not the only solution. Redemption gates, side pockets and redemptions in kind are alternative methods, but they are extreme solutions that may break the fiduciary duties and liquidity promises of asset managers. Swing pricing is also an important ALM tool, and is a challenging question when we consider the fair calibration of swing prices.

Figure 1: The sequential approach of liquidity stress testing
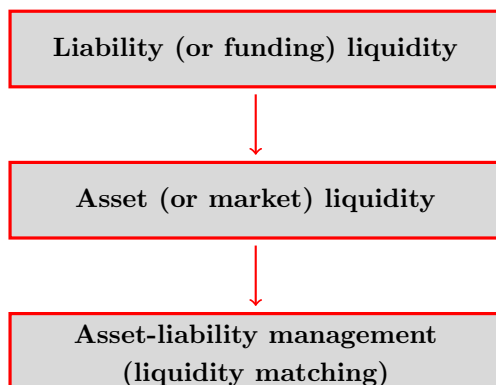
The three-stage process has many advantages in terms of modeling. First, it splits a complex question into three independent and more manageable problems. This is particularly the case of liability and asset modeling. Second, managing liquidity risk becomes a sequential process, where the starting point is clearly identified. As shown in Figure 1, we should begin with the liability risk. Indeed, if we observe no inflows or outflows, the process stops here. As such, the first stage determines the amount to sell in the market and it is measured with respect to the investor behavior. The liquidity risk has its roots in the severity of the redemption shock. Market liquidity is part of the second phase. Depending on the redemption size and the liquidity of the market, the fund manager will decide the best solution to adopt. And the sequential process will conclude with the action of the fund manager[2]. Finally, the third advantage concerns the feasibility of stress testing programs. In this approach, stress testing concerns the two independent dimensions. We can stress the liquidity on the liability side, or we can stress the liquidity on the asset side, or both, but the rule is simple.

In the sequential approach, the liability of the investment fund is the central node of the liquidity risk, and the vertex of the liquidity network. However, it is not so simple, because the three nodes can be interconnected (Figure 2). If market liquidity deteriorates sharply, investors may be incited to redeem in order to avoid a liquidity trap. In this case, funding liquidity is impacted by market liquidity, reinforcing the feedback loop between funding and market liquidity, which is described by Brunnermeier and Pedersen (2009). But this is not the only loop. For instance, the choice of an ALM decision may also influence funding liquidity. If one asset manager decides to suspend redemptions, it may be a signal for the investors of the other asset managers if they continue to meet redemptions. Again, we may observe a feedback loop between funding liquidity and asset-liability management.

---

[2]Of course, the fund manager's action is not uniquely determined, because it depends on several parameters. This means that two fund managers can take two different decisions even if they face the same situation in terms of redemption and market liquidity.

Finally, it is also obvious that market liquidity is related to ALM decisions, because of many factors such as trading policies, the first-mover advantage and crowding effects (Roncalli and Weisang, 2015a). It follows that the liquidity risk given in Figure 1 is best described by the dense and fully connected network given in Figure 2. Nevertheless, developing a statistical model that takes into account the three reinforcing loops is not straightforward and certainly too complex for professional use. Therefore, it is more realistic to adjust and update the sequential models with second-round effects than to have an integrated dynamic model.

Figure 2: The network risk of liquidity
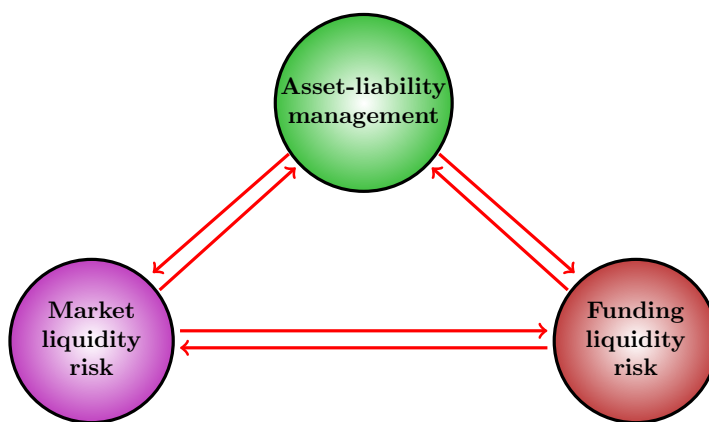
Liquidity is a long-standing issue and also an elusive concept. This is particularly true in asset management, where liquidity covers several interpretations. For example, some asset classes are considered as highly liquid whereas other asset classes are illiquid. In the first category, we generally find government bonds and large cap stocks. The last category includes real estate and private equities. However, categorizing liquidity of a security is not easy and there is no consensus. Let us consider for example Rule 22e-4(b) that is applied in the US. The proposed rule was based on the ability to convert the security to cash within a given period and distinguished six buckets: (a) convertible to cash within 1 business day, (b) convertible to cash within 2-3 business days, (c) convertible to cash within 4-7 calendar days, (d) convertible to cash within 8-15 calendar days, (e) convertible to cash within 16-30 calendar days (f) convertible to cash in more than one month. Finally, the adopted rule is the following:

1. highly liquid investments (convertible to cash within three business days);

2. moderately liquid investments (convertible to cash within four to seven calendar days);

3. less liquid investments (expected to be sold in more than seven calendar days);

4. illiquid investments (cannot be sold in seven calendar days or less without significant price impact).

Classifying a security into a bucket may be different from one fund manager to another. Moreover, the previous categories depend on the market conditions. Nevertheless, even if the current market liquidity is abundant, securities that can be categorized in the first bucket must also face episodes of liquidity shortage (Blanqué and Mortier, 2019a). A typical example concerns government bonds facing idiosyncratic risks. Blanqué and Mortier (2019a)

gave the case of Italian bonds in 2018 during the discussion on the budget deficit. However, most of the time, when we consider the liquidity of an asset class, we assume that it is static. Certainly, this way of thinking reflects the practice of portfolio management. Indeed, it is common to include a constant illiquidity premium when estimating the expected returns of illiquid assets. But investors should stick to their investments without rebalancing and trading if they want to capture this illiquidity premium. The split between liquid and illiquid investments does not help, because it is related to the absolute level of asset illiquidity, and not liquidity dynamics. However, the issue is more complex:

> "[...] there is also broad belief among users of financial liquidity – traders, investors and central bankers – that the principal challenge is not the average level of financial liquidity... but its variability and uncertainty" (Persaud, 2003).

This observation is important because it is related to the liquidity question from a regulatory point of view. The liquidity risk of private equities or real assets is not a big concern for regulators, because one knows that these asset classes are illiquid. Even if they become more illiquid at some point, this should not dramatically influence investors (asset managers and owners). Regulators and investors are more concerned by securities that are liquid under some market conditions and illiquid under other market conditions. At first sight, it is therefore a paradox that liquidity stress testing programs must mainly focus on highly or moderately liquid instruments than on illiquid instruments. In fact, liquidity does not like surprises and changes. This is why the liquidity issue is related to the cross-section of the expected illiquidity premium for illiquid assets, but to the time-series illiquidity variance for liquid assets.

This is all the more important that the liquidity risk must be measured and managed in a stress testing framework, which adds another layer of complexity. Indeed, stress scenarios are always difficult to interpret, and calibrating them is a balancing act, because they must correspond to extreme but also plausible events (Roncalli, 2020). This is why the historical method is the most used approach when performing stress testing. However, it is very poor and not flexible in terms of risk management. Parametric approaches must be preferred since stress periods are very heterogenous and outcomes are uncertain. Therefore, it makes more sense to estimate and use stressed liquidity parameters than directly estimate a stressed liquidity outcome. In this approach, the normal model is the baseline model on which we could apply scenario analysis on the different parameters that define the liquidity model. This is certainly the best way to proceed if we want to develop a factor-based liquidity stress testing program, which is an important issue for fund management. Otherwise, liquidity stress testing would be likely to remain a regulatory constraint or a pure exercise of risk measurement, but certainly not a risk management process supporting investment policies and fund management.

This paper is organized as follows. Section Two introduces the concept of redemption rates and defines the historical approach of liquidity stress testing. In Section Three, we consider parametric models that can be used to estimate redemption shocks. This implies making the distinction between the redemption event and the redemption amount. From a statistical point of view, this is equivalent to modeling the redemption frequency and the redemption severity. After having developed an aggregate population model, we consider an individual-based model. It can be considered as a first attempt to develop a behavioral model, which is the central theme of Section Four. We analyze the simple case where redemptions between investors are independent and then extend the model where redemptions are correlated to take into account spillover effects and contagion risk. Then, we develop factor-based models of liquidity stress testing in Section Five. Finally, Section Six offers some concluding remarks.

2 Understanding the liability side of liquidity risk

In order to assess the liquidity risk of an investment fund, we must model its '*funding*' liquidity. Therefore, managing the liquidity in asset management looks like a banking asset-liability management process (Roncalli, 2020). However, there is a major difference since banking ALM concerns both balance sheet and income statement. This is not the case of an investment fund, because we only focus on its balance sheet and the objective is to model the redemption flows.

2.1 Balance sheet of an investment fund

In order to define the liability risk, we first have to understand the balance sheet of a collective investment fund. A simplified illustration is given in Figure 3 for a mutual fund. The total (gross) assets $A(t)$ correspond to the market value of the investment portfolio. They include stocks, bonds and all financial instruments that are invested. On the liability side, we have two main balance sheet items. The first one corresponds to the debits $D(t)$, which are also called current or accrued liabilities. They are all the expenses incurred by the mutual fund. For instance, the current liabilities include money owed to lending banks, fees owed to the fund manager and the custodian, etc. The second liability item is the unit capital $C(t)$, which is owned by the investors. Each investor owns a number of units (or shares) and is referred to as a '*unitholder*'. This unit capital is equivalent to the equity concept of a financial institution. A unitholder is then also called a shareholder in reference to capital markets.

Figure 3: Balance sheet of mutual funds
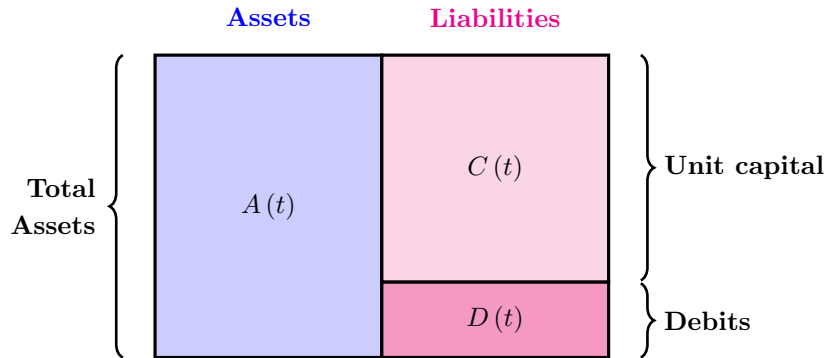
2.1.1 Definition of net asset value

The total net assets (TNA) equal the total value of assets less the current or accrued liabilities:

$$\text{TNA}(t) = A(t) - D(t)$$

The net asset value (NAV) represents the share price or the unit price. It is equal to:

$$\text{NAV}(t) = \frac{\text{TNA}(t)}{N(t)} \tag{1}$$

where the total number $N(t)$ of shares or units in issue is the sum of all units owned by all unitholders. The previous accounting rules show that the capital is exactly equal to the

total net assets, which is also called the assets under management (AUM). The investment fund's capital is therefore an endogenous variable and depends on the performance of the total net assets:

$$
\begin{aligned}
C\left(t\right) &= N\left(t\right)\cdot\mathrm{NAV}\left(t\right)\\
&= \mathrm{TNA}\left(t\right)
\end{aligned}
$$

At time $t+1$, we assume that the portfolio's return is equal to $R\left(t+1\right)$. Since $D\left(t\right)\ll A\left(t\right)$, it follows that:

$$
\begin{aligned}
\mathrm{TNA}\left(t+1\right) &= A\left(t+1\right)-D\left(t+1\right)\\
&= \left(1+R\left(t+1\right)\right)A\left(t\right)-D\left(t+1\right)\\
&\approx \left(1+R\left(t+1\right)\right)\cdot\mathrm{TNA}\left(t\right)
\end{aligned}
$$

meaning that:

$$
\mathrm{NAV}\left(t+1\right)\approx\left(1+R\left(t+1\right)\right)\cdot\mathrm{NAV}\left(t\right)
$$

The investment fund's capital is therefore time-varying. It increases when the performance of the asset is positive, and it decreases otherwise.

Remark 1 *In the sequel, we assume that the mutual fund is priced daily, meaning that the NAV of the mutual fund is calculated at the end of the market day. Therefore, the time t represents the current market day, whereas the time $t+1$ corresponds to the next market day.*

2.1.2 The effect of subscriptions and redemptions

Let us now introduce the impact of subscriptions and redemptions. In this case, new and current investors may purchase new mutual fund units, while existing investors may redeem all or part of their shares. Subscription and redemption orders must be known by the fund manager before $t+1$ in order to be executed. In this case, the number of units becomes:

$$
N\left(t+1\right)=N\left(t\right)+N^{+}\left(t+1\right)-N^{-}\left(t+1\right)
$$

where $N^{+}\left(t+1\right)$ is the number of units to be created and $N^{-}\left(t+1\right)$ is the number of units to be redeemed. At time $t+1$, we have:

$$
\begin{aligned}
\mathrm{NAV}\left(t+1\right) &= \frac{\mathrm{TNA}\left(t+1\right)}{N\left(t+1\right)}\\
&= \frac{\mathrm{TNA}\left(t+1\right)}{N\left(t\right)+N^{+}\left(t+1\right)-N^{-}\left(t+1\right)}
\end{aligned}
$$

We deduce that:

$$
\mathrm{TNA}\left(t+1\right)=N\left(t\right)\cdot\mathrm{NAV}\left(t+1\right)+\mathcal{F}^{+}\left(t+1\right)-\mathcal{F}^{-}\left(t+1\right) \tag{2}
$$

where $\mathcal{F}^{+}\left(t+1\right)=N^{+}\left(t+1\right)\cdot\mathrm{NAV}\left(t+1\right)$ and $\mathcal{F}^{-}\left(t+1\right)=N^{-}\left(t+1\right)\cdot\mathrm{NAV}\left(t+1\right)$ are the investment inflows and outflows. Again, we notice that the investment fund's capital is time-varying and depends on the fund flows.

From Equation (2), we deduce that:

$$
\begin{aligned}
\mathrm{TNA}\left(t+1\right) &= N\left(t\right)\cdot\mathrm{NAV}\left(t+1\right)+\mathcal{F}^{+}\left(t+1\right)-\mathcal{F}^{-}\left(t+1\right)\\
&\approx N\left(t\right)\cdot\left(1+R\left(t+1\right)\right)\cdot\mathrm{NAV}\left(t\right)+\mathcal{F}^{+}\left(t+1\right)-\mathcal{F}^{-}\left(t+1\right)\\
&= \left(1+R\left(t+1\right)\right)\cdot\mathrm{TNA}\left(t\right)+\mathcal{F}^{+}\left(t+1\right)-\mathcal{F}^{-}\left(t+1\right)
\end{aligned}
$$

The current net assets are approximatively equal to the previous net assets plus the performance value plus the net flow. We retrieve the famous formula of Sirri and Tufano (1998) when we want to estimate the net flow from the NAV and TNA of the fund:

$$
\begin{aligned}
\mathcal{F}(t+1) &= \mathcal{F}^+(t+1) - \mathcal{F}^-(t+1) \\
&= \text{TNA}(t+1) - (1 + R(t+1)) \cdot \text{TNA}(t) \\
&= \text{TNA}(t+1) - \left(\frac{\text{NAV}(t+1)}{\text{NAV}(t)}\right) \text{TNA}(t)
\end{aligned}
\tag{3}
$$

2.1.3 Liability risks

Since the capital is a residual, we face three liability risks. The first one deals with the accrued liabilities $D(t)$. Generally, the debits are a very small part of the liabilities. However, we can potentially face some situations where the debits are larger than the assets, implying that the net asset value becomes negative. In particular, this type of situation occurs when the fund is highly leveraged. The second risk concerns the inflows. If the investment fund has a big subscription, it may have some difficulties buying the financial instruments. For instance, this type of situation may occur when the fund must buy fixed-income securities in a bond bull market and it is difficult to find investors who are looking to sell bonds. The third liability risk is produced by the outflows. In this case, the fund manager must sell assets, which could be difficult in illiquid and stressed market conditions. The last two situations are produced when supply and demand dynamics are totally unbalanced (higher supply for buying assets or higher demand for selling assets). In this article, we focus on the third liability risk, which is also called redemption risk.

2.2 Measuring redemption risk

In order to assess an investment fund's redemption risk, we need an objective measurement system, which is well scaled. For instance, the outflows $\mathcal{F}^-(t)$ are not very interesting, because they depend on the investment fund's assets under management. In fact, they must be scaled in order to be a homogeneous measure that can be used to compare the redemption behavior across time, across funds and across investors.

2.2.1 Gross redemption rate

The (gross) redemption rate is defined as the ratio between the fund's redemption flows and total net assets:

$$
\mathcal{R}(t) = \frac{\mathcal{F}^-(t)}{\text{TNA}(t)}
\tag{4}
$$

We verify the property that $\mathcal{R}(t) \in [0,1]$. For example, if we observe an outflow of \$100 mn for a fund of \$5 bn, we have $\mathcal{R}(t) = 100/5\,000 = 2\%$. In the case where the outflow is \$10 mn and the fund size is \$100 mn, the redemption rate is equal to 10%. The redemption is more severe for the small fund than for the large fund.

We notice that Equation (4) is used to calculate the ex-post redemption rate, meaning that the value of outflows is known. Therefore, Equation (4) corresponds to the definition of the redemption rate, but it can also be used to estimate or predict the redemption flows. Indeed, we have:

$$
\hat{\mathcal{F}}^-(t+1) = \mathcal{R}(t+1) \cdot \text{TNA}(t)
\tag{5}
$$

In this case, $\mathcal{R}(t+1)$ is a random variable and is not known at the current time t. By assuming that redemption rates are stationary, the challenge is then to model the associated probability distribution $\mathbf{F}$.

2.2.2 Net redemption rate

The guidelines on the liquidity stress testing published by ESMA (2019) refer to both gross and net redemptions:

> "*LST should be adapted appropriately to each fund, including by adapting: [...] the assumptions regarding investor behaviour (gross and net redemptions)*" (ESMA, 2019, page 36).

Following this remark, we can also define the net flow rate by considering both inflows and outflows:

$$\mathcal{R}^{\pm}(t) = \frac{\mathcal{F}(t)}{\text{TNA}(t)} \tag{6}$$

This quantity is more complex than the previous one, because it cannot be used from an ex-ante point of view:

$$\hat{\mathcal{F}}(t+1) \neq \mathcal{R}^{\pm}(t+1) \cdot \text{TNA}(t)$$

The reason is that the outflows are bounded and cannot exceed the current assets under management. This is not the case for the inflows. For example, we consider a fund with a size of \$100 mn. By construction, we have[3] $\hat{\mathcal{F}}^{-}(t+1) \leq 100$, but we can imagine that $\hat{\mathcal{F}}^{+}(t+1) > 100$. The fund size can double or triple, in particular when the investment fund is young and small.

Nevertheless, the use of net flows is not foolish since the true liability risk of the fund is on the net flows. If the fund manager faces a large redemption, which is offset by a large subscription, there is no liquidity risk. The issue is that the use of net flows is difficult to justify in stress periods. In these cases, inflows generally disappear and the probability distribution of $\mathcal{R}^{\pm}(t)$ may not reflect the liability risk in a stress testing framework. For example, let us consider an asset class that has experienced a bull market over the last three years. Certainly, we will mainly observe positive net flows and a very small number of observations with negative net flows. We may think that these data are not relevant for building stress scenarios. More generally, if an asset manager uses net flow rates for stress testing purposes, only the observations during historical stress periods are relevant, meaning that the calibration is based on a small fraction of the dataset.

In fact, the use of net flows is motivated by other considerations. Indeed, the computation of $\mathcal{R}(t)$ requires us to know the outflows $\mathcal{F}^{-}(t)$ exactly. Moreover, as we will see later, $\mathcal{R}(t)$ must be computed for all the investor categories that are present in the fund (retail, private banking, institutional, etc.). This implies in-depth knowledge of the fund's balance sheet liability, meaning that the asset manager must have a database with all the flows of all the investors on a daily basis. From an industrial point of view, this is a big challenge in terms of IT systems between the asset manager and the custodian. This is why many asset managers don't have the disaggregated information on the liability flows. An alternative measure is to compute the net redemption rate, which corresponds to the negative part of the net flow rate:

$$\mathcal{R}^{-}(t) = \max\left(0, -\frac{\mathcal{F}(t)}{\text{TNA}(t)}\right)$$

It has the good mathematical property that $\mathcal{R}^{-}(t) \in [0, 1]$. Indeed, we have:

$$\mathcal{R}^{-}(t) = \max\left(0, \frac{\mathcal{F}^{-}(t) - \mathcal{F}^{+}(t)}{\text{TNA}(t)}\right) \tag{7}$$

---

[3]In order to simplify the calculus, we do not take into account the daily performance of the fund.

and its maximum value is reached when $\mathcal{F}^{-}(t) = \mathrm{TNA}(t)$ and $\mathcal{F}^{+}(t) = 0$. Moreover, we notice that the net redemption rate is equal to the gross redemption rate when there are no inflows:

$$\mathcal{R}^{-}(t) = \max\left(0, \frac{\mathcal{F}^{-}(t)}{\mathrm{TNA}(t)}\right) = \mathcal{R}(t)$$

Otherwise, we have:

$$\mathcal{R}^{-}(t) < \mathcal{R}(t)$$

From a risk management point of view, it follows that redemption shocks based on net redemptions may be underestimated compared to redemption shocks based on gross redemptions. However, we will see later that the approximation $\mathcal{R}(t) \approx \mathcal{R}^{-}(t)$ may be empirically valid under some conditions.

2.2.3 Liability classification

The computation of redemption rates only makes sense if they are homogeneous, coherent and comparable. Let us assume that we compute the redemption rate $\mathcal{R}(t)$ at the level of the asset management company, and we have the historical data for the last ten years. By assuming that there are 260 market days per year, we have a sample of 2 600 redemption rates. We can compute the mean, the standard deviation, different quantiles, etc. Does it help with building a stress scenario for a mutual fund? Certainly not, because redemptions depend on the specific investor behavior at the fund level and not on the overall investor behavior at the asset manager level. For instance, we can assume that an investor does not have the same behavior if he is invested in an equity fund or a money market fund. We can also assume that the redemption behavior is not the same for a central bank, a retail investor, or a pension fund. Therefore, we must build categories that correspond to homogenous behaviors. Otherwise, we will obtain categories, whose behavior is non-stationary. But, without the stationarity property, risk measurement is impossible and stress testing is a hazardous exercise.

Therefore, liability categorization is an important step before computing redemption rates. For instance, ESMA (2019) considers four factors regarding investor behavior: investor category, investor concentration, investor location and investor strategy. Even though the last three factors are significant, the most important factor remains the investor type. For instance, AMF (2017, page 12) gives an example with the following investor types: large institutional (tier one), small institutional (tier two), investment (or mutual) fund, private banking network and retail investor. Other categories can be added: central bank, sovereign, corporate, third-party distributor, employee savings plan, wealth management, etc. Moreover, it is also important to classify funds into homogeneous buckets such as balanced funds, bond funds, equity funds, etc. An example of an investor/fund categorization matrix is given in Table 1.

Remark 2 *The granularity of the investor/fund classification is an important issue. It is important to have a very detailed classification at the level of the database in order to group categories together from a computational point of view. In order to calibrate stress scenarios, we must have a sufficient number of observations in each cell of the classification matrix. Let us for instance consider the case of central banks. We can suppose that their behavior is very different to the other investors. Therefore, it is important for an asset manager to be aware of the liabilities with respect to central banks. Nevertheless, there are few central banks in the world, meaning we may not have enough observations for calibrating some cells (e.g. central bank/equity or central bank/real asset), and we have to merge some cells (across investor and fund categories).*

Table 1: An example of two-dimensional categorization matrix

Investor category	Absolute return	Balanced	Bond	Commodity	Enhanced treasury	Equity	Money market	Real asset	Structured
Central bank									
Corporate									
Institutional									
Insurance									
Internal									
Pension fund									
Retail									
Sovereign									
Third-party distributor									
Wealth management									

2.2.4 The arithmetic of redemption rates

We consider a fund. We note $\mathrm{TNA}_i(t)$ the assets under management of the investor i for this fund. By definition, we have:

$$\mathrm{TNA}_i(t) = N_i(t) \cdot \mathrm{NAV}(t)$$

where $\mathrm{NAV}(t)$ is the net asset value of the fund and $N_i(t)$ is the number of units held by the investor i for the fund. The fund's assets under management are equal to:

$$\mathrm{TNA}(t) = \sum_k \mathrm{TNA}_{(k)}(t)$$

where $\mathrm{TNA}_{(k)}(t) = \sum_{i \in \mathcal{IC}_{(k)}} \mathrm{TNA}_i(t)$, and $\mathcal{IC}_{(k)}$ is the kth investor category. It follows that:

$$
\begin{aligned}
\mathrm{TNA}(t) &= \sum_k \sum_{i \in \mathcal{IC}_{(k)}} \mathrm{TNA}_i(t) \\
&= \sum_k \sum_{i \in \mathcal{IC}_{(k)}} N_i(t) \cdot \mathrm{NAV}(t) \\
&= N(t) \cdot \mathrm{NAV}(t)
\end{aligned}
$$

where $N(t) = \sum_k \sum_{i \in \mathcal{IC}_{(k)}} N_i(t)$ is the total number of units in issue. We retrieve the definition of the assets under management (or total net assets) at the fund level. We can obtain a similar breakdown for the outflows[4]:

$$\mathcal{F}^-(t) = \sum_k \sum_{i \in \mathcal{IC}_{(k)}} \mathcal{F}_i^-(t) = \sum_k \mathcal{F}_{(k)}^-(t)$$

The redemption rate for the investor category $\mathcal{IC}_{(k)}$ is then equal to:

$$\mathcal{R}_{(k)}(t) = \frac{\mathcal{F}_{(k)}^-(t)}{\mathrm{TNA}_{(k)}(t)} \tag{8}$$

---

[4] We have $\mathcal{F}_k^-(t) = \sum_{i \in \mathcal{IC}_{(k)}} \mathcal{F}_i^-(t)$.

We deduce that the relationship between the investor-based redemption rates and the fund-based redemption rate is:

$$
\begin{aligned}
\mathcal{R}\left(t\right) & = \frac{\mathcal{F}^{-}\left(t\right)}{\mathrm{TNA}\left(t\right)} \\
& = \frac{\sum_{k} \mathcal{F}_{(k)}^{-}\left(t\right)}{\mathrm{TNA}\left(t\right)} \\
& = \frac{\sum_{k} \mathrm{TNA}_{(k)}\left(t\right) \cdot \mathcal{R}_{(k)}\left(t\right)}{\mathrm{TNA}\left(t\right)} \\
& = \sum_{k} \omega_{(k)}\left(t\right) \cdot \mathcal{R}_{(k)}\left(t\right)
\end{aligned}
\tag{9}
$$

where $\omega_{(k)}\left(t\right)$ represents the weights of the investor category $\mathcal{IC}_{(k)}$ in the fund:

$$
\omega_{(k)}\left(t\right) = \frac{\mathrm{TNA}_{(k)}\left(t\right)}{\mathrm{TNA}\left(t\right)}
$$

Equation (9) is very important, because it shows that the redemption rate at the fund level is a weighted-average of the redemption rates of the different investor categories.

Let us now consider different funds. We note $\mathcal{R}_{(f,k)}\left(t\right)$ as the redemption rate of the investor category $\mathcal{IC}_{(k)}$ for the fund f at time t. By relating the fund f to its fund category $\mathcal{FC}_{(j)}$, we obtain a database of redemption rates by investor category $\mathcal{IC}_{(k)}$ and fund category $\mathcal{FC}_{(j)}$:

$$
\mathcal{DB}_{(j,k)}\left(T\right) = \left\{ \mathcal{R}_{(f,k)}\left(t\right) : f \in \mathcal{FC}_{(j)}, t \in T \right\}
$$

$\mathcal{DB}_{(j,k)}\left(T\right)$ is then the sample of all redemption rates of the investor category $\mathcal{IC}_{(k)}$ for all the funds that fall into the fund category $\mathcal{FC}_{(j)}$ during the observation period T. We notice that $\mathcal{DB}_{(j,k)}\left(t\right)$ does not have a unique element for a given date t because we generally observe several redemptions at the same date for different funds and the same investor category.

2.3 Calibration of historical redemption scenarios

The key parameter for computing the redemption flows is the redemption rate, which is defined for an investor category and a fund category. It is not calibrated at the fund level, because past redemption data for a given specific fund are generally not enough to obtain a robust estimation. This is why we have pooled redemption data as described in the previous paragraph. Using these data, we can estimate the probability distribution $\mathbf{F}$ of the redemption rate and define several statistics that can help to build stress scenarios.

2.3.1 Data

In what follows, we consider the liability data provided by Amundi Asset Management from January, 1st 2019 to August, 19th 2020. The database is called '*Amundi Cube Database*' and contains $1\,617\,403$ observations if we filter based on funds with assets under management greater than €5 mn. The breakdown by investor categories[5] is given in Table 40 on page 92. The number of observations is $464\,399$ for retail investors, $310\,452$ for third-party distributors, $267\,600$ for institutionals, etc. The investor category which is the smallest is central banks with $15\,523$ observations. In terms of fund categories, bond, equity and balanced funds dominate with respectively $452\,942$, $436\,401$ and $361\,488$ observations. The smallest

---

[5]The Amundi database contains 13 investor and 13 fund categories.

categories are private loan funds and real estate funds. In terms of classification matrix, the largest matrix cells are retail/balanced, third-party distributor/equity, retail/equity, institutional/bond, retail/bond, third-party distributor/bond, retail/structured, etc.

Remark 3 *In what follows, we apply a filter that consists in removing observations that corresponds to dedicated mutual funds (FCP and SICAV) and mandates (see Table 41 on page 93). The motivation is to focus on mutual funds with several investors, and this issue will be extensively discussed in Section 4.1.3 on page 44.*

2.3.2   Net flow, net redemption and gross redemption rates

Figure 4: Retail investor
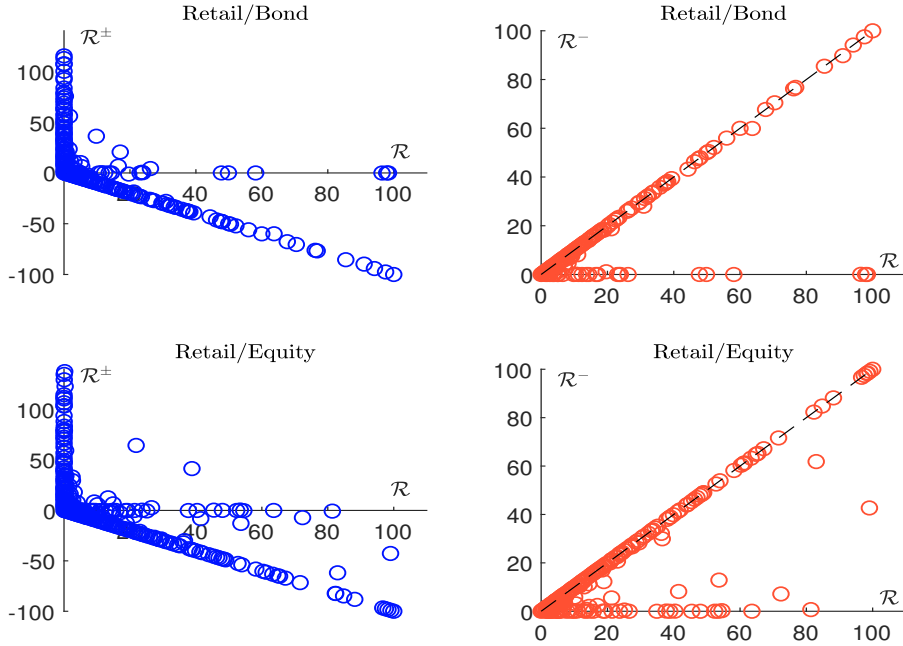
We first begin by comparing the gross redemption rate $\mathcal{R}$, the net flow rate $\mathcal{R}^{\pm}$ and the net redemption rate $\mathcal{R}^{-}$. Some results are given in Figures 4 and 5 for retail and insurance investors and bond and equity funds. In the case of insurance companies, we notice that the approximation $\mathcal{R} \approx \mathcal{R}^{-} \approx -\mathcal{R}^{\pm}$ is valid when the redemption rate is greater than 20%. This is not the case for retail investors, where we observe that some large redemptions may be offset by large subscriptions[6]. The difference between retail and insurance categories lies in the investor concentration. When an investor category is concentrated, there is a low probability that this offsetting effect will be observed. This is not the case when the granularity of the investor category is high. We also observe that the approximation $\mathcal{R} \approx \mathcal{R}^{-} \approx -\mathcal{R}^{\pm}$ depends on the fund category. For instance, it is not valid for money market funds. The reason is that we generally observe subscriptions in a bull market and redemptions in a bear market when the investment decision mainly depends on the performance of the asset class. This is why large redemptions and subscriptions tend to be mutually exclusive (in the mathematical sense) in equity or bond funds. The mutual exclusivity property is more difficult

---

[6]We observe the same phenomenon when we consider the data of third-party distributors (see Figure 37 on page 94).
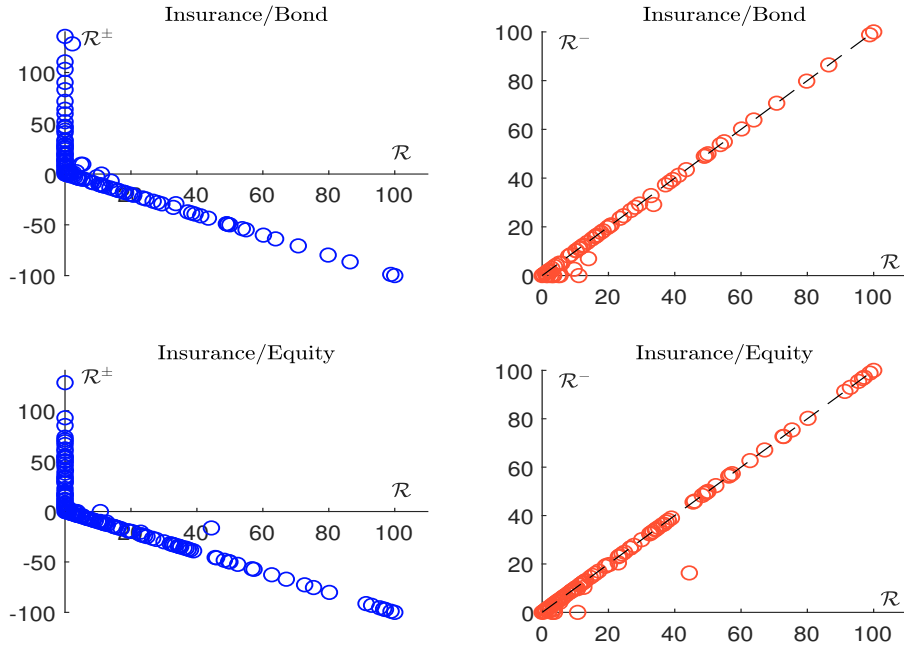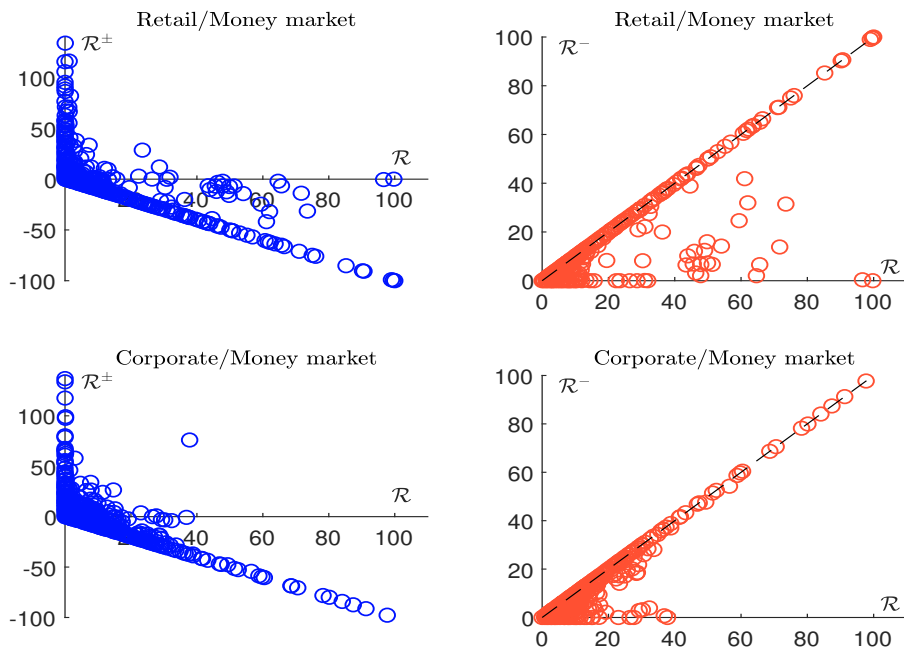
Figure 5: Insurance

Insurance/Bond

Insurance/Bond

Insurance/Equity

Insurance/Equity

Figure 6: Money market fund

Retail/Money market

Retail/Money market

Corporate/Money market

Corporate/Money market

to observe for money market, enhanced treasury or balanced funds, because their inflows are less dependent on market conditions. We conclude that net redemption rates may be used in order to perform stress scenarios under some conditions regarding the concentration of the investor category and the type of mutual fund.

2.3.3 Statistical risk measures

For a given investor/fund category, we note $\mathbf{F}$ as the probability distribution of the redemption rate. We can define several risk measures (Roncalli, 2020, pages 62-63):

- the mean:

$$\mathbb{M} = \int_0^1 x \, d\mathbf{F}(x)$$

- the standard deviation-based risk measure:

$$\mathbb{SD}(c) = \mathbb{M} + c \int_0^1 \left(x - \mathbb{M}^2\right) \, d\mathbf{F}(x)$$

- the quantile (or the value-at-risk) at the confidence level α:

$$\mathbb{Q}(\alpha) = \mathbf{F}^{-1}(\alpha)$$

- the average beyond the quantile (or the conditional value-at-risk):

$$\mathbb{C}(\alpha) = \mathbb{E}\left[\mathcal{R} \mid \mathcal{R} \geq \mathbf{F}^{-1}(\alpha)\right]$$

The choice of a risk measure depends on its use. For instance, $\mathbb{M}$ can be used by the fund manager daily, because it is the expected value of the daily redemption rate. If the fund manager prefers to have a more conservative measure, he can use $\mathbb{SD}(1)$. $\mathbb{M}$ and $\mathbb{SD}(c)$ make sense in normal periods from a portfolio management perspective, but they are less relevant in a stress period. This is why it is better to use $\mathbb{Q}(\alpha)$ and $\mathbb{C}(\alpha)$ from a risk management point of view. In the asset management industry, the consensus is to set $\alpha = 99\%$.

In Table 2, we have reported the values of $\mathbb{M}$, $\mathbb{Q}(99\%)$ and $\mathbb{C}(99\%)$ by considering the empirical distribution of gross redemption rates by client category. We do not consider the $\mathbb{SD}$-measure because we will see later that there is an issue when it is directly computed from a sample of historical redemption rates. On average, the expected redemption rate is roughly equal to 20 bps. It differs from one client category to another, since the lowest value of $\mathbb{M}$ is observed for central banks whereas the highest value of $\mathbb{M}$ is observed for corporates. The 99% value-at-risk is equal to 3.5%. This means that we observe a redemption rate of 3.5% every 100 days, that is every five months. Again, there are some big differences between the client categories. The riskiest category is corporate followed by sovereign and auto-consumption. If we focus on the conditional value-at-risk, we are surprised by the high values taken by $\mathbb{C}(99\%)$. If we consider all investor categories, $\mathbb{C}(99\%)$ is more than 15%, and the ratio $\mathbb{R}(99\%)$ between $\mathbb{C}(99\%)$ and $\mathbb{Q}(99\%)$ is equal to 4.51. This is a very high figure since this ratio is generally less than 2 for market and credit risks. For example, in the case of a Gaussian distribution $\mathcal{N}\left(0, \sigma^2\right)$, the ratio $\mathbb{R}(\alpha)$ between the conditional value-at-risk and the value-at-risk is equal to:

$$\mathbb{R}(\alpha) = \frac{\mathbb{C}(\alpha)}{\mathbb{Q}(\alpha)} = \frac{\phi\left(\Phi^{-1}(\alpha)\right)}{(1-\alpha)\Phi^{-1}(\alpha)}$$

This ratio is respectively equal to 1.37 and 1.15 when $\alpha = 90\%$ and $\alpha = 99\%$. Moreover, Roncalli (2020, page 118) showed that it is a decreasing function of α and:

$$\lim_{\alpha \to 1^-} \mathbb{R}(\alpha) = 1$$

We deduce that the ratio is lower than 1.5 for reasonable values of the confidence level α. Therefore, the previous figure $\mathbb{R}(99\%) = 4.51$ indicates that redemption risk is more skewed than market and credit risks.

Table 2: Redemption statistical measures in % by investor category

Client	$\mathbb{M}$	$\mathbb{Q}(99\%)$	$\mathbb{C}(99\%)$	$\mathbb{R}(99\%)$
Auto-consumption	0.38	7.44	24.86	3.34
Central bank	0.04	0.00	4.38	∞
Corporate	0.54	12.71	28.21	2.22
Corporate pension fund	0.13	0.50	13.06	26.22
Employee savings plan	0.06	1.13	4.86	4.30
Institutional	0.27	5.11	22.79	4.46
Insurance	0.26	5.25	21.24	4.05
Other	0.23	3.41	20.22	5.92
Retail	0.15	1.92	9.18	4.77
Sovereign	0.45	8.28	39.85	4.81
Third-party distributor	0.23	3.90	13.72	3.52
Total	0.22	3.50	15.79	4.51

Table 3 reports the statistical measures by fund category. Again, we observe some big differences. Money market and enhanced treasury funds face a high redemption risk followed by bond and equity funds. This is normal because treasury funds can be converted to cash very quickly, investors are motivated to redeem these funds when they need cash, and their holding period is short. At the global level, we also notice that the redemption behavior is similar between bond and equity funds. For instance, their 99% value-at-risk is close to 3% (compared to 6% for the enhanced treasury category and 22% for money market funds). Another interesting result is the lower redemption rate of balanced funds compared to bond and equity funds. This result is normal because balanced funds are more diversified. Therefore, investors in balanced funds are more or less protected by a bond crisis or an equity crisis. Finally, structured funds are the least exposed category to redemption risk, because they generally include a capital guarantee or protection option.

Table 3: Redemption statistical measures in % by fund category

Fund	$\mathbb{M}$	$\mathbb{Q}(99\%)$	$\mathbb{C}(99\%)$	$\mathbb{R}(99\%)$
Balanced	0.14	1.77	8.14	4.61
Bond	0.20	3.18	14.23	4.47
Enhanced treasury	0.40	6.30	31.15	4.94
Equity	0.18	2.68	12.94	4.84
Money market	1.06	21.76	46.13	2.12
Other	0.11	1.19	9.32	7.84
Structured	0.04	0.45	3.52	7.88
Total	0.22	3.50	15.79	4.51

Table 4: Historical $\mathbb{M}$-statistic in % by investor/fund category

	(1)	(2)	(3)	(4)	(5)	(6)	(7)	(8)
Auto-consumption	0.27	0.36	0.65	0.30	1.58	0.18		0.38
Central bank	0.01	0.06		0.11				0.04
Corporate	0.08	0.15	0.27	0.25	1.52	0.07		0.54
Corporate pension fund	0.17	0.05	0.10	0.10	0.55	0.00		0.13
Employee savings plan	0.03	0.05	0.13	0.06	0.06		0.08	0.06
Institutional	0.13	0.16	0.64	0.18	1.47	0.06		0.27
Insurance	0.17	0.15	0.12	0.16	0.90	0.08		0.26
Other	0.08	0.10	0.33	0.21	0.76	0.02		0.23
Retail	0.15	0.14	0.26	0.16	0.91	0.07	0.04	0.15
Sovereign	0.01	0.01	0.16	0.19	1.91	0.06		0.45
Third-party distributor	0.12	0.24	0.67	0.19	0.92	0.28	0.08	0.23
Total	0.14	0.20	0.40	0.18	1.06	0.11	0.04	0.22

Table 5: Historical $\mathbb{Q}$-statistic in % by investor/fund category

	(1)	(2)	(3)	(4)	(5)	(6)	(7)	(8)
Auto-consumption	2.93	7.57	12.62	5.46	25.98	3.23		7.44
Central bank	0.00	0.00		0.12				0.00
Corporate	0.30	1.58	4.90	3.88	24.14	0.00		12.71
Corporate pension fund	0.39	0.05	1.30	0.03	13.09	0.00		0.50
Employee savings plan	1.06	1.70	2.35	1.08	2.51		0.25	1.13
Institutional	0.84	1.94	8.68	3.10	34.82	0.00		5.11
Insurance	0.32	0.21	3.87	0.50	18.39	0.00		5.25
Other	0.73	0.56	2.40	2.20	14.75	0.05		3.41
Retail	2.01	1.50	4.72	1.65	18.36	1.17	0.45	1.92
Sovereign	0.11	0.14	7.98	0.22	66.36	0.00		8.28
Third-party distributor	1.32	4.59	11.13	3.38	14.66	3.96	1.11	3.90
Total	1.77	3.18	6.30	2.68	21.76	1.19	0.45	3.50

Table 6: Historical $\mathbb{C}$-statistic in % by investor/fund category

	(1)	(2)	(3)	(4)	(5)	(6)	(7)	(8)
Auto-consumption	21.08	23.37	40.73	21.24	54.96	15.50		24.86
Central bank	1.28	6.05		10.11				4.38
Corporate	7.31	14.98	22.80	22.48	38.37	6.52		28.21
Corporate pension fund	17.22	5.14	9.24	9.58	32.33	0.00		13.06
Employee savings plan	2.48	3.16	10.60	4.91	4.97		7.91	4.86
Institutional	10.99	15.40	62.30	16.27	58.10	6.26		22.79
Insurance	16.35	14.65	10.59	15.32	37.28	7.62		21.24
Other	7.45	9.84	32.56	18.61	46.88	2.17		20.22
Retail	7.02	8.34	15.99	8.95	44.38	5.03	3.03	9.18
Sovereign	0.39	1.35	15.20	17.97	86.47	5.73		39.85
Third-party distributor	6.69	14.53	42.24	11.22	32.68	20.16	6.85	13.72
Total	8.14	14.23	31.15	12.94	46.13	9.32	3.52	15.79

(1) = balanced, (2) = bond, (3) = enhanced treasury, (4) = equity, (5) = money market, (6) = other, (7) = structured, (8) = total

The historical statistical measures[7] for the classification matrix are given in Tables 4, 5 and 6. We notice that the two dimensions are important, since one dimension does not dominate the other. This means that a low-risk (resp. high-risk) investor category tends to present the lowest (resp. highest) redemption statistics whatever the fund category. In addition, the ranking of redemption statistics between fund categories is similar whatever the investor category. Nevertheless, we observe some exceptions and new stylized facts. For instance, we have previously noticed that bond and equity funds have similar redemption rates on average. This is not the case for the corporate, corporate pension fund and sovereign categories, for which historical $\mathbb{C}$-statistics are more important for equity funds than bond funds. For the corporate pension fund category, the risk is also higher for balanced funds than for bond funds.

2.3.4 Defining historical stress scenarios

According to BCBS (2017, page 60), a historical stress scenario "*aims at replicating the changes in risk factor shocks that took place in an actual past episode*". If we apply this definition to the redemption risk, the computation of the historical stress scenario is simple. First, we have to choose a stress period T^{stress} and second, we compute the maximum redemption rate:

$$\mathbb{X}\left(T^{\text{stress}}\right) = \max_{t \in T^{\text{stress}}} \mathcal{R}\left(t\right)$$

For example, if we apply this definition to our study period, we obtain the results given in Table 7. We recall that the study period runs from January 2019 to August 2020 and includes the Coronavirus pandemic crisis, which was a redemption stress period. We observe that the $\mathbb{X}$-statistic is generally equal to 100%! This is a big issue, because it is not helpful to consider that liquidity stress testing of liabilities leads to a figure of 100%. The problem is that the $\mathbb{X}$-statistic is not adapted to redemption risk. Let us consider an investor category $\mathcal{IC}_{(k)}$ and a fund category $\mathcal{FC}_{(j)}$. The $\mathbb{X}$-statistic is computed by taking the maximum of all redemption rates for all funds that belong to the fund category:

$$\mathbb{X}_{(j,k)}\left(T^{\text{stress}}\right) = \max_{t \in T^{\text{stress}}} \left\{\mathcal{R}_{(f,k)}\left(t\right) : f \in \mathcal{FC}_{(j)}\right\}$$

If there is one fund with only one investor and if this investor redeems 100%, $\mathbb{X}_{(j,k)}\left(T^{\text{stress}}\right)$ is equal to 100%. However, the asset manager does not really face a liquidity risk in this situation, because there is no other investor in this fund. So, the other investors are not penalized. We have excluded this type of fund. However, we face a similar situation in many other cases: small funds with a large fund holder, funds with a low number of unitholders, etc. Moreover, this type of approach penalizes big asset managers, which have hundreds of funds. Let us consider an example. For a given investor/fund category, the fund manager A has 100 funds of \$100 million, whereas the fund manager B has one fund of \$10 billion. From a theoretical point of view, A and B face the same redemption risk, since they both manage \$10 billions for the same investor/fund category. However, it is obvious that $\mathbb{X}_A \gg \mathbb{X}_B$, meaning that the historical stress scenario for the fund manager A will be much higher than the historical stress scenario for the fund manager B. This is just a probabilistic counting principle as shown in Appendix A.1 on page 78. If we consider the previous example, the historical stress scenario for the fund manager A is larger than 99.9% when the historical stress scenario for the fund manager B is larger than 6.68% (see Figure 38 on page 95). More generally, the two stress scenarios are related in the following manner:

$$\mathbb{X}_n = 1 - \left(1 - \mathbb{X}_1\right)^n$$

where $\mathbb{X}_1$ is the $\mathbb{X}$-measure for one fund and $\mathbb{X}_n$ is the $\mathbb{X}$-measure for n funds.

---

[7]They are not calculated if the number of observations is less than 200.

Table 7: Historical $\mathbb{X}$-statistic in % by investor/fund category

	(1)	(2)	(3)	(4)	(5)	(6)	(7)
Auto-consumption	100.00	100.00	100.00	100.00	99.65	100.00	
Central bank	9.17	29.60		50.00			
Corporate	78.64	83.44	100.00	94.14	97.72	100.00	
Corporate pension fund	100.00	100.00	15.79	100.00	94.78	0.00	
Employee savings plan	50.79	15.35	100.00	100.00	14.71		100.00
Institutional	99.09	100.00	100.00	100.00	100.00	100.00	
Insurance	99.99	100.00	56.96	100.00	99.93	77.13	
Other	50.00	100.00	100.00	100.00	100.00	100.00	
Retail	100.00	100.00	100.00	100.00	100.00	100.00	100.00
Sovereign	5.44	21.12	24.91	100.00	100.00	100.00	
Third-party distributor	100.00	100.00	100.00	100.00	97.04	100.00	97.98

(1) = balanced, (2) = bond, (3) = enhanced treasury, (4) = equity, (5) = money market, (6) = other, (7) = structured

Remark 4 *Another approach consists in computing the average redemption rate daily:*

$$\mathcal{R}_{(j,k)}\left(t\right) = \sum_{f \in \mathcal{FC}_{(j)}} \frac{\text{TNA}_{(f)}}{\sum_{f \in \mathcal{FC}_{(j)}} \text{TNA}_{(f)}} \mathcal{R}_{(f,k)}\left(t\right)$$

where the weights are proportional to the size of funds f that belong to the jth fund category $\mathcal{FC}_{(j)}$. In this case, we have:

$$\mathbb{X}_{(j,k)}\left(T^{\text{stress}}\right) = \max_{t \in T^{\text{stress}}} \mathcal{R}_{(j,k)}\left(t\right)$$

This method does not have the previous drawback, but it has other shortcomings such as an information loss. However, the biggest disadvantage is that the historical stress scenario is generally based on the largest fund, except when the funds have similar size.

Since $\mathbb{X}$-measures can not be used to build redemption shocks, we propose using $\mathbb{Q}$ or $\mathbb{C}$-measures. $\mathbb{Q}\left(99\%\right)$ is the daily value-at-risk at the 99% confidence level. This means that its return period is 100 days. On average, we must observe that redemption shocks are greater than $\mathbb{Q}\left(99\%\right)$ two and a half times per year. We can also use the conditional value-at-risk $\mathbb{C}\left(99\%\right)$ if we want more severe redemption shocks. The drawback of $\mathbb{C}\left(99\%\right)$ is that we don't know the return period of such event. However, it does make sense because it is a very popular measure in risk management, and it is well received by regulatory bodies and supervisors (Roncalli, 2020). Nevertheless, we must be cautious about the computed figures obtained in Tables 5 and 6 on page 18. For example, we don't have the same confidence level between the matrix cells, because the estimates are not based on the same number of observations. In the case of retail investors or third-party distributors, we generally use a huge number of observations whereas this is not the case with the other categories. In Table 8, we give an example of confidence level codification. We see that some cells are not well estimated since the number of observations is less than 10 000. For some of them, the number of observations is very low (less than 200), implying that the confidence on these estimates is very poor.

Therefore, the estimated values cannot be directly used as redemption shocks. However, they help risk managers and business experts to build redemption shocks. Starting from these figures, they can modify them and build a table of redemption shocks that respect the risk coherency $\mathcal{C}_{\text{investor}}$ between investor categories and the risk coherency $\mathcal{C}_{\text{fund}}$ between

Table 8: Confidence in estimated values with respect to the number of observations

	(1)	(2)	(3)	(4)	(5)	(6)	(7)
Auto-consumption	●●●	●●●	●●	●●●	●●	●●●	○○○
Central bank	●●	●	○○○	●	○○○	○○○	○○○
Corporate	●●	●●	●●	●●	●●	●●	○○○
Corporate pension fund	●●	●●	●	●●	●●	●●	○○○
Employee savings plan	●●	●●	●●	●●●	●●	○○○	●●
Institutional	●●	●●●	●●	●●●	●●	●●●	○○○
Insurance	●●	●●●	●●	●●●	●●	●●	○○○
Other	●●	●●●	●●	●●	●●	●●●	○○○
Retail	●●●	●●●	●●	●●●	●●●	●●●	●●●
Sovereign	●●	●●	●	●●	●●	●●	○○○
Third-party distributor	●●●	●●●	●●	●●●	●●●	●●●	●●

○○○ $0-10$, ○○ $11-50$, ○ $51-200$, ● $201-1\,000$, ●● $1\,001-10\,000$, ●●● $+10\,000$

fund categories[8]. The risk coherency $\mathcal{C}_{\text{investor}}$ means that if one investor category is assumed to be riskier than another, the global redemption shock of the first category must be greater than the global redemption shock of the second category:

$$\mathcal{IC}_{(k_1)} \succ \mathcal{IC}_{(k_2)} \Rightarrow \mathbb{S}_{(k_1)} \geq \mathbb{S}_{(k_2)}$$

For example, if we consider the $\mathbb{Q}$-measure, we can propose the following risk ordering:

1. central bank, corporate pension fund

2. employee savings plan, retail

3. other, third-party distributor

4. institutional, insurance

5. auto-consumption, corporate, sovereign

In this case, the redemption shock $\mathbb{S}_{(j,k)}$ for the (j,k)-cell depends on the global redemption shock $\mathbb{S}_{(k)}$ for the investor category $\mathcal{IC}_{(k)}$. For instance, we can set the following rule of thumb:

$$\mathbb{S}_{(j,k)} = m_{(j)} \cdot \mathbb{S}_{(k)} \tag{10}$$

where $m_{(j)}$ is the multiplicative factor of the fund category $\mathcal{FC}_{(j)}$. In a similar way, the risk coherency $\mathcal{C}_{\text{fund}}$ means that if one fund category is assumed to be riskier than another, the global redemption shock of the first category must be greater than the global redemption shock of the second category:

$$\mathcal{FC}_{(j_1)} \succ \mathcal{FC}_{(j_2)} \Rightarrow \mathbb{S}_{(j_1)} \geq \mathbb{S}_{(j_2)}$$

For example, if we consider the $\mathbb{Q}$-measure, we can propose the following risk ordering:

1. structured

2. balanced, other

3. bond, equity

---

[8]For instance, if we consider the sovereign category, it is difficult to explain the big difference of $\mathbb{C}\,(99\%)$ between bond and equity funds

4. enhanced treasury

5. money market

The redemption shock $\mathbb{S}_{(j,k)}$ for the (j,k)-cell depends then on the redemption shock $\mathbb{S}_{(j)}$ for the fund category $\mathcal{IC}_{(j)}$. Again, we can set the following rule of thumb:

$$\mathbb{S}_{(j,k)} = m_{(k)} \cdot \mathbb{S}_{(j)} \tag{11}$$

where $m_{(k)}$ is the multiplicative factor of the investor category $\mathcal{IC}_{(k)}$. We can also combine the two rules of thumb and we obtain the mixed rule:

$$\mathbb{S}_{(j,k)} = \frac{m_{(k)} \cdot \mathbb{S}_{(j)} + m_{(j)} \cdot \mathbb{S}_{(k)}}{2} \tag{12}$$

Let us illustrate the previous rules of thumb by considering the $\mathbb{Q}$-measure. Table 9 gives an example of $\mathbb{S}_{(j,k)}$ by considering the risk coherency[9] $\mathcal{C}_{\mathrm{investor}}$, whereas Table 10 corresponds to the risk coherency[10] $\mathcal{C}_{\mathrm{fund}}$. The mixed rule is reported in Table 11. These figures can then be modified by risk managers and business experts by considering the specificity of some matrix cells. For instance, it is perhaps not realistic to have the same redemption shock for balanced funds between auto-consumption and corporates. Moreover, these redemption shocks can also be modified by taking into account the $\mathbb{C}$-measure. For instance, the conditional value-at-risk for bond funds is much higher for third-party distributors than for sovereigns. Perhaps we can modify the redemption shock of 3.3% and have a larger value for third-party distributors. It is even more likely that the estimated values of $\mathbb{Q}$ and $\mathbb{C}$ are based on 75 591 observations for the third-party distributor category, and 2 261 for the sovereign category. Therefore, we can consider that the estimated value of 4.59% obtained in Table 5 on page 18 does make more sense than the proposed value of 3.3% obtained in Table 11 for the third-party distributor/bond matrix cell. In a similar way, we can consider that the estimated value of 0.14% does make less sense than the proposed value of 7.0% for the sovereign/bond matrix cell.

The previous analysis shows that building redemption shocks in a stress testing framework is more of an art than a science. A pure quantitative approach is dangerous because it is data-driven and it does not respect some coherency properties. However, historical statistics are very important because they provide an anchor point for risk managers and business experts in order to propose stress scenarios that are satisfactory from regulatory, risk management and fund management points of view. Historical data are also important because they help to understand the behavior of clients. It is different from one fund category to another, it also depends on the granularity of the classification, it may depend on the time period, etc. In what follows, we complete this pure historical analysis using more theoretical models. These models are important, because an historical approach is limited when we want to understand contagion effects between investors, correlation patterns between funds, time properties of redemption risk, the impact of the holding period, etc. The idea is not to substitute one model with another, but to rely on several approaches, because there is not just one single solution to the liability stress testing problem.

---

[9]We use the following values: $\mathbb{S}_{(k)} = 0.5\%$ for central banks and corporate pension funds, $\mathbb{S}_{(k)} = 2\%$ for employee savings plans and retail, $\mathbb{S}_{(k)} = 3.5\%$ for other and third-party distributors, $\mathbb{S}_{(k)} = 5\%$ for institutionals and insurance companies, and $\mathbb{S}_{(k)} = 8\%$ for auto-consumption, corporates and sovereigns. For the multiplication factor, we assume that $m_{(j)} = 0.25$ for structured, $m_{(j)} = 0.5$ for balanced and other, $m_{(j)} = 1$ for bond and equity, $m_{(j)} = 1.75$ for enhanced treasury, and $m_{(j)} = 6$ for money market.

[10]We use the following values: $\mathbb{S}_{(j)} = 0.5\%$ for structured, $\mathbb{S}_{(j)} = 1.5\%$ for balanced and other, $\mathbb{S}_{(j)} = 3\%$ for bond and equity, $\mathbb{S}_{(j)} = 5\%$ for enhanced treasury, and $\mathbb{S}_{(j)} = 20\%$ for money market. For the multiplication factor, we assume that $m_{(k)} = 0.25$ for central banks and corporate pension funds, $m_{(k)} = 0.5$ for employee savings plans and retail, $m_{(k)} = 1$ for other and third-party distributors, $m_{(k)} = 1.5$ for institutionals and insurance companies, and $m_{(k)} = 2$ for auto-consumption, corporates and sovereigns.

Table 9: Redemption shocks in % computed with the rule of thumb (10)

	(1)	(2)	(3)	(4)	(5)	(6)	(7)	(8)
Auto-consumption	4.0	8.0	14.0	8.0	48.0	4.0	2.0	8.0
Central bank	0.3	0.5	0.9	0.5	3.0	0.3	0.1	0.5
Corporate	4.0	8.0	14.0	8.0	48.0	4.0	2.0	8.0
Corporate pension fund	0.3	0.5	0.9	0.5	3.0	0.3	0.1	0.5
Employee savings plan	1.0	2.0	3.5	2.0	12.0	1.0	0.5	2.0
Institutional	2.5	5.0	8.8	5.0	30.0	2.5	1.3	5.0
Insurance	2.5	5.0	8.8	5.0	30.0	2.5	1.3	5.0
Other	1.8	3.5	6.1	3.5	21.0	1.8	0.9	3.5
Retail	1.0	2.0	3.5	2.0	12.0	1.0	0.5	2.0
Sovereign	4.0	8.0	14.0	8.0	48.0	4.0	2.0	8.0
Third-party distributor	1.8	3.5	6.1	3.5	21.0	1.8	0.9	3.5
Total	1.8	3.5	6.1	3.5	21.0	1.8	0.9	3.5

Table 10: Redemption shocks in % computed with the rule of thumb (11)

	(1)	(2)	(3)	(4)	(5)	(6)	(7)	(8)
Auto-consumption	3.0	6.0	10.0	6.0	40.0	3.0	1.0	7.0
Central bank	0.4	0.8	1.3	0.8	5.0	0.4	0.1	0.9
Corporate	3.0	6.0	10.0	6.0	40.0	3.0	1.0	7.0
Corporate pension fund	0.4	0.8	1.3	0.8	5.0	0.4	0.1	0.9
Employee savings plan	0.8	1.5	2.5	1.5	10.0	0.8	0.3	1.8
Institutional	2.3	4.5	7.5	4.5	30.0	2.3	0.8	5.3
Insurance	2.3	4.5	7.5	4.5	30.0	2.3	0.8	5.3
Other	1.5	3.0	5.0	3.0	20.0	1.5	0.5	3.5
Retail	0.8	1.5	2.5	1.5	10.0	0.8	0.3	1.8
Sovereign	3.0	6.0	10.0	6.0	40.0	3.0	1.0	7.0
Third-party distributor	1.5	3.0	5.0	3.0	20.0	1.5	0.5	3.5
Total	1.5	3.0	5.0	3.0	20.0	1.5	0.5	3.5

Table 11: Redemption shocks in % computed with the rule of thumb (12)

	(1)	(2)	(3)	(4)	(5)	(6)	(7)	(8)
Auto-consumption	3.5	7.0	12.0	7.0	44.0	3.5	1.5	7.5
Central bank	0.3	0.6	1.1	0.6	4.0	0.3	0.1	0.7
Corporate	3.5	7.0	12.0	7.0	44.0	3.5	1.5	7.5
Corporate pension fund	0.3	0.6	1.1	0.6	4.0	0.3	0.1	0.7
Employee savings plan	0.9	1.8	3.0	1.8	11.0	0.9	0.4	1.9
Institutional	2.4	4.8	8.1	4.8	30.0	2.4	1.0	5.1
Insurance	2.4	4.8	8.1	4.8	30.0	2.4	1.0	5.1
Other	1.6	3.3	5.6	3.3	20.5	1.6	0.7	3.5
Retail	0.9	1.8	3.0	1.8	11.0	0.9	0.4	1.9
Sovereign	3.5	7.0	12.0	7.0	44.0	3.5	1.5	7.5
Third-party distributor	1.6	3.3	5.6	3.3	20.5	1.6	0.7	3.5
Total	1.6	3.3	5.6	3.3	20.5	1.6	0.7	3.5

(1) = balanced, (2) = bond, (3) = enhanced treasury, (4) = equity, (5) = money market, (6) = other, (7) = structured, (8) = total

3 The frequency-severity modeling approach

The direct computation of value-at-risk, conditional value-at-risk and other statistics from historical redemption rates is particularly problematic. Indeed, we observe a large proportion of zeros in the redemption rate database. On average, we have 68.9% of zeros, this proportion reaches 99.5% for some investors and it is more than 99.9% for some matrix cells. Therefore, the data of redemption rates are "*clumped-at-zero*", meaning that the redemption rate is a semi-continuous random variable, and not a continuous random variable (Min and Agresti, 2002). This discontinuity is a real problem when estimating the probability distribution **F**. This is why we consider that the redemption rate is not the right redemption risk factor. We prefer to assume that the redemption risk is driven by two dimensions or two risk factors:

1. the redemption frequency, which measures the occurrence $\mathcal{E}$ of the redemption;

2. the redemption severity $\mathcal{R}^\star$, which measures the amount of the redemption.

It is obvious that this modeling approach finds its root in other risk models that deal with extreme events or counting processes, such as operational and insurance risks (Roncalli, 2020).

3.1 Zero-inflated models

In the frequency-severity approach, we distinguish the redemption event $\mathcal{E}$ that indicates if there is a redemption, and the redemption amount $\mathcal{R}^\star$ that measures the redemption rate in case of a redemption. An example is provided in Figure 7. The probability to observe a redemption is equal to 5%, and in the case of a redemption, the amount can be 2%, 5%, 15% and 50%. It follows that the redemption rate is the convolution of two risk factors.

Figure 7: Zero-inflated modeling of the redemption risk
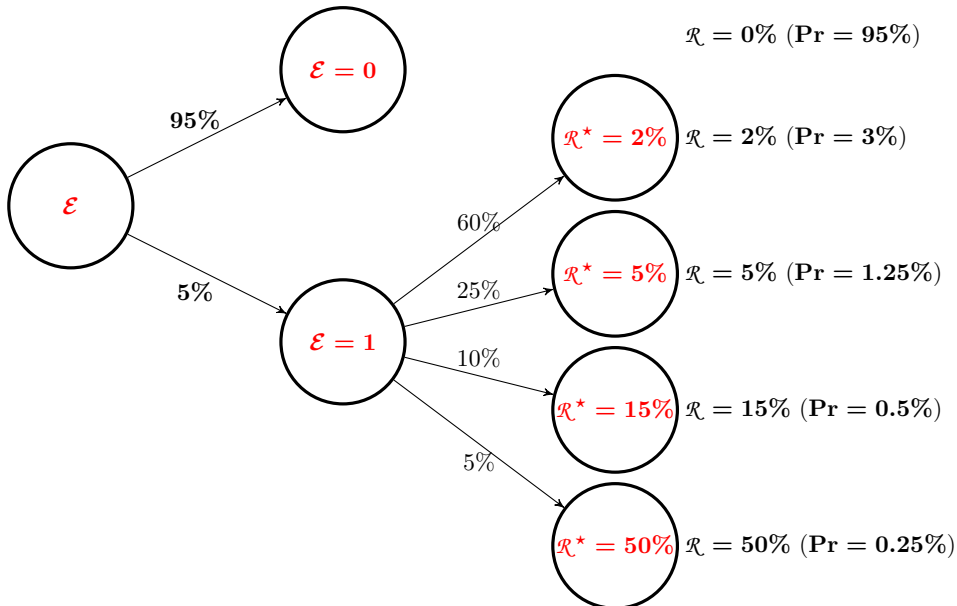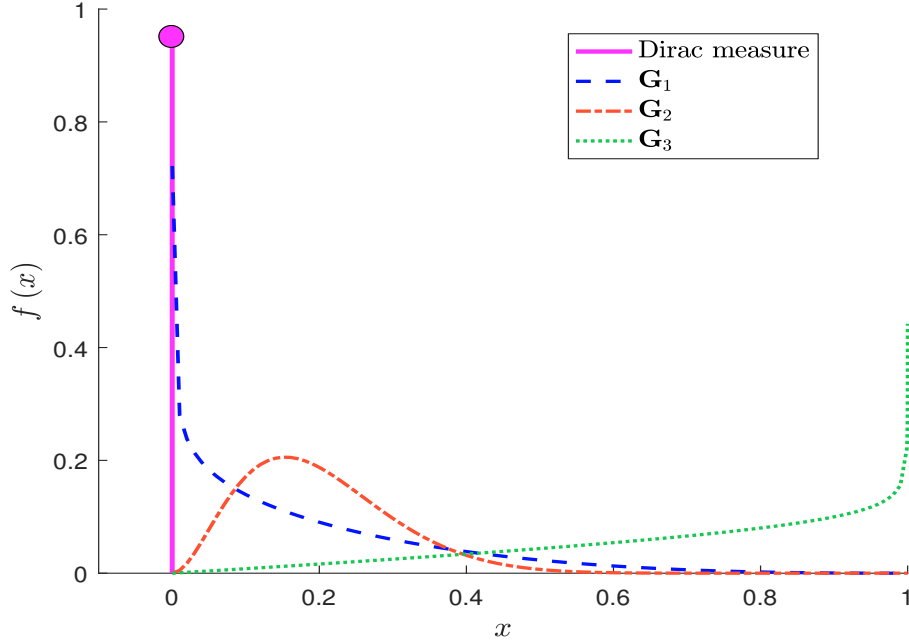
Figure 8: Zero-inflated probability density function

3.1.1 Zero-inflated probability distribution

We assume that the redemption event $\mathcal{E}$ follows a bernoulli distribution $\mathcal{B}(p)$, whereas the redemption severity[11] $\mathcal{R}^{\star}$ follows a continuous probability distribution $\mathbf{G}$. We have:

$$\Pr\{\mathcal{E} = 1\} = \Pr\{\mathcal{R} > 0\} = p$$

and:

$$\Pr\{\mathcal{R} \leq x \mid \mathcal{E} = 1\} = \mathbf{G}(x)$$

We deduce that the unconditional probability distribution of the redemption rate is given by:

$$
\begin{aligned}
\mathbf{F}(x) &= \Pr\{\mathcal{R} \leq x\} \\
&= \mathbb{1}\{x \geq 0\} \cdot (1-p) + \mathbb{1}\{x > 0\} \cdot p \cdot \mathbf{G}(x)
\end{aligned}
$$

Its density probability function is singular at $x = 0$:

$$f(x) = \begin{cases} 1 - p & \text{if } x = 0 \\ p \cdot g(x) & \text{otherwise} \end{cases}$$

where $g(x)$ is the density function of $\mathbf{G}$. Some examples are provided in Figure 8 when $p = 5\%$. We observe that the density function is composed of a dirac measure and a continuous function. In the case of $\mathbf{G}_1$, the distribution is right-skewed, meaning that the probability to observe small redemptions is high. In the case of $\mathbf{G}_2$, we have a bell curve, meaning that the redemption amount is located around the mean if there is a redemption. Finally, the distribution is left-skewed in the case of $\mathbf{G}_3$, meaning that the probability to observe high redemptions is high if there is of course a redemption, because we recall that the probability to observe a redemption is only equal to 5%.

---

[11]It is defined as the non-zero redemption rate.

From a probabilistic point of view, the redemption rate is then the product of the redemption event and the redemption severity:

$$\mathcal{R} = \mathcal{E} \cdot \mathcal{R}^{\star}$$

In Appendix A.2.1 on page 78, we show that:

$$\mathbb{E}[\mathcal{R}] = p\mathbb{E}[\mathcal{R}^{\star}] \tag{13}$$

and:

$$\sigma^2(\mathcal{R}) = p\sigma^2(\mathcal{R}^{\star}) + p(1-p)\mathbb{E}^2[\mathcal{R}^{\star}] \tag{14}$$

Moreover, the skewness coefficient is equal to:

$$\gamma_1(\mathcal{R}) = \frac{\vartheta_1(\mathcal{R}^{\star})}{\left(p\sigma^2(\mathcal{R}^{\star}) + p(1-p)\mathbb{E}^2[\mathcal{R}^{\star}]\right)^{3/2}} \tag{15}$$

where:

$$\vartheta_1(\mathcal{R}^{\star}) = p\gamma_1(\mathcal{R}^{\star})\sigma^3(\mathcal{R}^{\star}) + 3p(1-p)\sigma^2(\mathcal{R}^{\star})\mathbb{E}[\mathcal{R}^{\star}] + p(1-p)(1-2p)\mathbb{E}^3[\mathcal{R}^{\star}]$$

For the excess kurtosis coefficient, we obtain:

$$\gamma_2(\mathcal{R}) = \frac{\vartheta_2(\mathcal{R}^{\star})}{\left(p\sigma^2(\mathcal{R}^{\star}) + p(1-p)\mathbb{E}^2[\mathcal{R}^{\star}]\right)^2} \tag{16}$$

where:

$$\vartheta_2(\mathcal{R}^{\star}) = (p\gamma_2(\mathcal{R}^{\star}) + 3p(1-p))\sigma^4(\mathcal{R}^{\star}) + 4p(1-p)\gamma_1(\mathcal{R}^{\star})\sigma^3(\mathcal{R}^{\star})\mathbb{E}[\mathcal{R}^{\star}] + 6p(1-p)(1-2p)\sigma^2(\mathcal{R}^{\star})\mathbb{E}^2[\mathcal{R}^{\star}] + p(1-p)(1-6p+6p^2)\mathbb{E}^4[\mathcal{R}^{\star}]$$

In Figure 9 we have reported the moments of the redemption rate $\mathcal{R}$ by considering the following set of parameters:

#1 $\mathbb{E}[\mathcal{R}^{\star}] = 40\%$, $\sigma(\mathcal{R}^{\star}) = 20\%$, $\gamma_1(\mathcal{R}^{\star}) = 0$ and $\gamma_2(\mathcal{R}^{\star}) = 0$;

#2 $\mathbb{E}[\mathcal{R}^{\star}] = 20\%$, $\sigma(\mathcal{R}^{\star}) = 20\%$, $\gamma_1(\mathcal{R}^{\star}) = 0$ and $\gamma_2(\mathcal{R}^{\star}) = 0$;

#3 $\mathbb{E}[\mathcal{R}^{\star}] = 40\%$, $\sigma(\mathcal{R}^{\star}) = 40\%$, $\gamma_1(\mathcal{R}^{\star}) = -1$ and $\gamma_2(\mathcal{R}^{\star}) = 0$;

#4 $\mathbb{E}[\mathcal{R}^{\star}] = 40\%$, $\sigma(\mathcal{R}^{\star}) = 20\%$, $\gamma_1(\mathcal{R}^{\star}) = 0$ and $\gamma_2(\mathcal{R}^{\star}) = 1$.

We notice that the parameter values of $\mathcal{R}^{\star}$ have a major impact on the statistical moments, but the biggest effect comes from the frequency probability p. Indeed, we verify the following properties:

$$\begin{cases} \lim_{p \to 0^+} \mathbb{E}[\mathcal{R}] = \lim_{p \to 0^+} \sigma(\mathcal{R}) = 0 \\ \lim_{p \to 0^+} \gamma_1(\mathcal{R}) = \lim_{p \to 0^+} \gamma_2(\mathcal{R}) = \infty \end{cases} \tag{17}$$

This means that the redemption risk is very high for small frequency properties. In this case, the expected redemption rate and its standard deviation are very low, but skewness and kurtosis risk are very high! This creates a myopic situation where the asset manager may have the feeling that redemption risk is not a concern because of historical data. Indeed, when p is low, the probability of observing large redemption rates is small, implying that they are generally not observed in the database. For instance, let us consider two categories that have the same redemption severity distribution, but differ from their redemption frequency probability. One has a probability of 50%, the other has a probability of 1%. It is not obvious that the second category experienced sufficient severe redemption events such that the historical data are representative of the severity risk.

Figure 9: Statistical moments of the redemption rate $\mathcal{R}$ in zero-inflated models
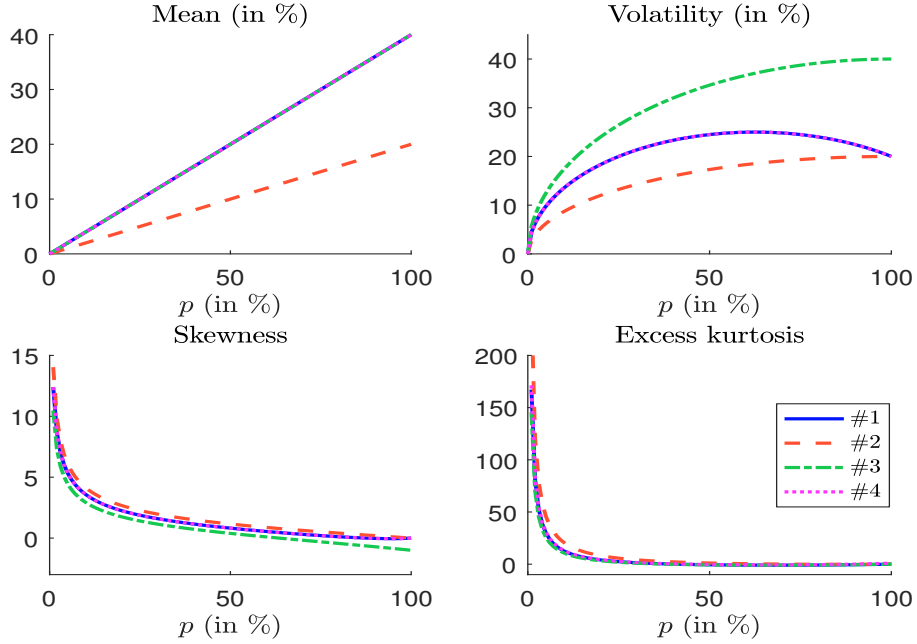
3.1.2 Statistical risk measures of the zero-inflated model

For the $\mathbb{M}$-measure, we have:

$$\mathbb{M} = p\mathbb{E}\left[\mathcal{R}^\star\right] \tag{18}$$

The formula of the value-at-risk is equal to:

$$\mathbb{Q}\left(\alpha\right) = \begin{cases} 0 & \text{if } p \leq 1 - \alpha \\ \mathbf{G}^{-1}\left(\dfrac{\alpha + p - 1}{p}\right) & \text{otherwise} \end{cases} \tag{19}$$

We notice that computing the quantile α of the unconditional distribution $\mathbf{F}$ is equivalent to compute the quantile $\alpha_{\mathbf{G}}$ of the severity distribution $\mathbf{G}$:

$$\alpha_{\mathbf{G}} = \max\left(0, \frac{\alpha + p - 1}{p}\right)$$

The relationship between p, α and $\alpha_{\mathbf{G}}$ is illustrated in Figure 39 on page 95. Let us focus on the 99% value-at-risk:

$$\mathbb{Q}\left(99\%\right) = \begin{cases} 0 & \text{if } p \leq 1\% \\ \mathbf{G}^{-1}\left(\dfrac{p - 1\%}{p}\right) & \text{otherwise} \end{cases}$$

If the redemption frequency probability is greater than 1%, the value-at-risk corresponds to the quantile $(p - 1\%)/p$. The relationship between p and $\alpha_{\mathbf{G}} = (p - 1\%)/p$ is shown in Figure 10. If p is greater than 20%, $\alpha_{\mathbf{G}}$ is greater than 95%. If p is less than 5%, we observe a high curvature of the relationship, implying that we face a high estimation risk. For instance, if p is equal to 1.5%, the 99% value-at-risk corresponds to the quantile 3.33% of the redemption severity. If p becomes 2.0%, the 99% value-at-risk is then equal to the

quantile 50% of the redemption severity! Therefore, there is a high sensitivity of the 99% value-at-risk when p is low, implying that a small error in the estimated value of p leads to a high impact on the value-at-risk.

Figure 10: Relationship between p and $\alpha_{\mathbf{G}}$ for the 99% value-at-risk
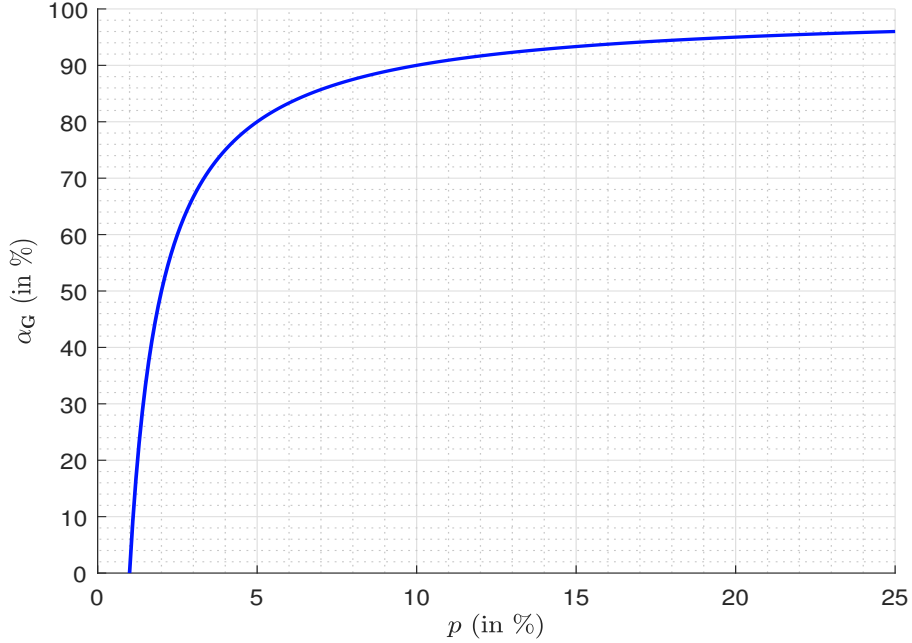
For the conditional value-at-risk, we obtain:

$$\mathbb{C}(\alpha) = \frac{1}{1-\alpha} \int_{\alpha}^{1} \mathbb{Q}(u) \, du \tag{20}$$

where $\mathbb{Q}(u)$ is the quantile function of $\mathcal{R}$ for the confidence level u. In the case where $p > 1 - \alpha$, we obtain:

$$\mathbb{C}(\alpha) = \frac{p}{1-\alpha} \int_{1-p^{-1}(1-\alpha)}^{1} \mathbf{G}^{-1}(u) \, du$$

Another expression of the conditional value-at-risk is:

$$\mathbb{C}(\alpha) = \frac{1}{1-\alpha} \int_{\mathbb{Q}(\alpha)}^{1} x \, d\mathbf{F}(x)$$

In the case where $p > 1 - \alpha$, we obtain:

$$\mathbb{C}(\alpha) = \frac{p}{1-\alpha} \int_{\mathbb{Q}(\alpha)}^{1} x g(x) \, dx$$

where $g(x)$ is the probability density function of $\mathbf{G}(x)$. All these formulas can be computed numerically thanks to Gauss-Legendre integration.

We now introduce a new risk measure which is very popular when considering parametric model. Roncalli (2020) defines the distribution-based (or parametric-based) stress scenario

$\mathbb{S}(\mathcal{T})$ for a given horizon time $\mathcal{T}$ such that the return time of this scenario is exactly equal to $\mathcal{T}$. From a mathematical point of view, we have:

$$\frac{1}{\Pr\{\mathcal{R} \geq \mathbb{S}(\mathcal{T})\}} = \mathcal{T}$$

$\Pr\{\mathcal{R} \geq \mathbb{S}(\mathcal{T})\}$ is the exceedance probability of the stress scenario, implying that the quantity $\Pr\{\mathcal{R} \geq \mathbb{S}(\mathcal{T})\}^{-1}$ is the return time of the exceedance event. For example, if we set $\mathbb{S}(\mathcal{T}) = \mathbb{Q}(\alpha)$, we have $\Pr\{\mathcal{R} \geq \mathbb{S}(\mathcal{T})\} = 1 - \alpha$ and $\mathcal{T} = (1 - \alpha)^{-1}$. The return time associated to a 99% value-at-risk is then equal to 100 days, the return time associated to a 99.9% value-at-risk is equal to $1\,000$ days (or approximately 4 years), etc. This parametric approach of stress testing is popular among professionals, regulators and academics when they use the extreme value theory for modeling the risk factors.

By combining the two definitions $\mathbb{S}(\mathcal{T}) = \mathbb{Q}(\alpha)$ and $\mathcal{T} = (1 - \alpha)^{-1}$, we obtain the mathematical expression of the parametric stress scenario:

$$\mathbb{S}(\mathcal{T}) = \mathbb{Q}\left(1 - \frac{1}{\mathcal{T}}\right) \tag{21}$$

If we consider the zero-inflated model, we deduce that:

$$\mathbb{S}(\mathcal{T}) = \begin{cases} 0 & \text{if } p \leq \mathcal{T}^{-1} \\ \mathbf{G}^{-1}\left(1 - \dfrac{1}{p\mathcal{T}}\right) & \text{otherwise} \end{cases} \tag{22}$$

The magnitude of $\mathcal{T}$ is the year, but the unit of $\mathcal{T}$ is the day. For example, since one year corresponds to 260 market days, the five-year stress scenario is equal to[12]:

$$\mathbb{S}(5) = \mathbf{G}^{-1}\left(1 - \frac{1}{1300\,p}\right)$$

3.1.3 The zero-inflated beta model

The choice of the severity distribution is an important issue. Since $\mathcal{R}^{\star}$ is a random variable between 0 and 1, it is natural to use the two-parameter beta distribution $\mathcal{B}(a, b)$. We have:

$$\mathbf{G}(x) = \mathfrak{B}(x; a, b)$$

where $\mathfrak{B}(x; a, b)$ is the incomplete beta function. The corresponding probability density function is equal to:

$$g(x) = \frac{x^{a-1}(1-x)^{b-1}}{\mathfrak{B}(a, b)}$$

where $\mathfrak{B}(a, b)$ is the beta function:

$$\mathfrak{B}(a, b) = \frac{\Gamma(a)\Gamma(b)}{\Gamma(a+b)}$$

Concerning the statistical moments, the formulas are given in Appendix A.2.2 on page 81.

We report some examples of density function in Figure 11. Instead of providing the parameters a and b, we have indicated the value μ and σ of the mean and the volatility. The first distribution is skewed, because the volatility is high compared to the mean. The other three distributions have a mode. Figure 12 shows the corresponding statistical moments of

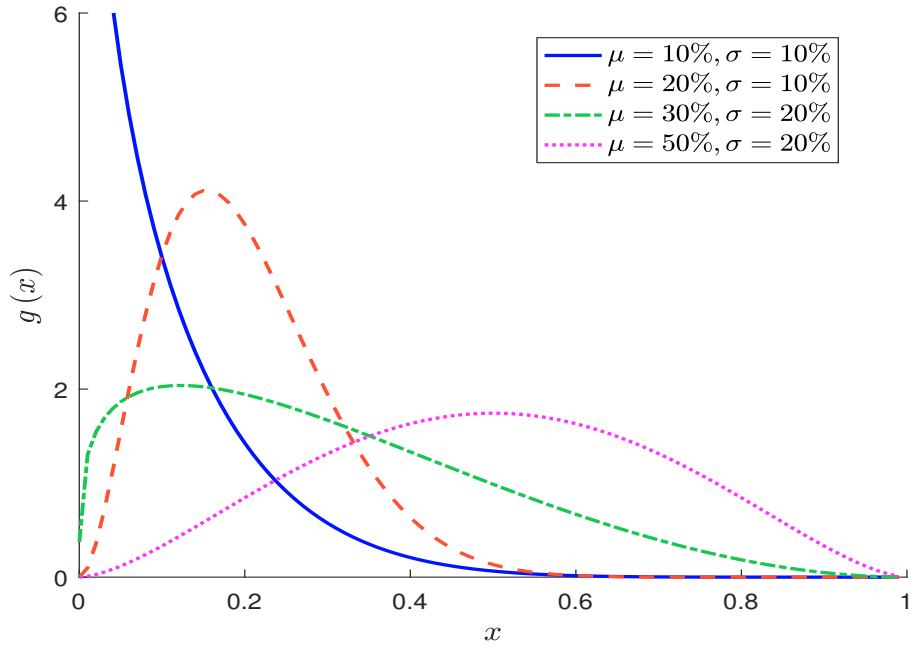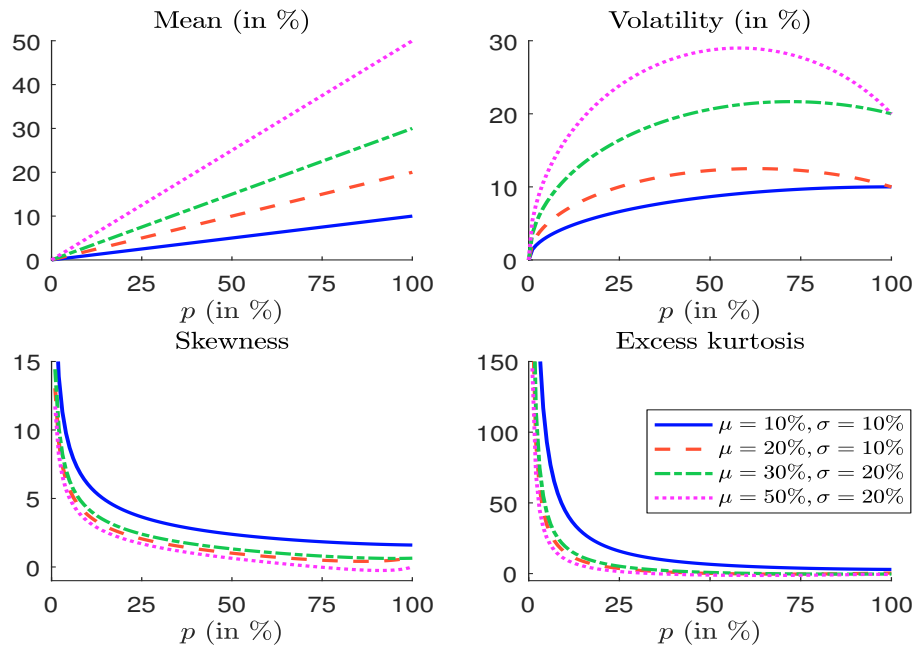Figure 11: Density function of the beta distribution

Figure 12: Statistical moments of the zero-inflated beta distribution

the associated zero-inflated model. We notice that the first and third distributions have the largest skewness and kurtosis.

In Figure 13, we report the 99% value-at-risk of the redemption rate. As explained before, the $\mathbb{Q}$-measure highly depends on the redemption frequency p. Again, we observe that the sensitivity of the value-at-risk is particularly important when p is small[13]. The ratio between the 99% conditional value-at-risk and the 99% value-at-risk is given in Figure 14. When the redemption frequency p is high, the ratio is less than 1.5 and we retrieve the typical figures that we observe for market and credit risks[14]. When the redemption frequency p is small, the ratio may be greater than 2.0. These results shows that the sensitivity to redemption risk is very high when the observed redemption frequency is low. The stress scenarios $\mathbb{S}(\mathcal{T})$ are given in Figure 15 when the redemption frequency p is equal to 1%. By definition, $\mathbb{S}(\mathcal{T})$ increases with the return time $\mathcal{T}$. From a theoretical point of view, the limit of the stress scenario is 100%:

$$\lim_{\mathcal{T} \to \infty} \mathbb{S}(\mathcal{T}) = \lim_{\mathcal{T} \to \infty} \mathbf{G}^{-1}\left(1 - \frac{1}{p\mathcal{T}}\right) = 1$$

However, we observe that stress scenarios reach a plateau at five years, meaning that stress scenarios beyond 5 years have no interest. This is true for small values of p, but it is even more the case for larger values of p as shown in Figures 40 and 41 on page 96.

Figure 13: $\mathbb{Q}(99\%)$-measure in % with respect to the redemption frequency
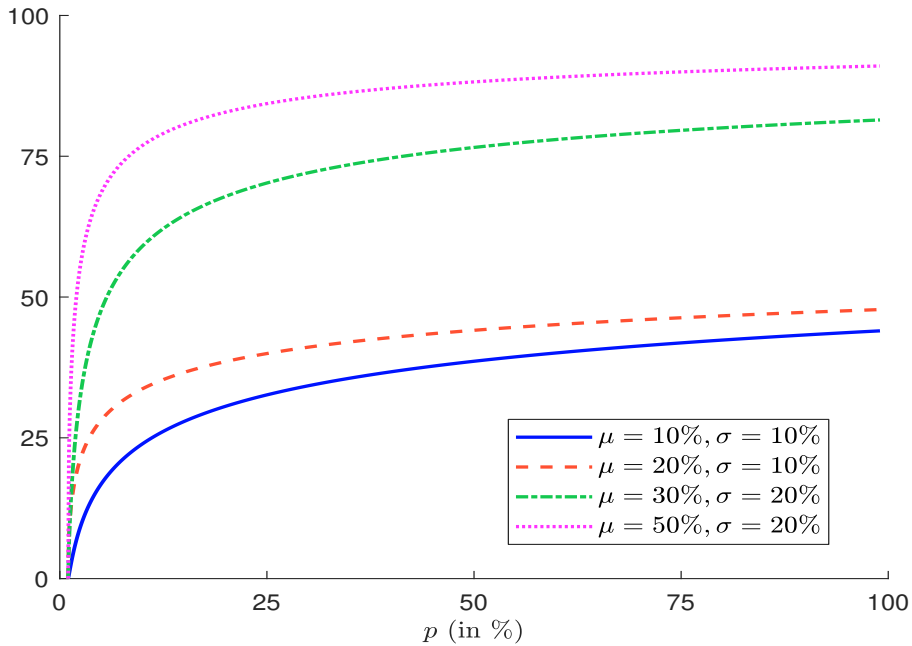
Remark 5 *In order to better understand the use of the $\mathbb{C}$-measure as a stress scenario, we compute the implied return time such that the stress scenario is exactly equal to the*

---

[12]We assume that the redemption frequency is greater than $1/1300$ or 7.69 bps. Otherwise, the quantile is equal to zero.

[13]Because of the impact of p on the confidence level $\alpha_{\mathbf{G}}$ — see Figure 10 on page 28.

[14]When p tends to one, the ratio is respectively equal to 1.15, 1.09, 1.06 and 1.03 for the four probability distributions of the redemption severity.

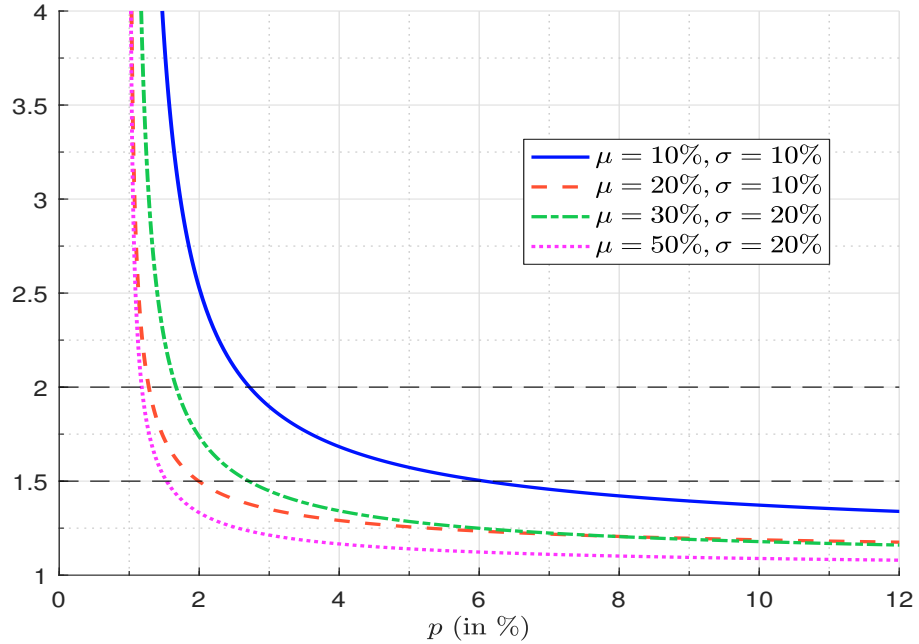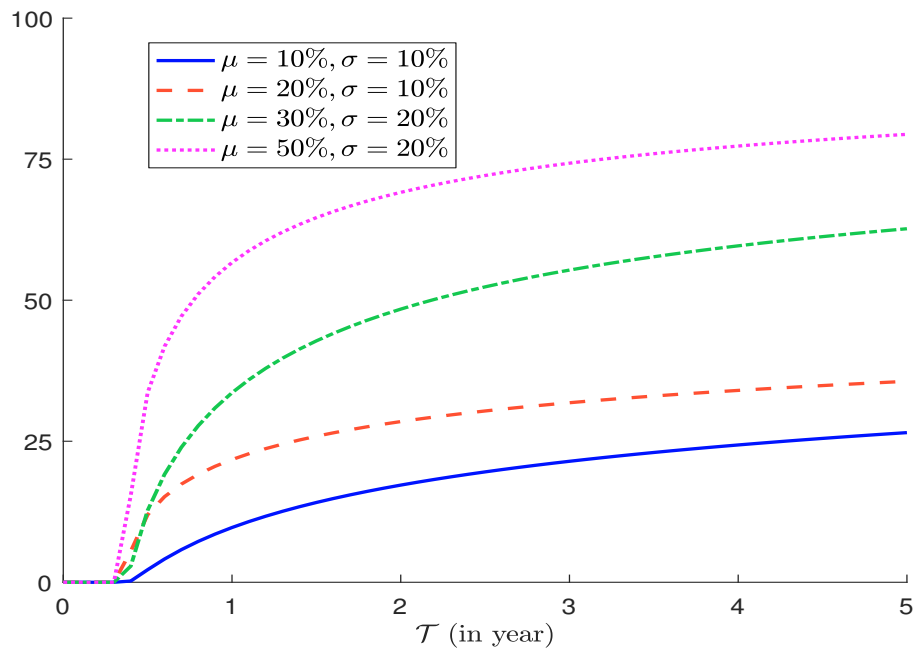Figure 14: Ratio $\mathbb{R}\,(99\%)$ with respect to the redemption frequency

Figure 15: Stress scenario $\mathbb{S}\,(\mathcal{T})$ in % ($p = 1\%$)

conditional value-at-risk:

$$\mathcal{T}_{\mathbb{C}(\alpha)} = \{\mathcal{T} : \mathbb{S}(\mathcal{T}) = \mathbb{C}(\alpha)\}$$

Results are given in Table 12. We notice that the value is between 0.77 and 1.03. On average, we can consider that the return time of the 99% conditional value-at-risk is about one year. This is 2.6 times the return time of the 99% value-at-risk[15].

Table 12: Implied return time $\mathcal{T}_{\mathbb{C}(99\%)}$ in year

	μ	10%	20%	30%	50%
	σ	10%	10%	20%	20%
	1%	1.03	0.86	0.87	0.77
	2%	1.00	0.94	0.89	0.85
	3%	0.99	0.95	0.90	0.86
p	5%	0.99	0.97	0.90	0.87
	10%	0.99	0.98	0.90	0.88
	50%	0.98	0.99	0.91	0.89
	99%	0.98	0.99	0.91	0.89

3.1.4 Extension to other probability distributions

The choice of the beta distribution is natural since the support is $[0, 1]$, but we can consider other continuous probability distributions for modeling $\mathcal{R}^\star$. For example, the Kumaraswamy distribution is another good candidate, but it is close to the beta distribution. When the support of the probability distribution is $[0, \infty)$, we apply the truncation formula[16]:

$$\mathbf{G}_{[0,1]}(x) = \frac{\mathbf{G}(x)}{\mathbf{G}(1)}$$

For instance, we can use the gamma or log-logistic distribution. However, our experience shows that some continuous probability distributions are not adapted such as the log-gamma and log-normal distributions, because the logarithm transform performs a bad scale for random variables in $[0, 1]$. Finally, we can also use the logit transformation, which is very popular for modeling the probability of default (PD) or the loss given default (LGD) in credit risk. Following Roncalli (2020, page 910), we assume that $\mathcal{R}^\star$ is a logit transformation of a random variable $X \in (-\infty, \infty)$, meaning that[17]:

$$X = \mathrm{logit}(\mathcal{R}^\star) = \ln\left(\frac{\mathcal{R}^\star}{1 - \mathcal{R}^\star}\right)$$

For instance, in the case of the logit-normal distribution, we have:

$$\mathrm{logit}(\mathcal{R}^\star) \sim \mathcal{N}(a, b^2)$$

---

[15]We recall that the return time of the 99% value-at-risk is equal to 100 market days or $\dfrac{100}{260} \approx 0.38$ years.

[16]For the probability density function, we have:

$$g_{[0,1]}(x) = \frac{g(x)}{\mathbf{G}(1)}$$

[17]We also have:

$$\mathcal{R}^\star = \mathrm{logit}^{-1}(X) = \frac{1}{1 + e^{-X}}$$

We deduce that:

$$
\begin{aligned}
\mathbf{G}\left(x\right) &= \Pr\left(\mathcal{R}^{\star} \leq x\right) \\
&= \Pr\left(X \leq \operatorname{logit}\left(x\right)\right) \\
&= \Phi\left(\frac{\operatorname{logit}\left(x\right) - a}{b}\right)
\end{aligned}
$$

and:

$$
g\left(x\right) = \frac{1}{bx\left(1 - x\right)}\phi\left(\frac{\operatorname{logit}\left(x\right) - a}{b}\right)
$$

A summary of these alternative approaches[18] is given in Table 13. In the sequel, we continue to use the beta distribution, because it is easy to calibrate and it is the most popular approach when modeling a random variable in $[0, 1]$. However, we cannot claim that it is the best fitting model. Such a debate has already taken place in operational risk with the log-normal distribution and the modeling of the severity distribution of operational risk losses (Roncalli, 2020). Nevertheless, we think that this debate is too early in the case of liability stress testing, and can wait when we will have more comprehensive redemption databases.

Table 13: List of continuous probability distributions

Distribution	Symbol	$\mathbf{G}\left(x\right)$	$g\left(x\right)$	Support
Beta	$\mathcal{B}\left(a, b\right)$	$\mathfrak{B}\left(x; a, b\right)$	$\dfrac{x^{a-1}\left(1 - x\right)^{b-1}}{\mathfrak{B}\left(a, b\right)}$	$[0, 1]$
Gamma	$\mathcal{G}\left(a, b\right)$	$\dfrac{\gamma\left(a, bx\right)}{\Gamma\left(a\right)}$	$\dfrac{b^{a} x^{a-1} e^{-bx}}{\Gamma\left(a\right)}$	$[0, \infty)$
Kumaraswamy	$\mathcal{K}\left(a, b\right)$	$1 - \left(1 - x^{a}\right)^{b}$	$abx^{a-1}\left(1 - x^{a}\right)^{b-1}$	$[0, 1]$
Log-logistic	$\mathcal{LL}\left(a, b\right)$	$\dfrac{x^{b}}{a^{b} + x^{b}}$	$\dfrac{b\left(x/a\right)^{b-1}}{a\left(1 + \left(x/a\right)^{b}\right)^{2}}$	$[0, \infty)$
Logit-normal	$\mathcal{LN}\left(a, b^{2}\right)$	$\Phi\left(\dfrac{\operatorname{logit}\left(x\right) - a}{b}\right)$	$\dfrac{1}{bx\left(1 - x\right)}\phi\left(\dfrac{\operatorname{logit}\left(x\right) - a}{b}\right)$	$[0, 1]$

3.2 Parametric stress scenarios

As explained previously, the zero-inflated beta model is appealing for producing stress scenarios. For that, we proceed in two steps. We first calibrate the parameters of the model, and then we compute the stress scenarios for a given return time.

3.2.1 Estimation of the zero-inflated beta model

Let $\Omega = \left\{\mathcal{R}_1, \ldots, \mathcal{R}_n\right\}$ be the sample of redemption rates for a given matrix cell. Three parameters have to be estimated: the redemption frequency p and the parameters a and b that control the shape of the beta distribution. We note n_0 as the number of observations that are equal to zero and $n_1 = n - n_0$ as the number of observations that are strictly positive[19]. In Appendix A.3 on page 81, we show that the maximum likelihood estimates are:

$$
\hat{p} = \frac{n_1}{n_0 + n_1}
$$

---

[18]$\gamma\left(\alpha, x\right)$ is the lower incomplete gamma function.

[19]We have $n_0 = \sum_{i=1}^{n} \mathbb{1}\left\{\mathcal{R}_i = 0\right\} = n - n_1$ and $n_1 = \sum_{i=1}^{n} \mathbb{1}\left\{\mathcal{R}_i > 0\right\} = \sum_{i=1}^{n} \mathcal{E}_i$.

and:

$$\left\{\hat{a}, \hat{b}\right\} = \arg\max_{a,b} - n_1 \ln \mathfrak{B}(a,b) + \sum_{\mathcal{R}_i > 0} (a - 1) \ln \mathcal{R}_i + \sum_{\mathcal{R}_i > 0} (b - 1) \ln (1 - \mathcal{R}_i)$$

The estimates $\hat{a}$ and $\hat{b}$ can be found by numerical optimization.

This is the traditional approach for estimating a zero-inflated model. However, it is not convenient since the parameters $\left(\hat{p}, \hat{a}, \hat{b}\right)$ should be modified by risk managers and business experts before computing redemption shocks. Indeed, the calibration process of parametric stress scenarios follows the same process when one builds historical stress scenarios, and estimated values $\left(\hat{p}, \hat{a}, \hat{b}\right)$ cannot be directly used because they do not necessarily respect some risk coherency principles and their robustness varies across matrix cells.

A second approach consists in using the method of moments. In this case, the estimator of p has the same expression:

$$\hat{p} = \frac{n_1}{n_0 + n_1} \tag{23}$$

For the parameters of the beta distribution, we first calculate the empirical mean $\hat{\mu}$ and the standard deviation $\hat{\sigma}$ of the positive redemption rates $\mathcal{R}^{\star}$, and then we use the following relationships (Roncalli, 2020, page 193):

$$\hat{a} = \frac{\hat{\mu}^2 (1 - \hat{\mu})}{\hat{\sigma}^2} - \hat{\mu} \tag{24}$$

and:

$$\hat{b} = \frac{\hat{\mu} (1 - \hat{\mu})^2}{\sigma^2} - (1 - \hat{\mu}) \tag{25}$$

The differences between the two methods are the following:

- In the case of the method of maximum likelihood, a and b are explicit parameters. Once the parameters p, a and b are estimated, we can calculate the mean μ and standard deviation σ for the severity distribution. In this approach, μ and σ are implicit, because they are deduced from a and b.

- In the case of the method of moments, a and b are implicit parameters. Indeed, they are calculated after having estimated the mean μ and standard deviation σ for the severity distribution. In this approach, μ and σ are explicit and define the severity distribution.

The first approach is known as the $p - a - b$ parameterization, whereas the second approach corresponds to the $p - \mu - \sigma$ parameterization. By construction, this last approach is more convenient in a liquidity stress testing framework, because the parameters μ and σ are intuitive and self-explanatory measures, which is not the case of a and b. Therefore, they can be manipulated by risk managers and business experts.

We have estimated the parameters p, a, b, μ and σ with the two methods. Table 14 shows the redemption frequency. On average, $\hat{p}$ is equal to 31%, but we observe large differences between the matrix cells. For instance, $\hat{p}$ is less than 5% for central banks, corporate pension funds and employee savings plans, whereas the largest values of $\hat{p}$ are observed for retail investors and third-party distributors. The values of $\hat{\mu}$ and $\hat{\sigma}$ are reported in Tables 15 and 16. The average redemption severity is 0.72%, whereas the redemption volatility is 4.55%. Again, we observe some large differences between the matrix cells.

Remark 6 *In Tables 42 and 43 on page 97, we have also reported the implicit values of $\hat{a}$ and $\hat{b}$ that are deduced from $\hat{\mu}$ and $\hat{\sigma}$. Moreover, we have reported the estimated values by the method of maximum likelihood on pages 98 and 99.*

Table 14: Estimated value of p in %

	(1)	(2)	(3)	(4)	(5)	(6)	(7)	(8)
Auto-consumption	21.63	19.41	30.00	25.46	50.60	6.39		22.16
Central bank	0.16	0.34			1.47			0.47
Corporate	15.04	6.19	6.25	2.87	39.81	0.21		14.54
Corporate pension fund	8.11	3.38	3.98	3.37	7.57	0.00		4.12
Employee savings plan	2.67	2.83	2.97	2.71	2.29		2.75	2.69
Institutional	19.36	6.28	1.96	6.51	32.83	1.04		8.23
Insurance	12.19	6.72	3.45	7.22	27.92	1.04		9.71
Other	9.67	3.87	3.68	19.35	21.52	2.22		8.82
Retail	44.59	45.04	58.76	70.50	45.75	17.51	27.32	45.61
Sovereign	16.30	3.18	1.05	10.07	18.23	0.06		10.14
Third-party distributor	33.77	37.36	45.97	45.94	65.94	32.86	6.52	40.61
Total	34.66	27.10	24.19	38.34	37.57	11.14	24.79	31.11

Table 15: Estimated value of μ in % (method of moments)

	(1)	(2)	(3)	(4)	(5)	(6)	(7)	(8)
Auto-consumption	1.24	1.88	2.15	1.19	3.11	2.81		1.70
Central bank								
Corporate	0.55	2.50			3.82			3.73
Corporate pension fund		1.54		2.84	7.26			3.21
Employee savings plan	1.29			2.08				2.10
Institutional	0.67	2.62		2.80	4.46			3.23
Insurance	1.36	2.20		2.19	3.21			2.66
Other	0.87	2.60		1.10	3.51	0.99		2.65
Retail	0.34	0.31	0.44	0.23	1.98	0.43	0.15	0.33
Sovereign	0.06			1.84	10.48			4.46
Third-party distributor	0.35	0.64	1.45	0.42	1.40	0.86	1.21	0.56
Total	0.40	0.73	1.64	0.48	2.82	0.98	0.18	0.72

Table 16: Estimated value of σ in % (method of moments)

	(1)	(2)	(3)	(4)	(5)	(6)	(7)	(8)
Auto-consumption	7.38	6.86	9.73	5.98	8.80	9.10		7.09
Central bank								
Corporate	5.55	9.57			7.49			8.70
Corporate pension fund		10.36		13.51	13.14			12.09
Employee savings plan	3.26			8.40				8.61
Institutional	5.46	9.99		9.23	11.46			10.86
Insurance	8.66	10.56		10.11	8.13			9.35
Other	3.61	9.36		7.27	11.88	6.70		10.68
Retail	2.80	2.58	3.32	2.10	7.52	3.22	2.64	2.88
Sovereign	0.25			9.90	21.63			14.94
Third-party distributor	2.68	3.48	7.63	2.58	4.71	5.84	6.98	3.37
Total	3.31	4.35	8.93	3.50	8.66	6.08	3.03	4.55

(1) = balanced, (2) = bond, (3) = enhanced treasury, (4) = equity, (5) = money market, (6) = other, (7) = structured, (8) = total

3.2.2 Stress scenarios based on the $p - \mu - \sigma$ parameterization

Using the previous estimates $(\hat{p}, \hat{\mu}, \hat{\sigma})$, risk managers and business experts can define the triplet (p, μ, σ) for the different matrix cells. For that, they must assess the confidence in estimated values with respect to the number of observations. For the frequency parameter, we use the value of n, which has been already reported in Table 8 on page 21. For the severity parameters $\hat{\mu}$ and $\hat{\sigma}$, we use the value of n_1, which is much smaller than n. Using the data given in Table 41 on page 93, we have built the confidence measure in Table 17. We confirm that the confidence measure in $\hat{\mu}$ and $\hat{\sigma}$ is lower than the confidence measure in $\hat{p}$. In particular, there are many matrix cells, where the number n_1 of observations is lower than 200. This explains why Tables 15 and 16 contain a lot of missing values. Therefore, except for a few matrix cells, the estimated values $\hat{\mu}$ and $\hat{\sigma}$ must be challenged by risk managers and business experts. Again, they can use risk coherency principles[20] $\mathcal{C}_{\text{investor}}$ and $\mathcal{C}_{\text{fund}}$ to build their own figures of p, μ and σ.

Table 17: Confidence in estimated values $\hat{\mu}$ and $\hat{\sigma}$ with respect to the number n_1 of observations

|	(1)	(2)	(3)	(4)	(5)	(6)	(7)
Auto-consumption	●●	●●	●●	●●●	●●	●	○○○
Central bank	○○○	○○○	○○○	○○○	○○○	○○○	○○○
Corporate	●	●	○	○	●●	○○○	○○○
Corporate pension fund	○	●	○○	●	●	○○○	○○○
Employee savings plan	●	○	○○	●	○	○○○	○
Institutional	●●	●●	○	●●	●●	○	○○○
Insurance	●	●	○	●●	●●	○	○○○
Other	●	●	○	●	●●	●	○○○
Retail	●●●	●●●	●●	●●●	●●	●●	●●●
Sovereign	●	○	○○○	●	●	○○○	○○○
Third-party distributor	●●●	●●●	●●	●●●	●●	●●	●

○○○ $0 - 10$, ○○ $11 - 50$, ○ $51 - 200$, ● $201 - 1\,000$, ●● $1\,001 - 10\,000$, ●●● $+10\,000$

Once the triplet (p, μ, σ) is defined for each matrix cell, we compute stress scenarios using the following formula:

$$\mathbb{S}\left(\mathcal{T}; p, \mu, \sigma\right) = \mathcal{B}^{-1}\left(1 - \frac{1}{p\mathcal{T}}; \frac{\mu^2\left(1 - \mu\right)}{\sigma^2} - \mu, \frac{\mu\left(1 - \mu\right)^2}{\sigma^2} - \left(1 - \mu\right)\right)$$

where $\mathcal{B}^{-1}\left(\alpha; a, b\right)$ is the α-quantile of the beta distribution with parameters a and b. The parametric stress scenario $\mathbb{S}\left(\mathcal{T}; p, \mu, \sigma\right)$ depends on the return time $\mathcal{T}$ and the three parameters of the zero-inflated model. An example is provided in Figure 16. For each plot, we indicate the triplet (p, μ, σ). For instance, the first plot corresponds to the triplet $(2\%, 1\%, 2\%)$, meaning that the daily redemption frequency is 2%, the expected redemption severity is 1% and the redemption volatility is 2%. In particular, these plots illustrate the high impact of σ, which is the key parameter when computing parametric stress scenarios. The reason is that the parameters p and μ determine the mean $\mathbb{E}\left[\mathcal{R}\right]$, whereas the uncertainty around this number is mainly driven by the parameter σ. The redemption volatility controls then the shape of the probability distribution of the redemption rate (both the skewness and the kurtosis), implying that σ has a major impact on the stress scenario $\mathbb{S}\left(\mathcal{T}\right)$ when $\mathcal{T}$ is large.

---

[20]They are defined on page 20.

Figure 16: Parametric stress scenarios $\mathbb{S}\left(\mathcal{T}; p, \mu, \sigma\right)$ in %
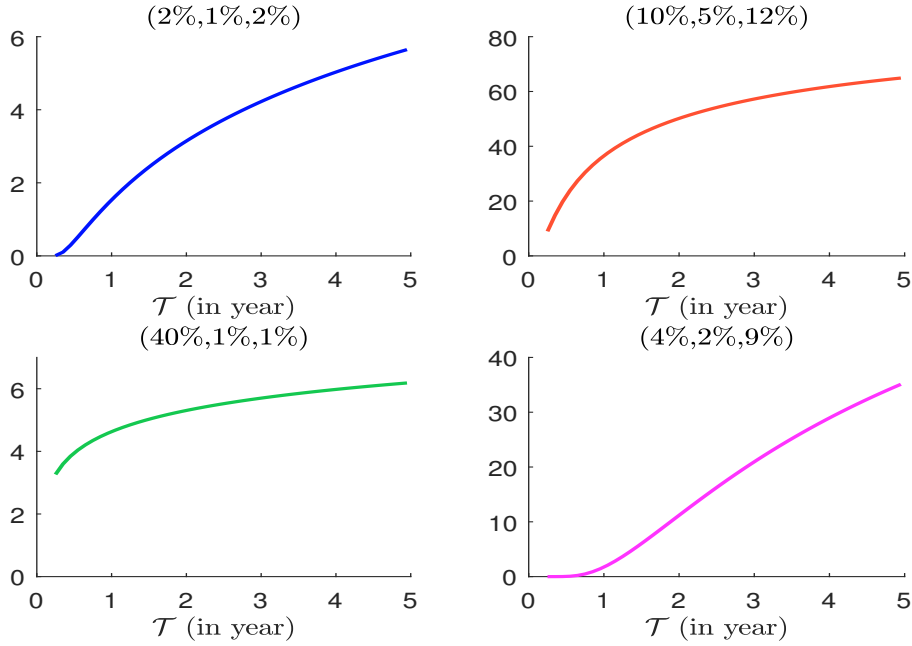
4 Behavioral modeling

In this section, we go beyond the zero-inflated model by considering the behavior of each investor. In particular, we show that the redemption rate depends on the liability structure of the mutual fund. Moreover, the behavior of investors may be correlated, in particular in a stress period. In this case, the modeling of spillover effects is important to define stress scenarios.

4.1 The individual-based model

The individual-based model and the zero-inflated model are highly connected. Indeed, the zero-inflated model can be seen as a special case of the individual-based model when we summarize the behavior of all unitholders by the behavior of a single client.

4.1.1 Definition

Let $\mathrm{TNA}\left(t\right)$ be the assets under management of an investment fund composed of n clients:

$$\mathrm{TNA}\left(t\right) = \sum_{i=1}^{n} \mathrm{TNA}_{i}\left(t\right)$$

where $\mathrm{TNA}_{i}\left(t\right)$ is the net asset of the individual i. The redemption rate of the fund is equal to the redemption flows divided by the total net assets:

$$
\begin{aligned}
\mathcal{R} &= \frac{\sum_{i=1}^{n} \mathrm{TNA}_{i} \cdot \mathcal{R}_{i}}{\mathrm{TNA}} \\
&= \sum_{i=1}^{n} \omega_{i} \cdot \mathcal{R}_{i}
\end{aligned}
$$

where ω_i represents the weight of the client i in the fund:

$$\omega_i = \frac{\text{TNA}_i}{\text{TNA}}$$

Since we have $\mathcal{R}_i = \mathcal{E}_i \cdot \mathcal{R}_i^\star$, we obtain:

$$\mathcal{R} = \sum_{i=1}^{n} \omega_i \cdot \mathcal{E}_i \cdot \mathcal{R}_i^\star$$

Generally, we assume that the clients are homogenous, meaning that $\mathcal{E}_i$ and $\mathcal{R}_i^\star$ are *iid* random variables. If we denote by $\tilde{p}$ and $\tilde{\mathbf{G}}$ the individual redemption probability and the individual severity distribution. The individual-based model is then characterized by the 4-tuple $\left(n, \omega, \tilde{p}, \tilde{\mathbf{G}}\right)$, where n is the number of clients and $\omega = (\omega_1, \ldots, \omega_n)$ is the vector of weights. Like the zero-inflated model, we consider a $\tilde{\mu} - \tilde{\sigma}$ parameterization of $\tilde{\mathbf{G}}$, meaning that the model is denoted by $\mathcal{IM}(n, \omega, \tilde{p}, \tilde{\mu}, \tilde{\sigma})$.

Remark 7 *When the individual severity distribution $\tilde{\mathbf{G}}$ is no specified, we assume that it is a beta distribution $\mathcal{B}\left(\tilde{a}, \tilde{b}\right)$, whose parameters $\tilde{a}$ and $\tilde{b}$ are calibrated with respect to the severity mean $\tilde{\mu}$ and the severity volatility $\tilde{\sigma}$ using the method of moments. In a similar way, we assume that the vector of weights is equally-weighted when it is not specified. In this case, the individual-based model is denoted by $\mathcal{IM}(n, \tilde{p}, \tilde{\mu}, \tilde{\sigma})$.*

Figure 17: Histogram of the redemption rate in % ($\tilde{p} = 50\%, \tilde{\mu} = 50\%, \tilde{\sigma} = 10\%$)
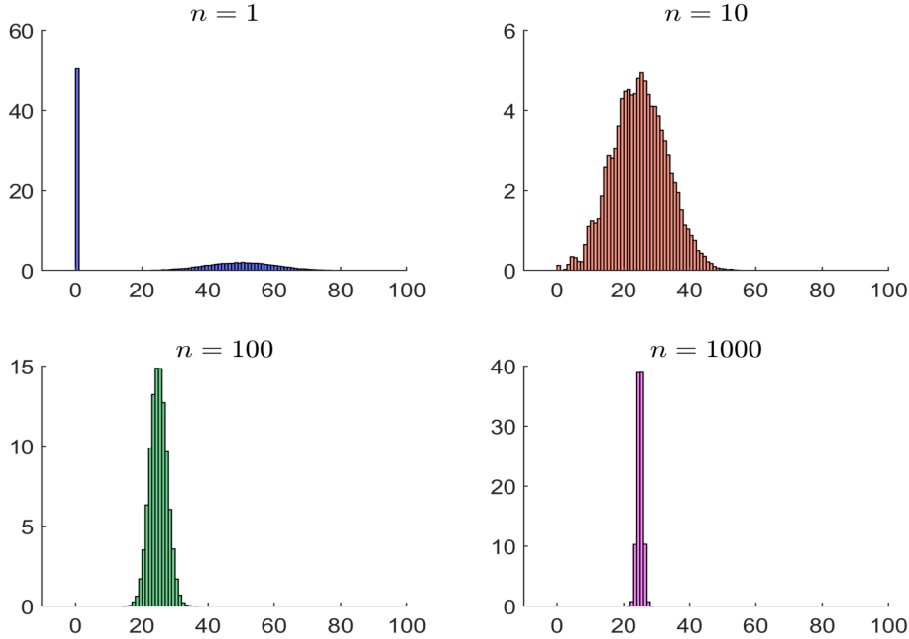
In Figure 17, we report the histogram of the redemption rate $\mathcal{R}$ in the case $\tilde{p} = 50\%$, $\tilde{\mu} = 50\%$ and $\tilde{\sigma} = 10\%$. In the case $n = 1$, we obtain a singular distribution. Indeed, there is a probability of 50% that there is no redemption. The singularity decreases with respect to the number n of investors, because the probability to have a redemption increases.

This is normal since the redemption frequency of a mutual fund depends on the number of unitholders. This explains that the redemption frequency is larger for a retail fund than for an institutional fund.

4.1.2 Statistical analysis

The skewness effect The singularity of the distribution function $\mathbf{F}$ at the point $\mathcal{R} = 0$ is entirely explained by the two parameters $\tilde{p}$ and n as shown in Appendix A.4.1 on page 83, because we have:

$$\Pr\{\mathcal{R} = 0\} = (1 - \tilde{p})^n$$

The fact that the probability distribution is not continuous has an impact on the skewness and the kurtosis. In Table 18, we have reported the probability $\Pr\{\mathcal{R} = 0\}$. If there is a few investors in the fund, the probability to observe no redemption in the fund is high. For instance, if $\tilde{p} = 5\%$ and $n = 10$, we have $\Pr\{\mathcal{R} = 0\} = 59.87\%$. If $\tilde{p} = 1\%$ and $n = 10$, we have $\Pr\{\mathcal{R} = 0\} = 90.44\%$. How to interpret these results? Since $\tilde{p}$ is the individual redemption probability, $1/\tilde{p}$ is the return time of a redemption at the investor level. For example, $\tilde{p} = 5\%$ (resp. $\tilde{p} = 1\%$) means that investors redeem every 20 days (resp. 100 days) on average. At the fund level, the return time to observe a redemption is equal to $(1 - \Pr\{\mathcal{R} = 0\})^{-1}$. For instance, in the case $\tilde{p} = 5\%$ and $n = 10$, we observe a redemption two days per week in the fund on average[21]. This analysis may help to distinguish active and passive investors. In the case of passive investors when the redemption event occurs once a year or less, $\tilde{p}$ is less than 40 bps. In the case of active investors that redeem once a month, $\tilde{p}$ is greater than 5%. Therefore, the skewness effect depends if the fund has active investors or not, and if the fund is granular or not.

Table 18: Probability to observe no redemption $\Pr\{\mathcal{R} = 0\}$ in %

p (in %)	Number n of investors							
	1	2	5	10	50	100	1000	10000
0.01	99.99	99.98	99.95	99.90	99.50	99.00	90.48	36.79
0.02	99.98	99.96	99.90	99.80	99.00	98.02	81.87	13.53
0.05	99.95	99.90	99.75	99.50	97.53	95.12	60.65	0.67
0.10	99.90	99.80	99.50	99.00	95.12	90.48	36.77	0.00
0.20	99.80	99.60	99.00	98.02	90.47	81.86	13.51	0.00
0.50	99.50	99.00	97.52	95.11	77.83	60.58	0.67	0.00
1.00	99.00	98.01	95.10	90.44	60.50	36.60	0.00	0.00
2.00	98.00	96.04	90.39	81.71	36.42	13.26	0.00	0.00
5.00	95.00	90.25	77.38	59.87	7.69	0.59	0.00	0.00
10.00	90.00	81.00	59.05	34.87	0.52	0.00	0.00	0.00
25.00	75.00	56.25	23.73	5.63	0.00	0.00	0.00	0.00
50.00	50.00	25.00	3.13	0.10	0.00	0.00	0.00	0.00

The mean effect The mean shape is easy to understand since it is the product of the redemption probability and the mean of the redemption severity:

$$\mathbb{E}[\mathcal{R}] = \tilde{p}\tilde{\mu}$$

Curiously, it depends neither on the number of investors in the fund, nor on the liability structure (see Figure 18). Since $\tilde{\mu} \in [0, 1]$, we notice that $\mathbb{E}[\mathcal{R}] \leq \tilde{p}$, meaning that we must

---

[21]The exact value is equal to $1/(1 - 59.87\%) = 2.4919$.

observe very low values of the redemption mean. And we verify this property if we consider the results[22] given in Table 4 on page 18. If we consider all investor and fund categories, the mean is equal to 22 bps. The largest value is observed for the sovereign/money market category and is equal to 1.91%.

Figure 18: Mean of the redemption rate $\mathcal{R}$ in %
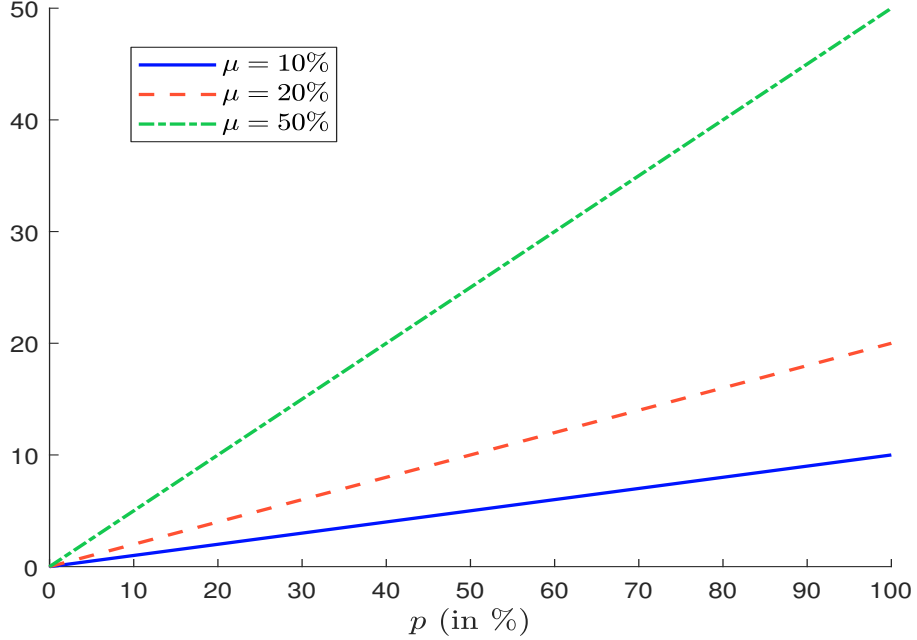
The volatility effect By assuming that the liability weights are equal ($\omega_i = 1/n$), the volatility of the redemption rate is equal to:

$$\sigma^2 \left(\mathcal{R} \right) = \frac{\tilde{p} \left(\tilde{\sigma}^2 + (1 - \tilde{p}) \, \tilde{\mu}^2 \right)}{n}$$

Globally, we observe that $\sigma^2 \left(\mathcal{R} \right)$ is an increasing function of $\tilde{p}$, $\tilde{\mu}$ and $\tilde{\sigma}$ as shown in Figure 19. When the redemption probability increases, we observe a convexity shape because we have:

$$\sigma^2 \left(\mathcal{R} \right) = \frac{\tilde{p} \left(\tilde{\sigma}^2 + \tilde{\mu}^2 \right)}{n} - \frac{\tilde{p}^2 \tilde{\mu}^2}{n}$$

However, this is not realistic since $\tilde{p} \leq 20\%$ in practice. Another interesting property is that $\sigma^2 \left(\mathcal{R} \right)$ tends to zero when the number of investors in the fund increases (Figure 20). If we compute the volatility of the redemption rate, we obtain the figures given in Table 48 on page 100. We observe that $\sigma \left(\mathcal{R} \right) \gg \mathbb{E} \left[\mathcal{R} \right]$, implying that $\mathcal{R}$ is a high-skewed random variable. This challenges the use of the $\mathbb{SD} \left(c \right)$ measure presented on page 16.

Correspondence between zero-inflated and individual-based models We notice that the zero-inflated model $\mathcal{ZI} \left(p, \mu, \sigma \right)$ is a special case of the individual-based model by

---

[22]Another way to compute the empirical mean of $\mathcal{R}$ is to calculate the product of the aggregate redemption frequency p (Table 14 on page 36) and the aggregate severity mean (Table 15 on page 36).

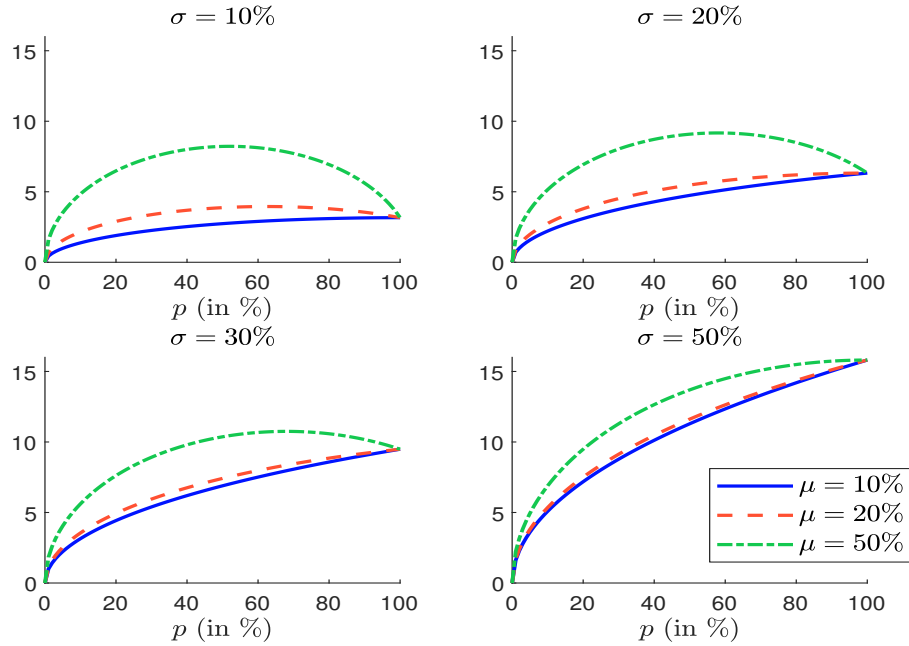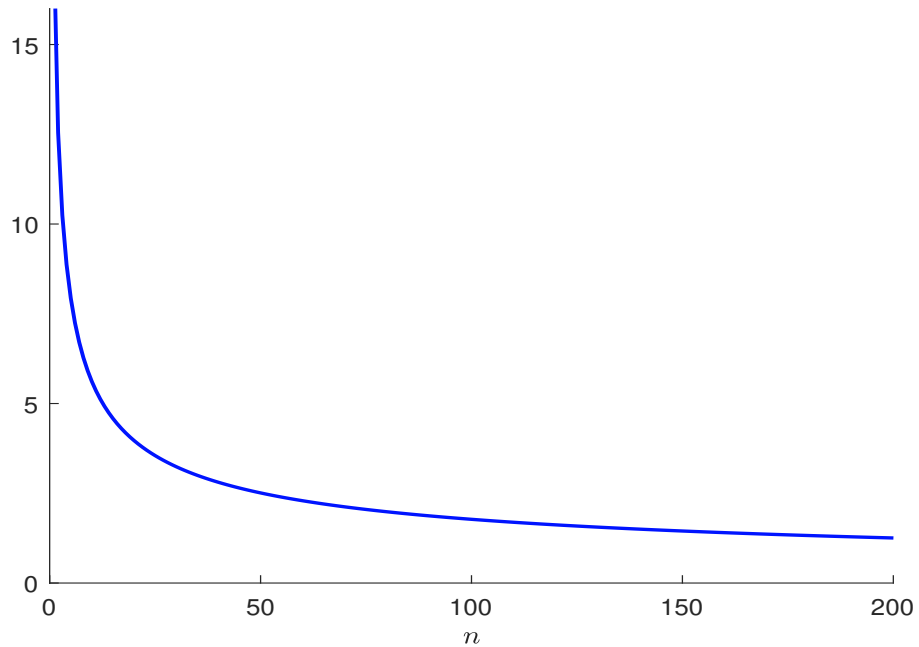Figure 19: Volatility of the redemption rate $\mathcal{R}$ in % ($n = 10$)

Figure 20: Volatility of the redemption rate $\mathcal{R}$ in % ($p = 10\%$, $\mu = 50\%$, $\sigma = 30\%$)

considering only one unitholder. Therefore, it is obvious that the zero-inflated model can not be seen as an explanatory model. It is a reduced-form model or a parametric model that can fit the data, but the interpretation of the $p - \mu - \sigma$ parameterization is not obvious, because $\mathcal{ZI}(p, \mu, \sigma)$ is an aggregate population model.

In this paragraph, we would like to find the relationships between the parameters of the zero-inflated model and those of the individual-based model, such that the two models are statistically equivalent:

$$\mathcal{ZI}(p, \mu, \sigma) \equiv \mathcal{IM}(n, \omega, \tilde{p}, \tilde{\mu}, \tilde{\sigma})$$

There are different approaches. A first one is to minimize the Kolmogorov-Smirnov statistics between $\mathcal{ZI}(p, \mu, \sigma)$ and $\mathcal{IM}(n, \omega, \tilde{p}, \tilde{\mu}, \tilde{\sigma})$. Another approach consists in matching their moments. We consider the second approach because we obtain analytical formulas, whereas the solution of the first approach can only be numerical. In Appendix A.5 on page 85, we show that:

$$p = 1 - (1 - \tilde{p})^n$$

and

$$\mu = \frac{\tilde{p}}{1 - (1 - \tilde{p})^n} \tilde{\mu}$$

whereas the parameter σ satisfies the following relationship:

$$
\begin{aligned}
\sigma^2 &= \left(\frac{\tilde{p} \mathcal{H}(\omega)}{1 - (1 - \tilde{p})^n} \right) \tilde{\sigma}^2 + \\
&\quad \left(\frac{\tilde{p}((1 - \tilde{p}) - (1 - \tilde{p})^n) \mathcal{H}(\omega) - \tilde{p}^2 (1 - \tilde{p})^n (1 - \mathcal{H}(\omega))}{(1 - (1 - \tilde{p})^n)^2} \right) \tilde{\mu}^2
\end{aligned}
$$

where $\mathcal{H}(\omega) = \sum_{i=1}^n \omega_i^2$ is the Herfindahl index. It is interesting to notice that p is a function of n and $\tilde{p}$, μ is a function of n, $\tilde{p}$ and $\tilde{\mu}$, but σ does not only depends on the parameters n, $\tilde{p}$, $\tilde{\mu}$ and $\tilde{\sigma}$:

$$
\begin{cases}
p = \varphi_1(n, \tilde{p}) \\
\mu = \varphi_2(n, \tilde{p}, \tilde{\mu}) \\
\sigma = \varphi_3(n, \tilde{p}, \tilde{\mu}, \tilde{\sigma}, \mathcal{H}(\omega))
\end{cases}
$$

Indeed, the aggregate severity volatility also depends on the Herfindahl index of the fund liability structure.

Remark 8 *The previous relationships can be inverted in order to define the parameters of the individual-based model with respect to the parameters of the zero-inflated model:*

$$
\begin{cases}
\tilde{p} = \varphi_1'(p; n) \\
\tilde{\mu} = \varphi_2'(p, \mu; n) \\
\tilde{\sigma} = \varphi_3'(p, \mu, \sigma; n, \mathcal{H}(\omega))
\end{cases}
$$

However, we notice that there are two degrees of freedom – n and $\mathcal{H}(\omega)$ – that must be fixed.

In Tables 19 and 20, we report some examples of calibration when n is equal to 10 and ω_i is equal to 10%. For instance, if the parameters of the individual-based model are $\tilde{p} = 1.00\%$, $\tilde{\mu} = 50\%$ and $\tilde{\sigma} = 10\%$, we obtain $p = 9.56\%$, $\mu = 5.23\%$ and $\sigma = 1.48\%$ for the zero-inflated model. If we know the weights of the investors in the investment fund, we can therefore calibrate the zero-inflated model from the individual-based model (Table 19), but also the individual-based model from the zero-inflated model (Table 20).

Table 19: Calibration of the zero-inflated model from the individual-based model

Parameter set	$\mathcal{IM}\,(n, \tilde{p}, \tilde{\mu}, \tilde{\sigma})$			$\mathcal{ZI}\,(p, \mu, \sigma)$		
	$\tilde{p}$	$\tilde{\mu}$	$\tilde{\sigma}$	p	μ	σ
#1	0.20%	50.00%	10.00%	1.98%	5.05%	1.11%
#2	1.00%	50.00%	10.00%	9.56%	5.23%	1.48%
#3	1.00%	30.00%	20.00%	9.56%	3.14%	2.14%

Table 20: Calibration of the individual-based model from the zero-inflated model

Parameter set	$\mathcal{ZI}\,(p, \mu, \sigma)$			$\mathcal{IM}\,(n, \tilde{p}, \tilde{\mu}, \tilde{\sigma})$		
	p	μ	σ	$\tilde{p}$	$\tilde{\mu}$	$\tilde{\sigma}$
#1	5.00%	2.00%	5.00%	0.51%	19.55%	49.34%
#2	10.00%	2.00%	5.00%	1.05%	19.08%	48.67%
#3	10.00%	5.00%	10.00%	1.05%	47.71%	97.14%

4.1.3 On the importance of the liability structure

We notice that the variance of the redemption rate depends on the Herfindahl index:

$$\mathcal{H}\,(\omega) = \sum_{i=1}^{n} \omega_i^2$$

This implies that the liability structure ω is an important parameter to understand the probability distribution of the redemption rate.

The arithmetics of the Herfindahl index We know that the Herfindahl index is bounded:

$$\frac{1}{n} \leq \mathcal{H}\,(\omega) \leq 1$$

$\mathcal{H}\,(\omega)$ is equal to one when one investor holds 100% of the investment fund ($\exists i : \omega_i = 1$), whereas the lower bound is reached for an equally-weighted liability structure ($\omega_i = n^{-1}$). Therefore, $\mathcal{H}\,(\omega)$ is a measure of concentration. A related statistic is the "*effective number of unitholders*":

$$\mathcal{N}\,(\omega) = \frac{1}{\mathcal{H}\,(\omega)}$$

$\mathcal{N}\,(\omega)$ indicates how many equivalent investors hold the investment fund. For instance, we consider two funds with the following liability structures $\omega^{(1)} = (25\%, 25\%, 25\%, 25\%)$ and $\omega^{(2)} = (42\%, 17\%, 15\%, 13\%, 9\%, 3\%, 1\%)$. Since we have $\mathcal{N}\,(\omega^{(1)}) = 4$ and $\mathcal{N}\,(\omega^{(2)}) = 3.94$, we may consider that the first fund is not more concentrated than the second fund even if the second fund has 7 unitholders.

We assume that the liability weights follow a geometric series with $\omega_i \propto q^i$ and $0 < q < 1$. We have[23]:

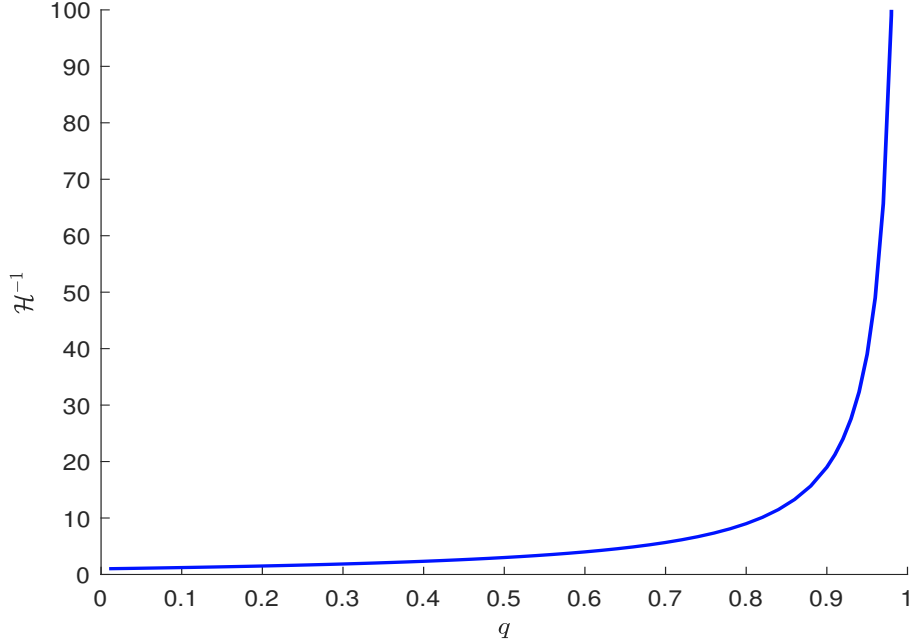$$\mathcal{N}\,(\omega) = \frac{1 - q^2}{(1 - q)^2}$$

---

[23] Because we have:

$$\mathcal{H}\,(\omega) = \frac{(1 - q)^2}{q^2} \sum_{i=1}^{\infty} q^{2i} = \frac{(1 - q)^2}{q^2} \frac{q^2}{(1 - q^2)} = \frac{(1 - q)^2}{1 - q^2}$$

As shown in Figure 21, we have an infinite number of unitholders, but a finite number of effective unitholders. For example, if $q \leq 0.98$, then $\mathcal{N}(\omega) < 100$.

Figure 21: Effective number of unitholders with a geometric liability structure $\omega_i \propto q^i$

Approximation of the probability distribution $\tilde{\mathbf{F}}(x \mid \omega)$ We recall that the unconditional probability distribution of the redemption rate is given by $\mathbf{F}(x) = \Pr\{\mathcal{R} \leq x\}$. Since the redemption rate depends on the liability structure ω in the individual-based model $\mathcal{IM}(n, \omega, \tilde{p}, \tilde{\mu}, \tilde{\sigma})$, we note $\tilde{\mathbf{F}}(x \mid \omega)$ the associated probability distribution:

$$\tilde{\mathbf{F}}(x \mid \omega) = \Pr\left\{\sum_{i=1}^{n} \omega_i \cdot \mathcal{E}_i \cdot \mathcal{R}_i^{\star} \leq x\right\}$$

We now consider the model $\mathcal{IM}(\mathcal{N}(\omega), \tilde{p}, \tilde{\mu}, \tilde{\sigma})$ and define $\tilde{\mathbf{F}}(x \mid \mathcal{H})$ as follows:

$$
\begin{aligned}
\tilde{\mathbf{F}}(x \mid \mathcal{H}) &= \Pr\left\{\frac{1}{\mathcal{N}(\omega)} \sum_{i=1}^{\mathcal{N}(\omega)} \mathcal{E}_i \cdot \mathcal{R}_i^{\star} \leq x\right\} \\
&= \Pr\left\{\mathcal{H}(\omega) \sum_{i=1}^{\mathcal{H}(\omega)^{-1}} \mathcal{E}_i \cdot \mathcal{R}_i^{\star} \leq x\right\}
\end{aligned}
$$

The issue is to know under which conditions we can approximate $\tilde{\mathbf{F}}(x \mid \omega)$ by $\tilde{\mathbf{F}}(x \mid \mathcal{H})$.

Let us consider some Monte Carlo experimentations. We assume that the liability weights are geometric distributed: $\omega_i \propto q^i$. In Figure 22, we compare the two probability distributions $\tilde{\mathbf{F}}(x \mid \omega)$ and $\tilde{\mathbf{F}}(x \mid \mathcal{H})$ for several sets of parameters[24] $(\tilde{p}, \tilde{\mu}, \tilde{\sigma})$. The weights ω_i for

---

[24] We recall that $\tilde{\mathbf{G}}$ is the beta distribution by default.

$q = 0.95$ are given in Figure 42 on page 100. We notice that the approximation of $\tilde{\mathbf{F}}\left(x \mid \omega\right)$ by $\tilde{\mathbf{F}}\left(x \mid \mathcal{H}\right)$ is good and satisfies the Kolmogorov-Smirnov test at the 99% confidence level. This is not the case if we assume that $q = 0.90$ or $q = 0.50$ (see Figures 43 and 44 on page 101).

Figure 22: Comparison of $\tilde{\mathbf{F}}\left(x \mid \omega\right)$ and $\tilde{\mathbf{F}}\left(x \mid \mathcal{H}\right)$ ($q = 0.95$ and $\mathcal{H}\left(\omega\right)^{-1} = 38$)
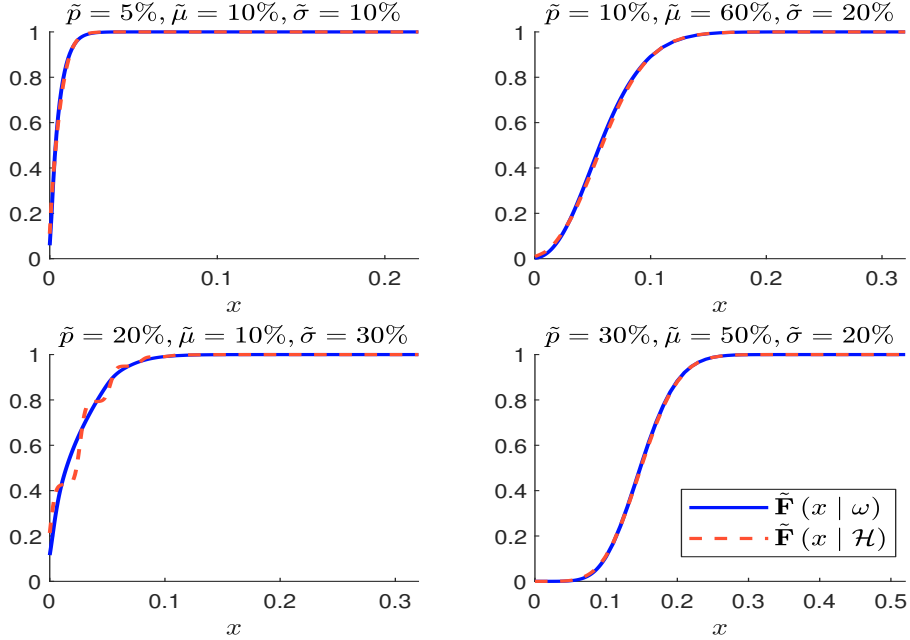
To better understand these results, we assume that $\tilde{p} = 0.3$, $\tilde{\mu} = 0.5$ and $\tilde{\sigma} = 0.4$. When q is equal to 0.50, the effective number of unitholders is low and is equal to 3. In this case, the probability distribution $\tilde{\mathbf{F}}\left(x \mid \mathcal{H}\right)$ is far from the probability distribution $\tilde{\mathbf{F}}\left(x \mid \omega\right)$ as shown in Figure 23. In fact, this case corresponds to an investment fund which is highly concentrated. The risk is then to observe redemptions from the largest unitholders. In particular, we notice that $\tilde{\mathbf{F}}\left(x \mid \mathcal{H}\right)$ presents some steps. The reason is that the redemption rate can be explained by the redemption of one unitholder, the redemption of two unitholders or the redemption of three unitholders. If we assume that q is equal to 0.90, the effective number of unitholders is larger and becomes 38. In this case, the probability distribution $\tilde{\mathbf{F}}\left(x \mid \mathcal{H}\right)$ is close to the probability distribution $\tilde{\mathbf{F}}\left(x \mid \omega\right)$, because the step effects disappear (see Figure 24). To summarize, the approximation of $\tilde{\mathbf{F}}\left(x \mid \omega\right)$ by $\tilde{\mathbf{F}}\left(x \mid \mathcal{H}\right)$ cannot be good when the effective number of unitholders (or $\mathcal{H}\left(\omega\right)^{-1}$) is low.

Remark 9 *In many cases, we don't know the comprehensive liability structure ω, but only the largest weights. In Appendix A.6 on page 86, we derive an upper bound $\mathcal{H}_m^+\left(\omega\right)$ of the Herfindahl index $\mathcal{H}\left(\omega\right)$ from the m largest weights. Therefore, we can deduce a lower bound of the effective number of unitholders:*

$$\mathcal{N}\left(\omega\right) > \mathcal{N}_m^-\left(\omega\right) = \frac{1}{\mathcal{H}_m^+\left(\omega\right)}$$

An example is provided in Table 21 when we assume that $\omega_i \propto q^i$. When the fund is highly concentrated, we obtain a good approximation of $\mathcal{N}\left(\omega\right)$ with the 10th or 20th largest

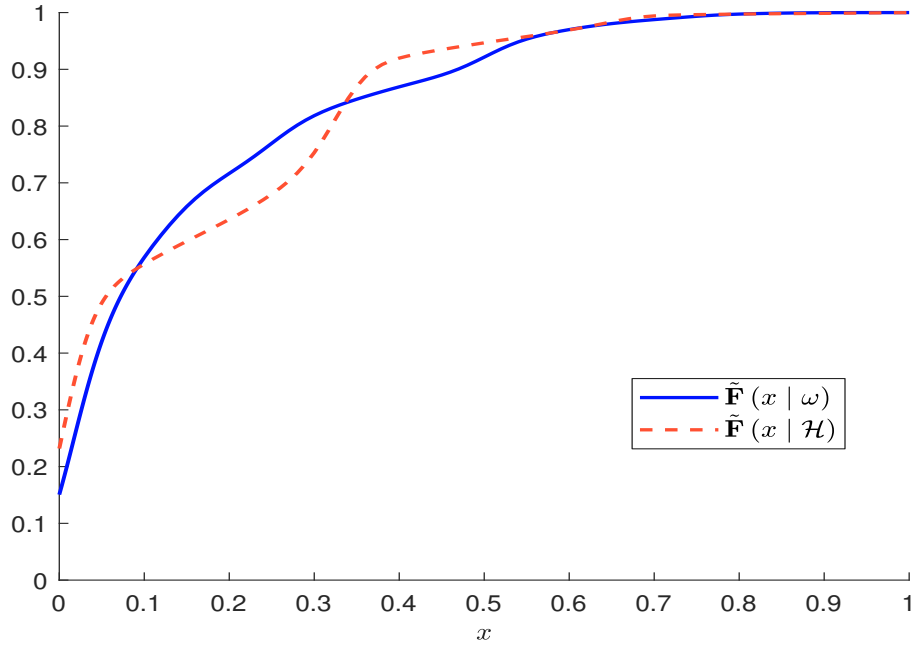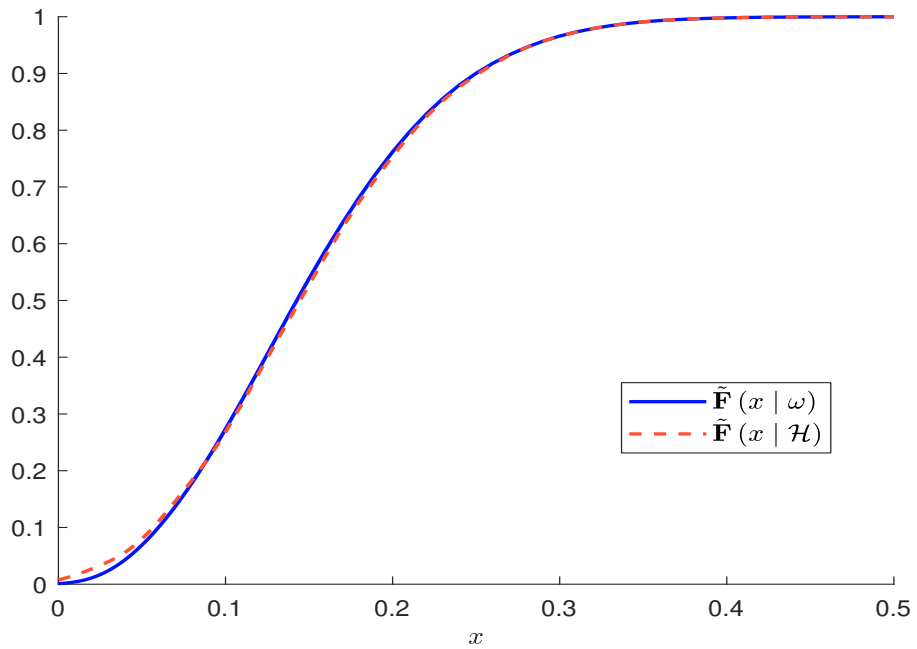Figure 23: The case $\mathcal{H}(\omega)^{-1} = 3$

Figure 24: The case $\mathcal{H}(\omega)^{-1} = 18$

unitholders. *Otherwise, $\mathcal{N}(\omega)$ is underestimated. However, this is not a real issue because we can think that generated stress scenarios will be overestimated. Indeed, using a lower value $\mathcal{N}(\omega)$ increases $\sigma(\mathcal{R})$ as shown in Figure 20 on page 42, implying that the redemption risk is generally overestimated.*

Table 21: Lower bound $\mathcal{N}_m^-(\omega)$ of the effective number of unitholders

m	$q = 0.50$	$q = 0.90$	$q = 0.95$	$q = 0.97$	$q = 0.99$	$q = 0.995$
5	3	14	24	37	104	204
10	3	17	28	42	109	209
20	3	19	34	50	119	219
50	3	19	39	63	145	248
∞	3	19	39	66	199	399

Stress scenarios based on the largest unitholders The previous results show that the main risk in a concentrated fund comes from the behavior of the largest unitholders. It justifies the use of stress scenarios based on the order statistics $\omega_{k:n}$:

$$\min \omega_i = \omega_{1:n} \leq \cdots \leq \omega_{k:n} \leq \omega_{k+1:n} \leq \cdots \leq \omega_{n:n} = \max \omega_i$$

Then, we can define the stress scenario that corresponds to the full redemption of the m largest unitholders:

$$\mathbb{S}(m) = \sum_{k=1}^{m} \omega_{n-k+1:n}$$

An example is given in Table 22 when the liability structure is defined by $\omega_i \propto q^i$. Of course, these stress scenarios $\mathbb{S}(m)$ make sense only if the fund presents some liability concentration. Otherwise, they are not informative.

Table 22: Stress scenarios $\mathbb{S}(m)$ when $\omega_i \propto q^i$

m	$q = 0.50$	$q = 0.90$	$q = 0.95$	$q = 0.97$	$q = 0.99$	$q = 0.995$
1	50.0%	10.0%	5.0%	3.0%	1.0%	0.5%
2	75.0%	19.0%	9.8%	5.9%	2.0%	1.0%
5	96.9%	41.0%	22.6%	14.1%	4.9%	2.5%
10	99.9%	65.1%	40.1%	26.3%	9.6%	4.9%

4.1.4   Calibration of stress scenarios

Using collective and mutual funds The calibration of the individual-based model is much more complicated than the calibration of the zero-inflated model. The reason is that it depends on the liability structure of the funds, which are not necessarily the same for the different funds. Let us consider the case of a single fund f. We can estimate the parameters $\tilde{p}$, $\tilde{\mu}$ and $\hat{\sigma}$ using the quadratic criterion:

$$\{\tilde{p}^{\star}, \tilde{\mu}^{\star}, \tilde{\sigma}^{\star}\} = \arg\min \varpi_{\tilde{p}} \left(\hat{p}_{(f)} - 1 + (1 - \tilde{p})^{\mathcal{H}_{(f)}^{-1}}\right)^2 + \varpi_{\tilde{\mu}} \left(\hat{p}_{(f)} \hat{\mu}_{(f)} - \tilde{p}\tilde{\mu}\right)^2 +$$
$$\varpi_{\tilde{\sigma}} \left(\hat{p}_{(f)} \left(\hat{\sigma}_{(f)}^2 + \left(1 - \hat{p}_{(f)}\right) \hat{\mu}_{(f)}^2\right) - \tilde{p}\left(\tilde{\sigma}^2 + (1 - \tilde{p})\tilde{\mu}^2\right) \mathcal{H}_{(f)}\right)^2 \quad (26)$$

where $\hat{p}_{(f)}$, $\hat{\mu}_{(f)}$ and $\hat{\sigma}_{(f)}$ are the empirical estimates of the parameters p, μ and σ, and $\mathcal{H}_{(f)}$ is the Herfindahl index associated with the fund. In practice, the liability structure changes every day, meaning that the Herfindahl index is time-varying. Therefore, we can use the average of Herfindahl indices. The weights $\varpi_{\tilde{p}}$, $\varpi_{\tilde{\mu}}$ and $\varpi_{\tilde{\sigma}}$ indicate the relative importance of each moment condition. If we consider several funds, the previous criterion becomes:

$$
\begin{aligned}
\{\tilde{p}^{\star}, \tilde{\mu}^{\star}, \tilde{\sigma}^{\star}\} \quad = \quad & \arg\min \varpi_{\tilde{p}} \sum_f \varpi_{(f)} \left(\hat{p}_{(f)} - 1 + (1 - \tilde{p})^{\mathcal{H}_{(f)}^{-1}} \right)^2 + \\
& \varpi_{\tilde{\mu}} \sum_f \varpi_{(f)} \left(\hat{p}_{(f)} \hat{\mu}_{(f)} - \tilde{p}\tilde{\mu} \right)^2 + \\
& \varpi_{\tilde{\sigma}} \sum_f \varpi_{(f)} \left(\hat{p}_{(f)} \left(\hat{\sigma}_{(f)}^2 + \left(1 - \hat{p}_{(f)}\right) \hat{\mu}_{(f)}^2 \right) - \tilde{p} \left(\tilde{\sigma}^2 + (1 - \tilde{p}) \tilde{\mu}^2 \right) \mathcal{H}_{(f)} \right)^2
\end{aligned}
\tag{27}
$$

where $\varpi_{(f)}$ is the relative weight of the fund f.

In practice, the estimates $\tilde{p}^{\star}$, $\tilde{\mu}^{\star}$ and $\tilde{\sigma}^{\star}$ are very sensitive to the Herfindahl index because of the first and third moment conditions. To illustrate this point, we consider the institutional category and we assume that there is only one fund. On page 36, we found that $\hat{p}_{(f)} = 8.23\%$, $\hat{\mu}_{(f)} = 3.23\%$ and $\hat{\sigma}_{(f)} = 10.86\%$. If $\mathcal{H}_{(f)} = 5$, we obtain $\tilde{p}^{\star} = 1.70\%$, $\tilde{\mu}^{\star} = 15.61\%$ and $\tilde{\sigma}^{\star} = 53.31\%$. If $\mathcal{H}_{(f)} = 20$, we obtain $\tilde{p}^{\star} = 0.43\%$, $\tilde{\mu}^{\star} = 62.04\%$ and $\tilde{\sigma}^{\star} = 212.48\%$. In the case of the retail category, we found that $\hat{p}_{(f)} = 45.61\%$, $\hat{\mu}_{(f)} = 0.33\%$ and $\hat{\sigma}_{(f)} = 2.88\%$. If $\mathcal{H}_{(f)} = 1\,000$, we obtain $\tilde{p}^{\star} = 0.06\%$, $\tilde{\mu}^{\star} = 247\%$ and $\tilde{\sigma}^{\star} = 2\,489\%$. If $\mathcal{H}_{(f)} = 10\,000$, we obtain $\tilde{p}^{\star} = 0.01\%$, $\tilde{\mu}^{\star} = 2\,472\%$ and $\tilde{\sigma}^{\star} = 24\,891\%$. These results are not realistic since $\tilde{\mu}^{\star} > 1$ and $\tilde{\sigma}^{\star} > 1$.

Using mandates and dedicated funds Collective investment and mutual funds are pooled investment vehicles, meaning that they are held by several investors. We now consider another type of funds with a single unitholder. They correspond to mandates and funds that are dedicated to a unique investor. In this case, the Herfindahl index is equal to one, and the solution of Problem (26) corresponds to the parameter set of the zero-inflated model:

$$
\left\{ \tilde{p}^{\star} = \hat{p}_{(f)}, \tilde{\mu}^{\star} = \hat{\mu}_{(f)}, \tilde{\sigma}^{\star} = \hat{\sigma}_{(f)} \right\}
$$

In our database, we can separate the observations between collective and mutual funds on one side and mandates and dedicated funds on the other side. In Tables 23, 24 and 25, we have estimated the parameters $\tilde{p}$, $\tilde{\mu}$ and $\tilde{\sigma}$ by only considering mandates and dedicated funds. These results highly differ than those obtained for collective and mutual funds (Tables 14, 15 and 16 on page 36). First, we can calibrate a smaller number of cells. Indeed, we recall that the estimates are not calculated if the number of observations is less than 200. Second, the magnitude of the estimates is very different. If we consider all fund and investor categories, we obtain $\tilde{p} = 3.34\%$, $\tilde{\mu} = 2.13\%$ and $\tilde{\sigma} = 10.27\%$, whereas we have previously found $p = 31.11\%$, $\mu = 0.72\%$ and $\sigma = 4.55\%$. As expected, we verify that $\tilde{p} \ll p$ and $\tilde{\sigma} \gg \tilde{\sigma}$ because of the following reasons:

- the redemption probability is larger in a collective fund than in a dedicated fund because they are several investors;

- the volatility of the redemption severity is smaller in a collective fund than in a dedicated fund because the behavior of the different investors is averaged, implying that the dispersion of redemption is reduced.

Table 23: Estimated value of $\tilde{p}$ in %

	(1)	(2)	(3)	(4)	(5)	(6)	(7)	(8)
Central bank	0.13	0.21		0.73	2.99			0.49
Corporate	0.49	1.14		0.13		0.57		0.71
Corporate pension fund	2.16	1.40		1.60	3.06	0.41	0.47	1.57
Institutional	1.47	1.35	0.41	2.13	1.65	0.40	0.00	1.46
Insurance	2.09	2.12		1.52	0.59	0.13		1.93
Sovereign	0.23	0.44		0.35	0.16	0.03		0.32
Third-party distributor	12.71	8.07	3.46	25.40	11.68	7.17		14.22
Total	3.95	2.63	1.73	5.82	2.92	0.68	7.46	3.34

Table 24: Estimated value of $\tilde{\mu}$ in %

	(1)	(2)	(3)	(4)	(5)	(6)	(7)	(8)
Central bank								
Corporate								
Corporate pension fund	4.39	2.94						4.11
Institutional	3.88	4.05		3.29				4.00
Insurance		3.46						4.23
Sovereign								
Third-party distributor	0.77	1.52		0.44				0.77
Total	1.89	2.47		1.48	2.64	3.91		2.13

Table 25: Estimated value of $\tilde{\sigma}$ in %

	(1)	(2)	(3)	(4)	(5)	(6)	(7)	(8)
Central bank								
Corporate								
Corporate pension fund	15.37	10.65						14.53
Institutional	16.42	13.88		12.30				14.64
Insurance		13.01						14.08
Sovereign								
Third-party distributor	5.28	5.84		3.29				4.65
Total	9.61	10.35		8.29	10.39	15.06		10.27

(1) = balanced, (2) = bond, (3) = enhanced treasury, (4) = equity, (5) = money market, (6) = other, (7) = structured, (8) = total

Curiously, we do not observe that $\tilde{\mu} \approx \mu$. One explanation may be that investors in mandates are not the same as investors in collective funds. Indeed, we may consider that they are more sophisticated and bigger when they are able to put in place a mandate or a dedicated fund. For instance, they can be more active.

The results obtained with data from mandates and dedicated funds are more realistic than those obtained with data from collective and mutual funds. The drawback is that they are based on a smaller number of observations and there are many cells where we don't have enough observations for computing the estimates. Therefore, these estimates must be completed by expert judgements.

Computing the stress scenarios Once we have estimated the parameters $\tilde{p}$, $\tilde{\mu}$ and $\tilde{\sigma}$, we can compute the stress scenarios using the Monte Carlo method. Nevertheless, we face an issue here, because the stress scenario is not unique to an investor category. Indeed, it depends on the liability structure of the fund. While the individual-based model is more realistic and relevant than the zero-inflated model, then it appears to be limited from a practical point of view. Nevertheless, it is useful to understand the importance of the liability structure on the redemption rate.

4.2 Correlation risk

4.2.1 Specification of the model

We now consider an extension of the previous model by introducing correlations between the investors. We obtain the same expression of the redemption rate:

$$\mathcal{R} = \sum_{i=1}^{n} \omega_i \cdot \mathcal{E}_i \cdot \mathcal{R}_i^{\star}$$

However, the random variables $(\mathcal{E}_1, \ldots, \mathcal{E}_n, \mathcal{R}_1^{\star}, \ldots, \mathcal{R}_n^{\star})$ are not necessarily independent. We discuss three different correlation patterns:

1. We can assume that $\mathcal{E}_i$ and $\mathcal{E}_j$ are correlated. This is the simplest and most understandable case. Indeed, we generally observe long periods with low redemption frequencies followed by short periods with high redemption frequencies, in particular when there is a crisis or a panic.

2. We can assume that the redemption severities $\mathcal{R}_i^{\star}$ and $\mathcal{R}_j^{\star}$ are correlated. For example, it would mean that high (resp. low) redemptions are observed at the same time. Nevertheless, this severity correlation is different from the previous frequency correlation. Indeed, the severities are independent from the number of redemptions, implying that the severity correlation only concerns the unitholders that have already decided to redeem.

3. We can assume that $\mathcal{E}_i$ and $\mathcal{R}_i^{\star}$ are correlated. We notice that we can write the redemption rate for a given category as follows:

$$\mathcal{R} = \sum_{i=1}^{n} \omega_i \cdot \mathcal{R}_i$$

where $\mathcal{R}_i = \mathcal{E}_i \cdot \mathcal{R}_i^{\star}$ is the individual redemption rate for the ith investor. The breakdown between the binary variable $\mathcal{E}_i$ and the continuous variable $\mathcal{R}_i^{\star}$ helps us to model the "*clumping-at-zero*" pattern. But there is no reason that the value taken by the redemption severity $\mathcal{R}_i^{\star}$ depends whether $\mathcal{E}_i$ takes the value 0 or 1, because $\mathcal{R}_i^{\star}$ is observed only if $\mathcal{E}_i = 1$.

Finally, only the first two correlation patterns are relevant from a financial point of view, because the third correlation model has no statistical meaning. Nevertheless, it is obvious that the first correlation model is more appropriate because the second correlation model confuses low-severity and high-severity regimes. During a liquidity crisis, both the redemption frequency and the redemption severity increase (Coval and Stafford, 2007; Duarte and Eisenbach, 2013; Kacperczyk and Schnabl, 2013; Roncalli and Weisang, 2015a; Schmidt *et al.*, 2016). The first effect may be obtained by stressing the parameter $\tilde{p}$ or by considering a high-frequency regime deduced from the first correlation model, but the second effect

can only be obtained by stressing the parameter $\tilde{\mu}$ and cannot be explained by the second correlation model. Therefore, we only consider the first correlation pattern by modeling the random vector $(\mathcal{E}_1, \ldots, \mathcal{E}_n)$ with a copula decomposition. We continue to assume that $\mathcal{E}_i \sim \mathcal{B}(\tilde{p})$ are identically distributed, but the dependence function of $(\mathcal{E}_1, \ldots, \mathcal{E}_n)$ is given by the copula function $\mathbf{C}(u_1, \ldots, u_n)$. The individual-based model is then a special case of this copula-based model when the copula function is the product copula $\mathbf{C}^{\perp}$.

In what follows, we consider the Clayton copula[25]:

$$\mathbf{C}_{(\theta_c)}(u_1, \ldots, u_n) = \left(u_1^{-\theta_c} + \cdots + u_n^{-\theta_c} - n + 1\right)^{-1/\theta_c}$$

or the Normal copula:

$$\mathbf{C}_{(\theta_c)}(u_1, \ldots, u_n) = \Phi\left(\Phi^{-1}(u_1) + \cdots + \Phi^{-1}(u_n); \mathcal{C}_n(\theta_c)\right)$$

The Clayton parameter satisfies $\theta_c \geq 0$ whereas the Normal parameter θ_c lies in the range $[-1, 1]$. These two copula families are very interesting since they are positively ordered with respect to the concordance stochastic ordering. For the Clayton copula, we have:

$$\mathbf{C}_{(0)} = \mathbf{C}^{\perp} \prec \mathbf{C}_{(\theta_c)} \prec \mathbf{C}^{+} = \mathbf{C}_{(\infty)}$$

meaning that the product copula is reached when $\theta_c = 0$ and the upper Fréchet bound corresponds to the limiting case $\theta_c \to \infty$. For the Normal copula, we restrict our analysis to $\theta_c \in [0, 1]$ because there is no sense to obtain negative correlations. Therefore, we have:

$$\mathbf{C}_{(0)} = \mathbf{C}^{\perp} \prec \mathbf{C}_{(\theta_c)} \prec \mathbf{C}^{+} = \mathbf{C}_{(1)}$$

The Normal parameter θ_c is easy to interpret because it corresponds to the Pearson linear correlation between two Gaussian random variables. The interpretation of the Clayton copula θ_c is more tricky. Nevertheless, we can compute the associated Kendall's tau and Spearman's rho rank correlations[26]. Their expressions are given in Table 26. Therefore, we can deduce the Pearson correlation ρ.

Table 26: Relationship between the copula parameter θ_c, the Kendall's tau τ, the Spearman's rho ϱ and the Pearson correlation ρ

	τ	ϱ	ρ
Clayton	$\dfrac{\theta_c}{\theta_c + 2}$	$\sin\left(\dfrac{\pi\theta_c}{2\theta_c + 4}\right)$	$\sin\left(\dfrac{\pi\theta_c}{2\theta_c + 4}\right)$
Normal	$\dfrac{2}{\pi}\arcsin(\theta_c)$	$\dfrac{6}{\pi}\arcsin\left(\dfrac{\theta_c}{2}\right)$	θ_c

The previous formulas can be used to map the copula parameter space into the Kendall, Spearman or Pearson correlation space. Some numeric values are given in Table 27. For example, the Clayton copula $\theta_c = 2$ corresponds to a Kendall's tau of 50%, a Spearman's rho of 69% and a Pearson correlation of 70.7%. The following analyses will present the results with respect to the Pearson correlation, which is the most readable and known parameter.

---

[25]We use the notations of Roncalli (2020, Chapter 11).

[26]For the Clayton copula, we calculate an approximation of the Spearman's rho:

$$\varrho \approx \frac{6}{\pi}\arcsin\left(\frac{1}{2}\sin\left(\frac{\pi\theta_c}{2\theta_c + 4}\right)\right) \approx \sin\left(\frac{\pi\theta_c}{2\theta_c + 4}\right)$$

Table 27: Mapping of the copula parameter space

	Clayton copula				Normal copula		
θ_c	τ	ϱ	ρ	θ_c	τ	ϱ	ρ
0.00	0.00%	0.00%	0.00%	0.00	0.00%	0.00%	0.00%
1.00	33.33%	48.26%	50.00%	0.20	12.82%	19.13%	20.00%
2.00	50.00%	69.02%	70.71%	0.50	33.33%	48.26%	50.00%
5.00	71.43%	89.25%	90.10%	0.75	53.99%	73.41%	75.00%
10.00	83.33%	96.26%	96.59%	0.90	71.29%	89.15%	90.00%
50.00	96.15%	99.80%	99.82%	0.99	90.99%	98.90%	99.00%

Remark 10 *We denote the copula-based model by $\mathcal{CM}\left(n, \omega, \tilde{p}, \tilde{\mu}, \tilde{\sigma}, \rho\right)$ (or $\mathcal{CM}\left(n, \tilde{p}, \tilde{\mu}, \tilde{\sigma}, \rho\right)$ when the vector of weights are equally-weighted). We have the following equivalence:*

$$\mathcal{IM}\left(n, \omega, \tilde{p}, \tilde{\mu}, \tilde{\sigma}\right) = \mathcal{CM}\left(n, \omega, \tilde{p}, \tilde{\mu}, \tilde{\sigma}, 0\right)$$

4.2.2 Statistical analysis

The skewness effect In Appendix A.7.1 on page 87, we show that:

$$\Pr\left\{\mathcal{R} = 0\right\} = \mathbf{C}_{(\theta_c)}\left(1 - \tilde{p}, \ldots, 1 - \tilde{p}\right)$$

Since $\mathbf{C}^{\perp} \prec \mathbf{C}_{(\theta_c)} \prec \mathbf{C}^{+}$, we obtain the following bounds[27]:

$$\left(1 - \tilde{p}\right)^n \leq \Pr\left\{\mathcal{R} = 0\right\} \leq 1 - \tilde{p}$$

We notice that the probability to observe zero redemptions converges to zero only when the number n of unitholders tends to ∞ and the copula is the product copula. By assuming that the redemption frequency $\tilde{p}$ is equal to 10%, we obtain the results given in Figure 45 on page 102 and we verify the previous statistical property. In Figure 25, we show the relationship between the Pearson correlation ρ and the probability $\Pr\left\{\mathcal{R} = 0\right\}$. As expected, it is an increasing function. We notice that the introduction of the correlation is very important to understand the empirical results we have calculated in Table 14 on page 36 and some unrealistic values we have obtained in Table 18 on page 40. For instance, the fact that $\Pr\left\{\mathcal{R} = 0\right\}$ is equal to 54.39% for the retail category can only be explained by a significant frequency correlation since the number n of unitholders is high for this category.

By construction, the frequency correlation modifies the probability distribution of the redemption frequency $\mathcal{F}$, which is defined as the proportion of unitholders that redeem:

$$\mathcal{F} = \frac{1}{n}\sum_{i=1}^{n} \mathbb{1}\left\{\mathcal{E}_i = 1\right\}$$

$\mathcal{F}$ is a random variable, whose range is between 0 and 1. $\mathcal{F}$ depends on the frequency parameter $\tilde{p}$, the number n of unitholders and the copula function $\mathbf{C}_{(\theta_c)}$ (or the Pearson

---

[27]Because we have:

$$\mathbf{C}^{\perp}\left(1 - \tilde{p}, \ldots, 1 - \tilde{p}\right) = \prod_{i=1}^{n}\left(1 - \tilde{p}\right) = \left(1 - \tilde{p}\right)^n$$

and:

$$\mathbf{C}^{+}\left(1 - \tilde{p}, \ldots, 1 - \tilde{p}\right) = \min\left(1 - \tilde{p}, \ldots, 1 - \tilde{p}\right) = 1 - \tilde{p}$$

Figure 25: Probability to observe no redemption $\Pr\{\mathcal{R} = 0\}$ in % with respect to the frequency correlation ρ ($\tilde{p} = 10\%$)

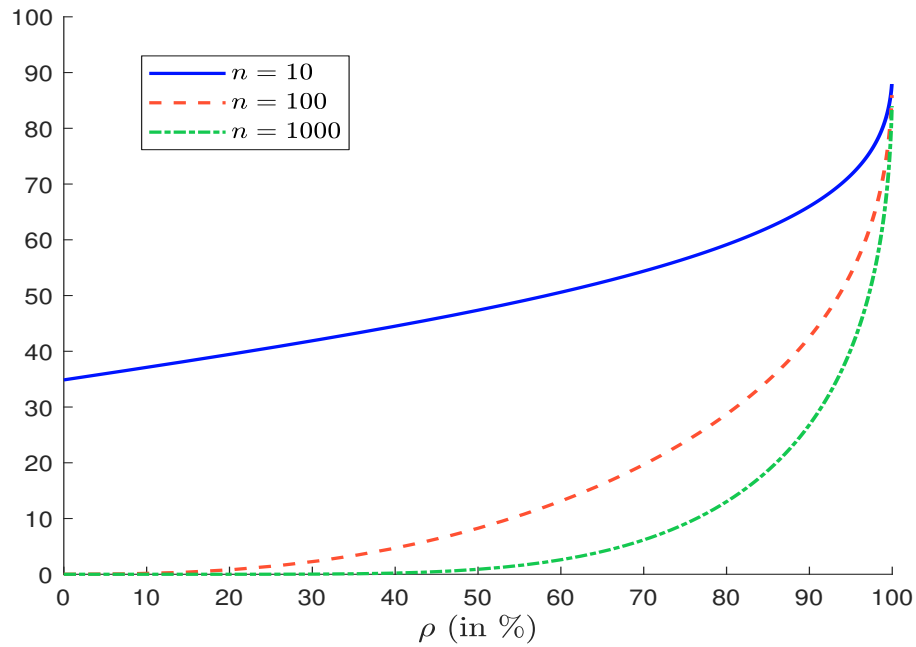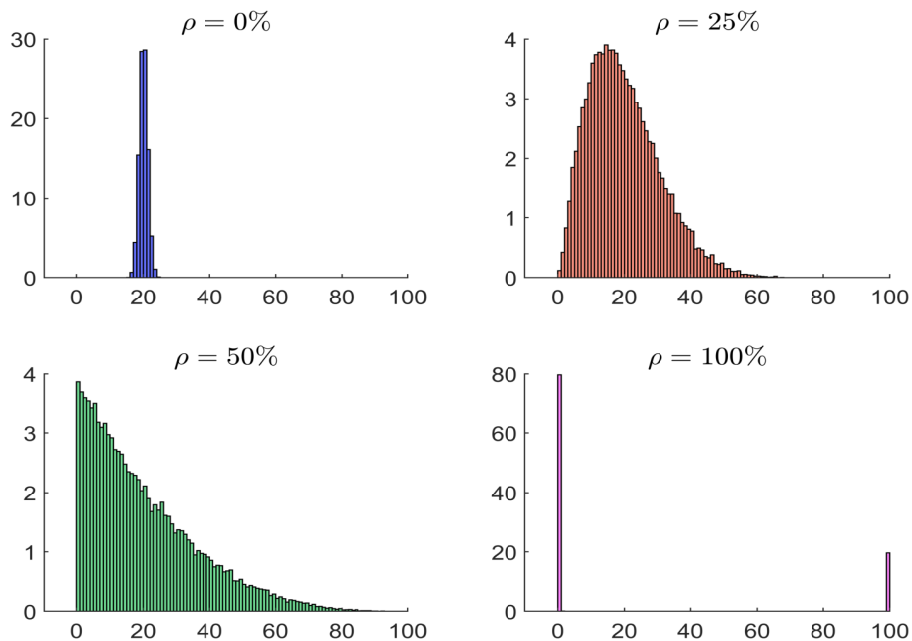Figure 26: Redemption frequencies in % with respect to the frequency correlation ρ ($\tilde{p} = 20\%, n = 1\,000$)

correlation ρ). When $\mathbf{C}_{(\theta_c)}$ is the product copula $\mathbf{C}^{\perp}$, the redemption events are independent and we obtain:

$$\mathcal{F} \sim \frac{\mathcal{B}(n, \tilde{p})}{n}$$

because the sum of independent Bernoulli random variables is a binomial random variable. Therefore, we obtain the following approximation when n is sufficiently large:

$$
\begin{aligned}
\frac{\mathcal{B}(n, \tilde{p})}{n} &\approx \frac{\mathcal{N}(n\tilde{p}, n\tilde{p}(1-\tilde{p}))}{n} \\
&= \mathcal{N}\left(\tilde{p}, \frac{\tilde{p}(1-\tilde{p})}{n}\right)
\end{aligned}
$$

When the copula $\mathbf{C}_{(\theta_c)}$ corresponds to the upper Fréchet bound $\mathbf{C}^{+}$, the redemption frequency follows the Bernoulli distribution and does not depend on the number of unitholders:

$$\mathcal{F} \sim \mathcal{B}(\tilde{p})$$

We have represented these two extreme cases in Figure 26 when $\tilde{p} = 20\%$ and $n = 1\,000$. We have also reported the probability distribution of $\mathcal{F}$ when the Pearson correlation of the copula function is equal to 25% and 50%. We notice that the skewness risk increases with the frequency correlation. Therefore, the parameter ρ will have a high impact on the stress testing results. In particular, when the frequency correlation is high, the risk is to observe a large proportion of redemptions even if the number of unitholders is large. In this case, the diversification effect across unitholders is limited. An illustration is provided in Figure 46 on page 102 that shows the probability to observe 100% of redemptions[28] when n is set to 20.

The mean effect   In Appendix A.7.3 on page 88, we show that the frequency correlation has no impact on the average redemption rate since we obtain the same expression as previously:

$$\mathbb{E}[\mathcal{R}] = \tilde{p}\tilde{\mu}$$

Therefore, the redemption frequency changes the shape of the probability distribution of $\mathcal{R}$, but not its mean.

The volatility effect   The volatility of the redemption rate is equal to:

$$\sigma^2(\mathcal{R}) = \left(\tilde{p}\tilde{\sigma}^2 + \left(\tilde{p} - \breve{\mathbf{C}}_{(\theta_c)}(\tilde{p}, \tilde{p})\right)\tilde{\mu}^2\right)\mathcal{H}(\omega) + \left(\breve{\mathbf{C}}_{(\theta_c)}(\tilde{p}, \tilde{p}) - \tilde{p}^2\right)\tilde{\mu}^2$$

where $\breve{\mathbf{C}}_{(\theta_c)}$ is the survival copula associated to $\mathbf{C}_{(\theta_c)}$. Since we have $\mathbf{C}^{\top} \prec \mathbf{C}_{(\theta_c)} \prec \mathbf{C}^{+}$, we obtain the following inequalities:

$$\tilde{p}\left(\tilde{\sigma}^2 + (1-\tilde{p})\tilde{\mu}^2\right)\mathcal{H}(\omega) \leq \sigma^2(\mathcal{R}) \leq \tilde{p}\tilde{\sigma}^2\mathcal{H}(\omega) + \tilde{p}(1-\tilde{p})\tilde{\mu}^2$$

If we consider the equally-weighted case and assume that n tends to infinity, we obtain:

$$0 \leq \sigma^2(\mathcal{R}) = \left(\breve{\mathbf{C}}_{(\theta_c)}(\tilde{p}, \tilde{p}) - \tilde{p}^2\right)\tilde{\mu}^2 \leq \tilde{p}(1-\tilde{p})\tilde{\mu}^2$$

This implies that the volatility risk is not equal to zero for an infinitely fine-grained liability structure if the frequency correlation is different from zero.

---

[28]It corresponds to the statistic $\Pr\{\mathcal{F} = 1\}$.

Figure 27: Volatility of the redemption rate $\mathcal{R}$ in % with respect to the number n of unithold-ers ($\tilde{p} = 10\%, \tilde{\mu} = 50\%, \tilde{\sigma} = 30\%$)
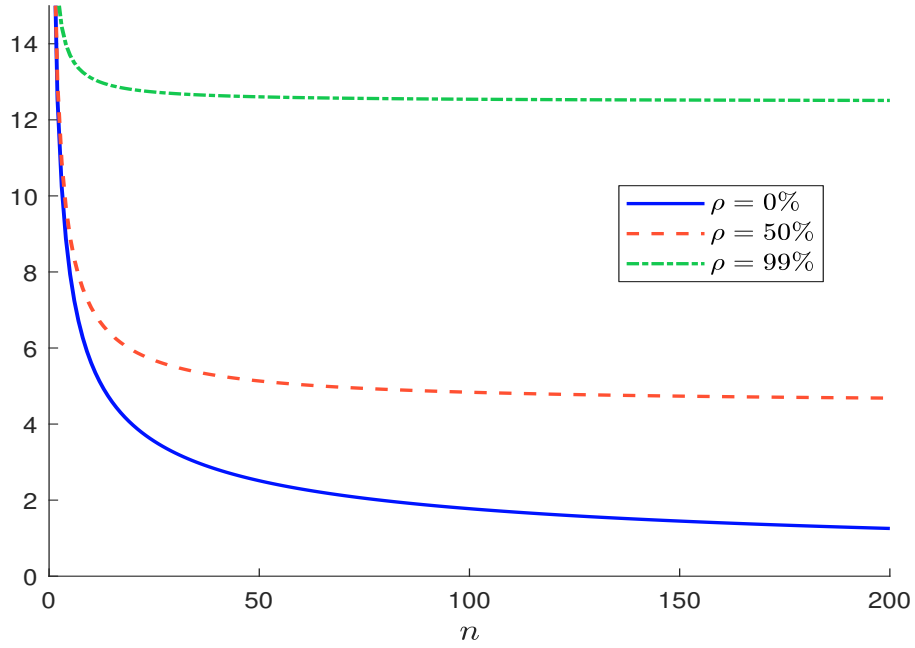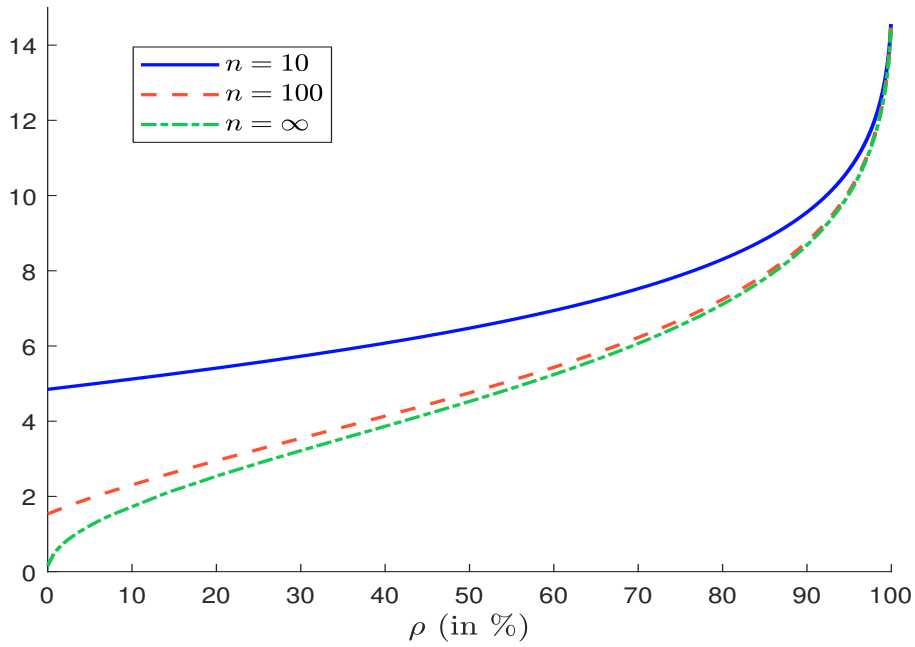

Figure 28: Volatility of the redemption rate $\mathcal{R}$ in % with respect to the frequency correlation ($\tilde{p} = 10\%, \tilde{\mu} = 50\%, \tilde{\sigma} = 10\%$)

The impact of the frequency correlation is illustrated in Figures 27 and 28. We notice that the decrease of the volatility risk highly depends on the correlation parameter ρ. These figures confirm that the volatility risk is minimum when the frequency correlation is equal to zero. The consequence is that the frequency correlation is a key parameter when building stress testing scenarios. This is perfectly normal since ρ can been seen as a parameter that controls spillover effects and the magnitude of redemption contagion. All these results corroborate the previous intuition that the individual-based model without redemption correlation may be not appropriate for building a robust stress testing program.

The shape effect   The impact of the frequency correlation on the skewness and the volatility can then change dramatically the shape of the probability distribution of the redemption rate. In Figure 17 on page 39, we have already studied the histogram of the redemption rate in the case $\tilde{p} = 50\%$, $\tilde{\mu} = 50\%$ and $\tilde{\sigma} = 10\%$. Let us reproduce the same exercise by assuming that the frequency correlation is equal to 50%. The results are given in Figure 29. The shape of the probability distributions is completely different except in the case of a single unitholder[29]. To better illustrate the impact of the frequency correlation, we report in Figure 30 the histogram of the redemption rate by fixing $n = 10$. In the case of a perfect correlation of 100% and an equally-weighted liability structure, we obtain two different cases:

1. there is zero redemption with a probability $1 - \tilde{p}$;

2. there are n redemptions with a probability $\tilde{p}$, and the redemption severity $\mathcal{R}^{\star}$ is the average of the individual redemption severities:

$$\mathcal{R}^{\star} = \frac{1}{n} \sum_{i=1}^{n} \mathcal{R}_i^{\star}$$

It follows that the probability distribution of the redemption rate is equal to:

$$\mathbf{F}\left(x\right) = \mathbb{1}\left\{x \geq 0\right\} \cdot \left(1 - \tilde{p}\right) + \mathbb{1}\left\{x > 0\right\} \cdot \tilde{p} \cdot \bar{\mathbf{G}}\left(x\right)$$

We retrieve the zero-inflated model $\mathcal{ZI}\left(\tilde{p}, \tilde{\mu}, n^{-1/2}\tilde{\sigma}\right)$ or the individual-based model with a single unitholder $\mathcal{IM}\left(1, \tilde{p}, \tilde{\mu}, n^{-1/2}\tilde{\sigma}\right)$. The only difference is the severity distribution $\bar{\mathbf{G}}$, whose variance is divided by a factor n. Spillover and contagion risks come then from the herd behavior of unitholders. Instead of having n different investors, we have a unique investor in the fund, because the decision to redeem by one investor induces the decision to redeem by all the other remaining investors.

4.2.3   Evidence of the correlation risk

Correlation risk within the same investor category   In order to illustrate that redemption frequencies are correlated, we build the time series of the frequency rate $\mathcal{F}_t$ for a given category[30]:

$$\mathcal{F}_t = \sum_{i=1}^{n} \omega_{i,t} \cdot \mathbb{1}\left\{\mathcal{E}_{i,t} = 1\right\} = \sum_{i=1}^{n} \omega_{i,t}\mathcal{E}_{i,t}$$

---

[29]Other illustrations are provided in Appendix C on page 103. Figures 47, 48 and 49 correspond to the cases $\rho = 25\%$, $\rho = 75\%$ and $\rho = 90\%$.

[30]We can use an equally-weighted scheme $\omega_{i,t} = 1/n$.

Figure 29: Histogram of the redemption rate in % with respect to the number n of unitholders ($\tilde{p} = 50\%, \tilde{\mu} = 50\%, \tilde{\sigma} = 10\%, \rho = 50\%$)
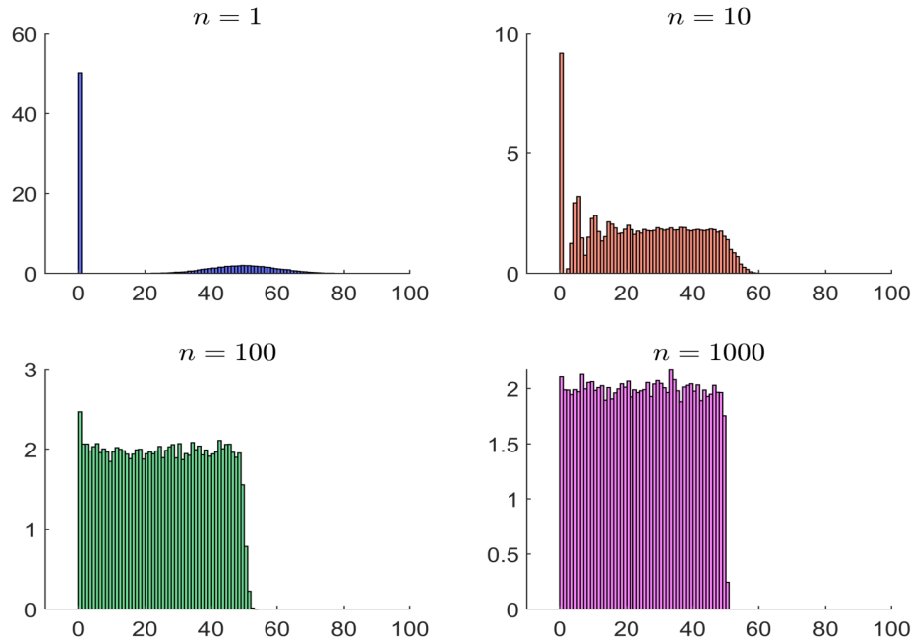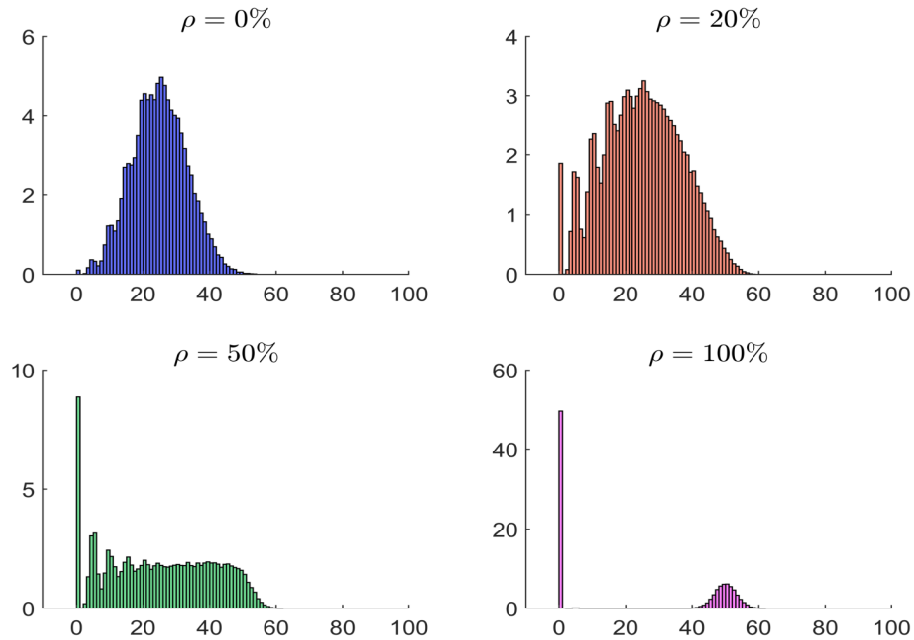

Figure 30: Histogram of the redemption rate in % with respect to the frequency correlation ($\tilde{p} = 50\%, \tilde{\mu} = 50\%, \tilde{\sigma} = 10\%, n = 10$)

where $\mathcal{E}_{i,t}$ is the redemption indicator for the investor i at time t. Using the sample $(\mathcal{F}_1, \ldots, \mathcal{F}_T)$, we compute the empirical mean $\overline{\mathcal{F}}$ and the standard deviation $\hat{\sigma}(\mathcal{F})$. Then, the copula parameter θ_c can be calibrated by solving the following nonlinear equation[31]:

$$\mathbf{C}_{(\theta_c)}\left(\overline{\mathcal{F}}, \overline{\mathcal{F}}\right) = \frac{\hat{\sigma}^2(\mathcal{F}) - \overline{\mathcal{F}}\left(\mathcal{H}(\omega) - \overline{\mathcal{F}}\right)}{1 - \mathcal{H}(\omega)}$$

The copula parameter θ_c can be transformed into the Kendall, Spearman or Pearson correlation using the standard formulas given in Table 26 on page 52. For instance, if $\mathbf{C}_{(\theta_c)}$ is the Clayton copula, the Pearson correlation is equal to:

$$\rho = \sin\left(\frac{\pi\theta_c}{2\theta_c + 4}\right)$$

An example is provided in Table 28 when the fund liability structure is equally-weighted and has 20 unitholders. For instance, if the empirical mean $\overline{\mathcal{F}}$ and the standard deviation $\hat{\sigma}(\mathcal{F})$ are equal to 25% and 20%, the calibrated Pearson correlation is equal to 44.5%.

Table 28: Calibrated Pearson correlation (Clayton copula, $\mathcal{H}(\omega) = 1/20$)

$\hat{\sigma}(\mathcal{F})$	$\overline{\mathcal{F}}$				
	10.0%	20.0%	25.0%	30.0%	40.0%
10.0%	39.1%	5.1%	1.1%		
20.0%	93.9%	58.7%	44.5%	34.7%	23.5%
30.0%	100.0%	91.5%	82.3%	72.8%	57.7%
40.0%		100.0%	98.7%	95.6%	87.4%

Remark 11 *At first sight, calibrating the frequency correlation seems to be an easy task. However, it is very sensitive to the different parameters $\overline{\mathcal{F}}$, $\hat{\sigma}(\mathcal{F})$ and $\mathcal{H}(\omega)$. Moreover, it depends on the copula specification. For instance, we obtain the results given in Table 49 on page 104 when the dependence function is the Normal copula. We observe that the Pearson correlations calibrated with the Clayton copula are different from those calibrated with the Normal copula.*

Remark 12 *Another way to illustrate the frequency correlation is to split a given investor category into two subsamples $\mathcal{S}_1$ and $\mathcal{S}_2$ and calculate the time series of the redemption frequency for the two subsamples $\mathcal{S}_k$ $(k = 1, 2)$:*

$$\mathcal{F}_{k,t} = \frac{1}{\sum_{i \in \mathcal{S}_k} \omega_{i,t}} \sum_{i \in \mathcal{S}_k} \omega_{i,t} \mathcal{E}_{i,t}$$

Then, we can calculate the Pearson correlation $\rho(\mathcal{F}_1, \mathcal{F}_2)$ and calibrate the associated copula parameter θ_c using Equation (58) on page 91.

Correlation risk between investor categories The correlation risk is present within a given investor category, but it may also concern two different investor categories. In order to distinguish them, we use the classical statistical jargon of inter-class and intra-class correlations. In Table 29, we report the intra-class Spearman correlation[32] for four

---

[31]See Equation (56) on page 90.

[32]The correlations of retail/insurance and institutional/insurance for balanced funds and the correlations of retail/third-party distributor and retail/insurance for money market funds are not significant at the confidence level of 95%.

Table 29: Intra-class Spearman correlation

Category #1	Category #2	Balanced	Bond	Equity	Money Market
Retail	Third-party distributor	53.0%	52.9%	52.1%	3.3%
Retail	Institutional	10.4%	23.2%	22.0%	−6.5%
Retail	Insurance	3.0%	18.8%	31.6%	−12.3%
Third-party distributor	Institutional	13.5%	48.0%	54.1%	24.0%
Third-party distributor	Insurance	23.1%	21.5%	22.8%	39.2%
Institutional	Insurance	2.5%	16.2%	16.4%	29.8%
Average		17.6%	30.1%	33.2%	12.9%

investor categories (retail, third-party distributor, institutional and insurance) and four fund categories (balanced, bond, equity and money market). We observe a high inter-class correlation between retail investors and third-party distributors except for money market funds. We notice that equity and bond funds present very similar frequency correlations. On average, it is equal to 30%. For balanced and money market funds, we obtain lower figures less than 20%. These results are coherent with the academic research, since redemption runs and contagions in bond and equity funds have been extensively studied and illustrated (Lakonishok *et al.*, 1992; Wermers, 1999; Sias, 2004; Wylie, 2005; Coval and Stafford, 2007; Shleifer and Vishny, 2011; Cai *et al.*, 2019).

Figure 31: Dependogram of redemption frequencies between retail investors and third-party distributors
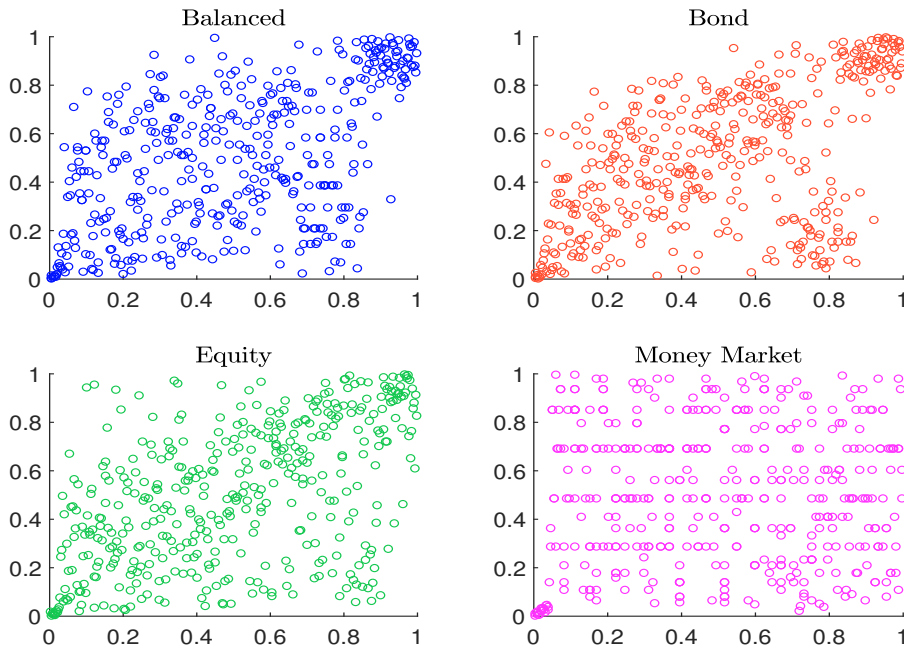
Remark 13 *Another way to illustrate the intra-class correlation is to report the dependogram (or empirical copula) of redemption frequencies. An example is provided in Figure 31 for retail investors and third-party distributors. We observe that these dependogram does not correspond to the product copula* [33].

---

[33]Examples of dependogram with the Normal copula and different correlations are provided in Figure 50 on page 105.

4.2.4 Computing the stress scenarios

The parameters of the copula-based model is made up by the parameters of the individual-based model ($\tilde{p}$, $\tilde{\mu}$ and $\tilde{\sigma}$) and the copula parameter θ_c (or the associated frequency correlation). Once these parameters are estimated for a given investor/fund category, we transform the $\tilde{\mu} - \tilde{\sigma}$ parameterization into the $a - b$ parameterization of the beta distribution and compute the risk measures $\mathbb{M}$, $\mathbb{Q}(\alpha)$, $\mathbb{C}(\alpha)$ and $\mathbb{S}(\mathcal{T})$ by using the following Monte Carlo algorithm:

1. we set $k \longleftarrow 1$;

2. we generate[34] $(u_1, \ldots, u_n) \sim \mathbf{C}_{(\theta_c)}$;

3. we compute the redemption events $(\mathcal{E}_1, \ldots, \mathcal{E}_n)$ such that:

$$\mathcal{E}_i = \mathbb{1}\{u_i \geq 1 - \tilde{p}\}$$

4. we simulate the redemption severities $(\mathcal{R}_1^\star, \ldots, \mathcal{R}_n^\star)$ from the beta distribution[35] $\mathcal{B}(a, b)$;

5. we compute the redemption rate for the kth simulation iteration:

$$\mathcal{R}_{(k)} = \sum_{i=1}^{n} \omega_i \mathcal{E}_i \mathcal{R}_i^\star$$

6. if k is equal to n_S, we return the simulated sample $(\mathcal{R}_{(1)}, \ldots, \mathcal{R}_{(n_S)})$, otherwise we set $k \longleftarrow k + 1$ and go back to step 2.

Figure 32 shows the relationship between the correlation frequency[36] and $\mathbb{C}(99\%)$ for different parameter sets when the liability structure has 20 equally-weighted unitholders. The impact of the correlation risk is not negligible in some cases. This is particularly true when the frequency correlation is close to 100%, but its impact is also significant when the frequency correlation is larger than 20%. On average, we observe that the risk measure $\mathbb{C}(99\%)$ increases by 15%, 20% and 35% when the frequency correlation is respectively equal to 20%, 30% and 50% compared the independent case.

Remark 14 *The algorithm to simulate the copula-based model $\mathcal{CM}(n, \omega, \tilde{p}, \tilde{\mu}, \tilde{\sigma}, \rho)$ can be used to simulate the individual-based model $\mathcal{IM}(n, \omega, \tilde{p}, \tilde{\mu}, \tilde{\sigma})$ by setting $\mathbf{C}_{(\theta_c)} = \mathbf{C}^{\perp}$. This is equivalent to replace step 2 and simulate n independent uniform random numbers $(u_1, \ldots, u_n)$.*

4.3 Time aggregation risk

In the case of daily redemptions, the correlation risk only concerns the cross-correlation between investors for a given market day. When we consider fire sales or liquidity crisis, the one-day study period is not adapted and must be extended to a weekly or monthly basis. In this case, we may face time aggregation risk, meaning that redemption flows for the subsequent market days may depend on the current redemption flows.

---

[34]Clayton and Normal copulas are easy to simulate using the method of transformation (Roncalli, 2020, page 803).

[35]Generally, the generation of beta random numbers is present in mathematical programming languages (Matlab, Python). Otherwise, we can use the method of rejection sampling (Roncalli, 2020, pages 886-887).

[36]It corresponds to the Pearson correlation of the Clayton copula.

Figure 32: Conditional value-at-risk $\mathbb{C}\left(99\%\right)$ with respect to the frequency correlation
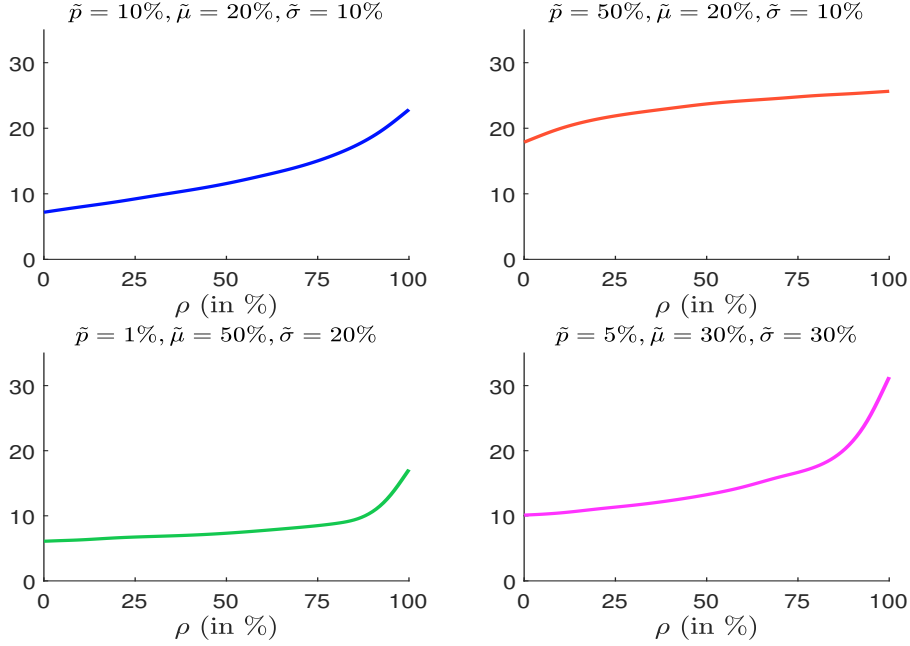
4.3.1 Analysis of non-daily redemptions

We recall that the total net assets at time $t+1$ can be decomposed as follows:

$$\text{TNA}\left(t+1\right) = \left(1 + R\left(t+1\right)\right) \cdot \text{TNA}\left(t\right) + \mathcal{F}^{+}\left(t+1\right) - \mathcal{F}^{-}\left(t+1\right)$$

By assuming that $\mathcal{F}^{+}\left(t+1\right) = 0$, we obtain:

$$\text{TNA}\left(t+1\right) \approx \left(1 + R\left(t+1\right) - \mathcal{R}\left(t+1\right)\right) \cdot \text{TNA}\left(t\right)$$

This formula is valid on a daily basis. If we consider a period of n_h market days (e.g. a weekly period), we have:

$$\text{TNA}\left(t+n_h\right) \approx \text{TNA}\left(t\right) \prod_{h=1}^{n_h} \left(1 + R\left(t+h\right) - \mathcal{R}\left(t+h\right)\right)$$

Therefore, it is not obvious to decompose the difference $\text{TNA}\left(t+n_h\right) - \text{TNA}\left(t\right)$ into a "*performance*" effect and a "*redemption*" effect since the two effects are related. Indeed, the mathematical definition of the n_h-day redemption rate is:

$$\mathcal{R}\left(t; t+n_h\right) = \frac{\sum_{h=1}^{n_h} \mathcal{F}^{-}\left(t+h\right)}{\text{TNA}\left(t\right)}$$

whereas the fund return over the period $\left[t, t+n_h\right]$ is given by the compound formula:

$$R\left(t; t+h\right) = \prod_{h=1}^{n_h} \left(1 + R\left(t+h\right)\right) - 1$$

Because of the cross-products (Brinson *et al.*, 1991), we cannot separate the two effects:

$$\text{TNA}\left(t+n_h\right) \neq \left(1 + R\left(t; t+n_h\right) - \mathcal{R}\left(t; t+n_h\right)\right) \cdot \text{TNA}\left(t\right)$$

4.3.2 The autocorrelation risk

In the case where the performance effect is negligible — $R(t+h) \ll \mathcal{R}(t+h)$, we have:

$$\mathcal{R}(t, t+n_h) \approx 1 - \prod_{h=1}^{n_h} (1 - \mathcal{R}(t+h)) \tag{28}$$

We can then calculate the probability distribution of $\mathcal{R}(t, t+n_h)$ by the Monte Carlo method. A first solution is to consider that the redemption rates are time-independent. A second solution is to consider that redemption rates are auto-correlated:

$$\mathcal{R}(t) = \rho_{\text{time}} \mathcal{R}(t-1) + \varepsilon(t) \tag{29}$$

where ρ_{time} is the autocorrelation parameter and $\varepsilon(t)$ is a random variable such that $\mathcal{R}(t) \in [0,1]$. Such modeling is complex because of the specification of $\varepsilon(t)$. However, this approach can be approximated by considering a time-series copula representation:

$$(\mathcal{R}(t+1), \ldots, \mathcal{R}(t+n_n)) \sim \mathbf{C}\left(\tilde{\mathbf{F}}(x), \ldots, \tilde{\mathbf{F}}(x); \Sigma_{\text{time}}(n_h)\right) \tag{30}$$

where $\tilde{\mathbf{F}}$ is the probability distribution of $\mathcal{R}(t)$ defined by the individual-based (or copula-based) model, $\mathbf{C}$ is the Normal copula, whose parameters are given by the Toeplitz correlation matrix[37] $\Sigma_{\text{time}}(n_h)$ such that $\Sigma_{\text{time}}(n_h)_{i,j} = \rho_{\text{time}}^{|i-j|}$. To calculate the probability distribution of $\mathcal{R}(t, t+n_h)$, we first simulate the individual-based (or copula-based) model in order to estimate the probability distribution $\tilde{\mathbf{F}}(x)$ of daily redemptions. Then, we generate the sample of the time-series $(\mathcal{R}(t+1), \ldots, \mathcal{R}(t+n_n))$ by using the method of the empirical quantile function (Roncalli, 2020, pages 806-809). Finally, we calculate the redemption rate $\mathcal{R}(t, t+n_h)$ using Equation (28). An example is provided in Figure 33 when the correlation between investors is equal to zero[38]. We have also measured the impact of the autocorrelation value ρ_{time} on the value-at-risk and the conditional value-at-risk. Results are given in Tables 30 and 31 for six different individual-based models $\mathcal{IM}(n, \tilde{p}, \tilde{\mu}, \tilde{\sigma})$. When the value of the risk measure is small, we notice that the impact of ρ_{time} is high. For instance, when $n = 500$, $\tilde{p} = 1\%$, $\tilde{\mu} = 25\%$ and $\tilde{\sigma} = 10\%$, the value-at-risk $\mathbb{Q}(99\%)$ is equal to 1.9% in the independent case. This figure increases respectively by $+9\%$ and $+19\%$ when ρ_{time} is equal to 25% and 50%. We also notice that the impact on the conditional value-at-risk is close to that on the value-at-risk.

Remark 15 *The compound approach defined by Equation (28) certainly overestimates stress scenarios. Indeed, we implicitly assume that the redemptions rates $\mathcal{R}(t+h)$ are identically distributed, meaning that there is no time effect on the individual redemption behaviour. However, we can think that an investor that redeems at time $t+1$ will not redeem at time $t+2$ and $t+3$. In practice, we observe that redemptions of a given investor are mutually exclusive during a short period of time. This property is not verified by Equation (28). At time $t+h$, we notice $\mathcal{IS}(t+h)$ the set of investors that have redeemed some units before*

---

[37] For instance, in the case of a weekly period, the Toeplitz correlation matrix is equal to:

$$\Sigma_{\text{time}}(5) = \begin{pmatrix} 1 & \rho_{\text{time}} & \rho_{\text{time}}^2 & \rho_{\text{time}}^3 & \rho_{\text{time}}^4 \\ \rho_{\text{time}} & 1 & \rho_{\text{time}} & \rho_{\text{time}}^2 & \rho_{\text{time}}^3 \\ \rho_{\text{time}}^2 & \rho_{\text{time}} & 1 & \rho_{\text{time}} & \rho_{\text{time}}^2 \\ \rho_{\text{time}}^3 & \rho_{\text{time}}^2 & \rho_{\text{time}} & 1 & \rho_{\text{time}} \\ \rho_{\text{time}}^4 & \rho_{\text{time}}^3 & \rho_{\text{time}}^2 & \rho_{\text{time}} & 1 \end{pmatrix}$$

[38] The same example with a correlation of 50% between investors is given in Figure 52 on page 106.

Figure 33: Histogram of the weekly redemption rate in % with respect to the autocorrelation ρ_{time} ($\tilde{p} = 50\%, \tilde{\mu} = 50\%, \tilde{\sigma} = 10\%, \rho = 0\%, n = 10$)
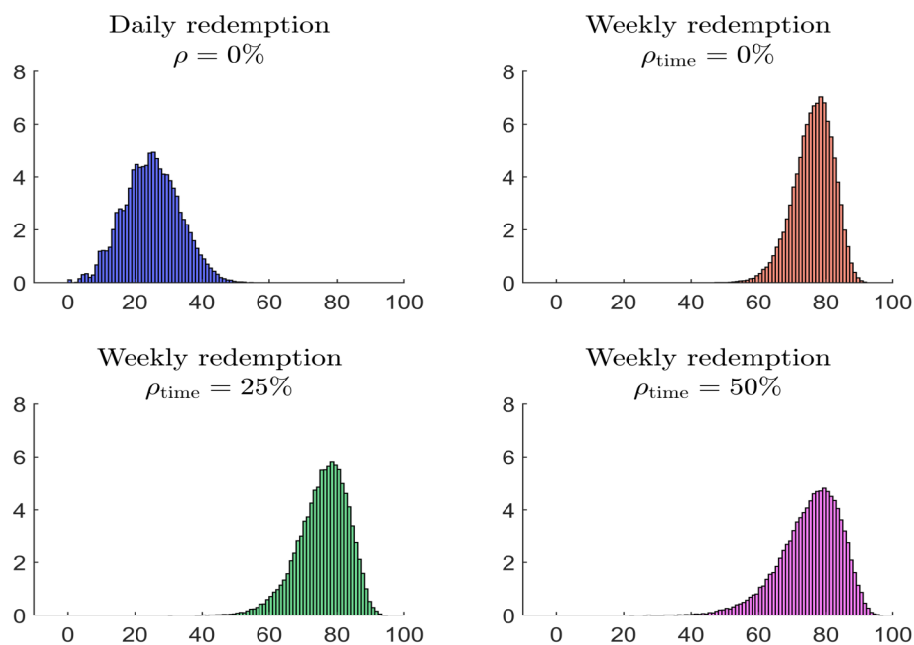

Table 30: Impact of the autocorrelation ρ_{time} on the value-at-risk $\mathbb{Q}\,(99\%)$

n	$\tilde{p}$	$\tilde{\mu}$	$\tilde{\sigma}$	ρ_{time}				
				0%	25%	50%	75%	100%
10 000	0.1%	25%	10%	0.2%	+6%	+14%	+24%	+36%
500	1.0%	25%	10%	1.9%	+9%	+19%	+33%	+50%
50	2.0%	50%	10%	10.5%	+12%	+29%	+49%	+79%
100	5.0%	50%	30%	18.2%	+8%	+18%	+29%	+45%
10	20.0%	50%	30%	65.8%	+6%	+13%	+21%	+28%
10	50.0%	50%	30%	90.1%	+2%	+4%	+6%	+8%

Table 31: Impact of the autocorrelation ρ_{time} on the conditional value-at-risk $\mathbb{C}\,(99\%)$

n	$\tilde{p}$	$\tilde{\mu}$	$\tilde{\sigma}$	ρ_{time}				
				0%	25%	50%	75%	100%
10 000	0.1%	25%	10%	0.2%	+6%	+16%	+27%	+41%
500	1.0%	25%	10%	2.0%	+9%	+21%	+37%	+56%
50	2.0%	50%	10%	11.4%	+13%	+32%	+54%	+84%
100	5.0%	50%	30%	19.2%	+9%	+20%	+32%	+50%
10	20.0%	50%	30%	68.8%	+6%	+13%	+21%	+28%
10	50.0%	50%	30%	91.3%	+2%	+4%	+6%	+7%

$t + h$. We have $\mathcal{IS}(t + 1) = \{1, \ldots, n\}$. The mutually exclusive property implies that[39]:

$$i \in \mathcal{IS}(t + h) \Rightarrow \mathcal{E}_i(t + 1) = \ldots = \mathcal{E}_i(t + n_h) = 0$$

It follows that:

$$\mathcal{R}(t + h) = \sum_{i \notin \mathcal{IS}(t+h)} \omega_i(t + h) \cdot \mathcal{E}_i(t + h) \cdot \mathcal{R}_i^{\star}(t + h)$$

and:

$$\omega_i(t + h + 1) = \frac{\omega_i(t + h)}{\sum\limits_{i \notin \mathcal{IS}(t+h)} \omega_i(t + h)}$$

Because $\omega_i(t + h - 1) \neq \omega_i(t + h)$ and $\mathcal{IS}(t + h - 1) \neq \mathcal{IS}(t + h)$, it is obvious that $\mathcal{R}(t + h - 1) \neq \mathcal{R}(t + h)$. Therefore, the redemption decisions taken in the recent past (e.g. two or three days ago) have an impact on the future redemptions for the next days. This is a limit of the compound approach. The solution would be to develop a comprehensive individual-based model, whose random variables are replaced by stochastic processes. Nevertheless, the complexity of such model is not worth it with respect to the large uncertainty of stress testing exercises.

4.3.3 The sell-herding behavior risk

Herding risk is related to momentum trading. According to Grinblatt *et al.* (1995), herding behavior corresponds to the situation where investors buy and sell the same securities at the same time. Herding risk happens during good and bad times, and is highly documented in economic research (Wermers, 1999; O'Neal, 2004; Ivković and Weisbenner, 2009; Ferreira *et al.*, 2012; Lou, 2012; Cashman *et al.*, 2014; Chen and Qin, 2017; Goldstein *et al.*, 2017; Choi *et al.*, 2019; Dötz and Weth, 2019). However, we generally notice that sell herding may have more impact on asset prices than buy herding. Therefore, the sell-herding behavior risk may be associated to a price destabilizing or spillover effect. In the case of redemption risk, the spillover mechanism corresponds to two related effects:

- A first spillover effect is that the unconditional probability of redemption is not equal to the conditional probability of the redemption given the returns of the fund during the recent past period:

$$\Pr\{\mathcal{R}(t + h) \leq x\} \neq \Pr\{\mathcal{R}(t + h) \leq x \mid (R(t + 1), \ldots, R(t + h - 1))\}$$

- A second spillover effect is that the unconditional probability of return is not equal to the conditional probability of the return given the redemptions of the fund during the recent past period:

$$\Pr\{R(t + h) \leq x\} \neq \Pr\{R(t + h) \leq x \mid (\mathcal{R}(t + 1), \ldots, \mathcal{R}(t + h - 1))\}$$

This implies that the transmission of a negative shock on the redemption rate $\mathcal{R}(t + 1)$ may also impact the redemption rates $\{\mathcal{R}(t + 2), \mathcal{R}(t + 3), \ldots\}$ because of the feedback

---

[39]For instance, if the investor has done a redemption at time $t + 1$, the probability that he will perform a new redemption at time $t + 2$ is very small, meaning that:

$$\mathcal{E}_i(t + 1) = 1 \Rightarrow \mathcal{E}_i(t + 2) = \ldots = \mathcal{E}_i(t + n_h) = 0$$

Figure 34: Spillover between fund redemptions and fund returns
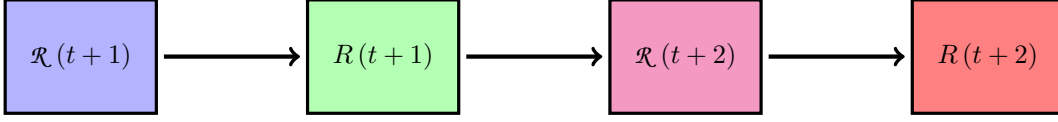
loop on the fund performance. An illustration is provided in Figure 34. A large negative redemption $\mathcal{R}(t+1)$ may induce a negative abnormal performance $R(t+1)$, and this negative performance may encourage the remaining investors of the fund to redeem, because negative returns accelerate redemption flows. This type of behavior is generally observed in the case of fire sales and less liquid markets.

As explained in the introduction, an integrated model that combines liability risk and asset risk is too ambitious and too complex. Moreover, this means modeling the policy reaction function of other investors and asset managers. Nevertheless, if we want to take into account sell herding, spillover or fire sales, we must build an econometric model. For example, the simplest way is to consider the linear dynamic model:

$$\begin{cases} R(t) = \phi_1 \mathcal{R}(t) + u_1(t) \\ \mathcal{R}(t+1) = \overline{\mathcal{R}} + \phi_2 R(t) + u_2(t+1) \end{cases}$$

We obtain an AR(1) process:

$$\mathcal{R}(t) = \overline{\mathcal{R}} + \phi \mathcal{R}(t-1) + u(t)$$

where $\phi = \phi_1 \phi_2$ and $u(t) = u_2(t) + \phi_2 u_1(t-1)$ is a white noise process. It follows that:

$$\mathbb{E}\left[\mathcal{R}(t+h)\right] = \frac{1}{1 - \phi_1 \phi_2} \overline{\mathcal{R}}$$

Therefore, spillover scenarios can be estimated by applying a scaling factor to the initial shock[40].

4.3.4 Empirical results

In order to illustrate the time dependency between redemptions, we build the time series of the redemption rate $\mathcal{R}_{(j,k)}(t)$, the redemption frequency $\mathcal{F}_{(j,k)}(t)$ and the redemption severities $\mathcal{R}^{\star}_{(j,k)}(t)$ for each classification matrix cell (j,k), which is defined by a fund category $\mathcal{FC}_{(j)}$ and an investor category $\mathcal{IC}_{(k)}$. For that, we calculate $\mathcal{R}_{(f,k)}(t)$ the redemption rate of the fund f for the investor category $\mathcal{IC}_{(k)}$ at time t. Then, we estimate the daily redemption rate $\mathcal{R}_{(j,k)}(t)$ as the average of the redemption rates of all funds that belong to the fund category $\mathcal{FC}_{(j)}$:

$$\mathcal{R}_{(j,k)}(t) = \frac{1}{\left|\mathcal{S}_{(j,k)}(t)\right|} \sum_{f \in \mathcal{S}_{(j,k)}(t)} \mathcal{R}_{(f,k)}(t) \tag{31}$$

where[41] $\mathcal{S}_{(j,k)}(t) = \left\{f : f \in \mathcal{FC}_{(j)}, \mathrm{TNA}_{(f,k)}(t) > 0\right\}$. We also estimate the daily redemption frequency as follows:

$$\mathcal{F}_{(j,k)}(t) = \frac{1}{\left|\mathcal{S}_{(j,k)}(t)\right|} \sum_{f \in \mathcal{S}_{(j,k)}(t)} \mathbf{1}\left\{\mathcal{R}_{(f,k)}(t) > 0\right\} \tag{32}$$

---

[40]The previous analysis can be extended to more sophisticated process, e.g. VAR (p) processes.

[41]We only consider funds which have unitholders that belong to the investor category $\mathcal{IC}_{(k)}$. This is equivalent to impose that the assets under management held by the investor category $\mathcal{IC}_{(k)}$ are strictly positive: $\mathrm{TNA}_{(f,k)}(t) > 0$.

whereas the daily redemption severity is given by the following formula:

$$\mathcal{R}^{\star}_{(j,k)}(t) = \frac{1}{\left|\mathcal{S}^{\star}_{(j,k)}(t)\right|} \sum_{f \in \mathcal{S}^{\star}_{(j,k)}(t)} \mathcal{R}_{(f,k)}(t) \tag{33}$$

where $\mathcal{S}^{\star}_{(j,k)}(t) = \left\{ f : f \in \mathcal{FC}_{(j)}, \mathrm{TNA}_{(f,k)} > 0, \mathcal{R}_{(f,k)}(t) > 0 \right\}$.

Table 32: Autocorrelation of the redemption rate in %

	Balanced	Bond	Equity	Money market
Institutional	25.9**	−2.2	−1.5	24.2**
Insurance	−1.5	9.9	5.4	17.8**
Retail	1.9	−2.1	9.8	11.7**
Third-party distributor	2.7	7.4	5.5	23.2**

The computation of $\mathcal{R}_{(j,k)}(t)$, $\mathcal{F}_{(j,k)}(t)$ and $\mathcal{R}^{\star}_{(j,k)}(t)$ does make sense only if there is enough observations $\left|\mathcal{S}_{(j,k)}(t)\right|$ and $\left|\mathcal{S}^{\star}_{(j,k)}(t)\right|$ at time t. This is why we focus on the most representative investor categories (retail, third-party distributor, institutional and insurance) and fund categories (balanced, bond, equity and money market). In Table 32, we report the maximum between the autocorrelation $\rho\left(\mathcal{R}(t), \mathcal{R}(t-1)\right)$ of order one and the autocorrelation $\rho\left(\mathcal{R}(t), \mathcal{R}(t-2)\right)$ of order two. Moreover, we indicate with the symbol ** the matrix cells where the p-value of the autocorrelation is lower than 5%. Except for money market funds and the institutional/balanced matrix cell, redemptions are not significantly autocorrelated. If we consider redemption frequencies and severities, we observe more autocorrelation (see Tables 50 and 51 on page 106). However, for bond and equity funds, the results show that the autocorrelation is significant and high for the redemption frequency, but low for the redemption severity.

5 Factor-based liquidity stress testing

The last section of this article is dedicated to the factors that may explain a redemption stress. First, we investigate whether it is due to a redemption frequency shock or a redemption severity shock. Second, we study how market risk may explain extreme redemption rates, and we focus on three factors: stock returns, bond returns and volatility levels.

5.1 Where does the stress come from?

We may wonder whether the time variation of redemption rates is explained by the time variation of redemption frequencies or redemption severities. Using the time series built in Section 4.3.4 on page 66, we consider three linear regression models:

$$\begin{cases} \mathcal{R}(t) = \beta_0 + \beta_1 \mathcal{F}(t) + u(t) \\ \mathcal{R}(t) = \beta_0 + \beta_1 \mathcal{R}^{\star}(t) + u(t) \\ \mathcal{R}(t) = \beta_0 + \beta_1 \mathcal{F}(t) + \beta_2 \mathcal{R}^{\star}(t) + u(t) \end{cases}$$

In the first model, we explain the redemption rate using the redemption frequency. In the second model, the explanatory variable is the redemption severity. Finally, the third model combines the two previous models. For each classification matrix cell (j, k), we have reported the centered coefficient of determination $\mathfrak{R}^2_c$ in Tables 33, 34 and 35.

Table 33: Coefficient of determination $\mathfrak{R}_c^2$ in % — $\mathcal{R}(t) = \beta_0 + \beta_1 \mathcal{F}(t) + u(t)$

	Balanced	Bond	Equity	Money market
Institutional	2.4	36.2	53.4	17.2
Insurance	0.9	11.6	10.8	17.8
Retail	37.2	34.5	14.7	18.4
Third-party distributor	11.5	31.6	17.7	11.5

Table 34: Coefficient of determination $\mathfrak{R}_c^2$ in % — $\mathcal{R}(t) = \beta_0 + \beta_1 \mathcal{R}^\star(t) + u(t)$

	Balanced	Bond	Equity	Money market
Institutional	87.2	74.8	44.5	87.5
Insurance	99.2	84.0	83.3	90.1
Retail	77.6	88.4	98.1	80.8
Third-party distributor	93.1	91.5	92.1	95.0

Table 35: Coefficient of determination $\mathfrak{R}_c^2$ in % — $\mathcal{R}(t) = \beta_0 + \beta_1 \mathcal{F}(t) + \beta_2 \mathcal{R}^\star(t) + u(t)$

	Balanced	Bond	Equity	Money market
Institutional	88.2	84.7	81.7	93.3
Insurance	99.3	86.2	86.4	94.9
Retail	92.5	95.4	99.3	92.3
Third-party distributor	97.0	96.3	95.7	97.3

If we consider the first linear regression model, we notice that $\mathfrak{R}_c^2$ is greater than 50% only for the institutional/equity category. $\mathfrak{R}_c^2$ takes a value around 35% for the retail/balanced, retail/bond and institutional/bond categories, otherwise it is less than 20%. Results for the second linear regression are better. This indicates that the redemption severity is a better explanatory variable than the redemption frequency. The only exception is the institutional/equity category. The combination of the two variables allows us to improve the explanatory power of the model, but we also notice that the redemption severity is the primary factor. The matrix cell with the highest $\mathfrak{R}_c^2$ is retail/equity, whereas the matrix cell with the lowest $\mathfrak{R}_c^2$ is institutional/equity. The scatter plot between $\mathcal{R}(t)$, $\mathcal{F}(t)$ and $\mathcal{R}^\star(t)$ for these two extreme cases are reported in Figures 35 and 36. For the retail/equity category, we verify that the redemption severity explains the redemption rate. For the institutional/equity category, the redemption severity is not able to explain the high values of the redemption rate.

The previous results are very interesting since the redemption severity is the primary factor for explaining the redemption shocks. Therefore, a high variation of the redemption rate is generally due to an increase of the redemption severity. Nevertheless, there are some exceptions where stress scenarios are also explained by an increase in the redemption frequency.

Remark 16 *We have used the coefficient $\mathfrak{R}_c^2$ to show the power explanation of the two variables $\mathcal{F}(t)$ and $\mathcal{R}^\star(t)$ without considering the effect of the constant. For some matrix cells, we notice that the constant may be important (see Tables 52, 53 and 54 on page 106).*

Figure 35: Relationship between $\mathcal{R}(t)$, $\mathcal{F}(t)$ and $\mathcal{R}^\star(t)$ (retail/equity)
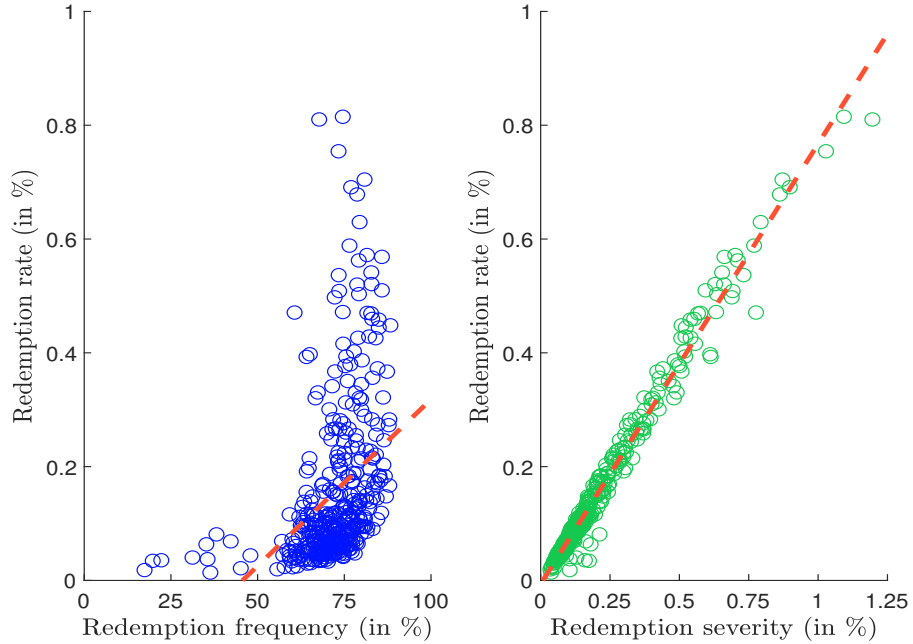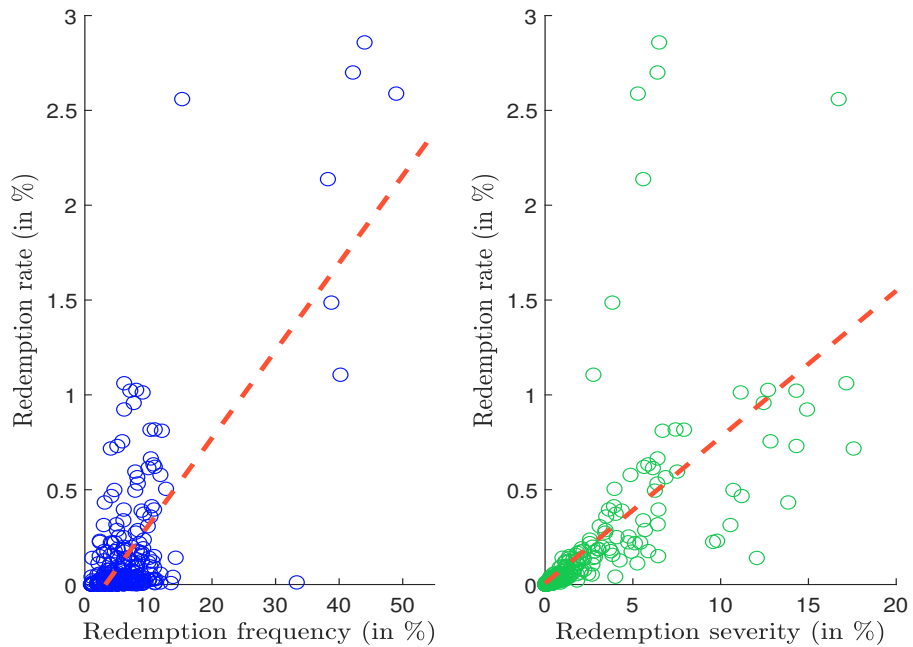

Figure 36: Relationship between $\mathcal{R}(t)$, $\mathcal{F}(t)$ and $\mathcal{R}^\star(t)$ (institutional/equity)

5.2 What market risk factors matter in stress testing?

5.2.1 The flow-performance relationship

Numerous academic research papers suggest that investor flows depend on past performance. According to Sirri and Tufano (1998) and Huang *et al.* (2007), there is an asymmetry concerning the flow-performance relationship: equity mutual funds with good performance gain a lot of money inflows, while equity mutual funds with poor performance suffer smaller outflows. However, this asymmetry concerns relative performance. Indeed, according to Ivković and Weisbenner (2009), "*inflows are related only to relative performance*" while "*outflows are related only to absolute fund performance*". Therefore, these authors suggest that investors sell the asset class when this one has a bad performance. In the case of corporate bonds, Goldstein *et al.* (2017) find that relative performance also matters in terms of explaining outflows. In order to better understand these results, we consider the following analytical model[42]:

$$\begin{cases} R_f(t) = \alpha_f(t) + \beta_f(t) R_{\mathrm{mkt}}(t) + \varepsilon(t) \\ \mathcal{R}_f(t) = \gamma_f + \delta_f \alpha_f(t-1) + \varphi_f R_f(t-1) + \eta(t) \end{cases}$$

where $R_f(t)$ is the return of the fund f, $R_{\mathrm{mkt}}(t)$ is the return of the market risk factor and $\mathcal{R}_f(t)$ is the redemption rate of the fund f. $\varepsilon(t)$ and $\eta(t)$ are two independent white noise processes. Using the first equation, we can estimate the relative performance of the fund, which is measured by its alpha component $\alpha_f(t)$. The second equation states that the redemption rate $\mathcal{R}_f(t)$ of the fund depends on the past relative performance $\alpha_f(t-1)$ and the past absolute performance $R_f(t-1)$. Then, we can test two assumptions: $\mathcal{H}_1 : \delta_f < 0$ and $\mathcal{H}_2 : \varphi_f < 0$. Accepting $\mathcal{H}_1$ implies that outflows depend on the relative performance, while accepting $\mathcal{H}_2$ implies that outflows depend on the absolute performance. In both cases, the value of the coefficient is negative, because we expect that a negative performance will increase the redemption rate. The previous framework can be extended to take into account a more sophisticated model for determining the relative performance[43] $\alpha_f(t)$ or to consider lagged variables (Bellando and Tran-Dieu, 2011; Ferreira *et al.*, 2012; Lou, 2012; Cashman *et al.*, 2014; Barber *et al.*, 2016; Fricke and Fricke, 2017). More generally, we have:

$$\mathcal{R}_f(t) = \gamma_f + \sum_{h=1}^{p} \left(\phi_f^{(h)} \mathcal{R}_f(t-h) + \delta_f^{(h)} \alpha_f(t-h) + \varphi_f^{(h)} R_f(t-h) \right) + \eta(t) \tag{34}$$

Even if this type of flow-performance relationship is interesting to understand the investor behavior, it is however not adapted in the case of a stress testing program for two reasons. The first reason is that Equation (34) is calibrated using low frequency data, e.g. quarterly or monthly data. Therefore, the goal of Equation (34) is to describe long-term behavior of investors, whereas stress testing of liabilities concerns short-term periods. The second reason is the inadequacy of this approach with macro stress testing approaches developed by regulators and institutional bodies.

5.2.2 The macro stress testing approach

If we consider stress testing programs developed in the banking sector (Roncalli, 2020, pages 893-922), we distinguish historical, probabilistic and macroeconomic approaches. While the first two methods have been developed in the previous sections, we focus on the third method, which is the approach used by the regulators (Board of Governors of the Federal Reserve

---

[42]See Arora *et al.* (2019).

[43]For instance, we can use the three-factor Fama-French model or the four-factor Carhart model.

System, 2017; EBA, 2020a,b; ECB, 2019; Ong, 2014). The macroeconomic approach consists in defining stress scenarios by a set of risk factors corresponding to some exogenous shocks. In this article, we focus on three market risk factors:

- the performance of the bond market;

- the performance of the stock market;

- market volatility.

Therefore, we assume that there is a linear relationship between the redemption rate and these factors:

$$\mathcal{R}(t) = \beta_0 + \beta_1 \mathcal{F}_{\text{bond}}(t) + \beta_2 \mathcal{F}_{\text{stock}}(t) + \beta_3 \mathcal{F}_{\text{vol}}(t) + u(t) \qquad (35)$$

where $\mathcal{F}_{\text{bond}}(t)$ and $\mathcal{F}_{\text{stock}}(t)$ are the h-day total returns of the FTSE World Broad Investment-Grade Bond index and the MSCI World index, $\mathcal{F}_{\text{vol}}(t)$ is the difference of the VIX index between $t - h$ and t, and h is the time horizon.

In Table 36, we report the coefficient of determination $\mathfrak{R}_c^2$ for the one-day time horizon. These figures are disappointing since the impact of the market risk factors are very low[44]. For instance, the highest $\mathfrak{R}$-squared is reached for the third-party distributor/money market category, but it is equal to 4.4%. If we consider a longer time horizon, results do not improve and we always have $\mathfrak{R}_c^2 \ll 5\%$ (see Tables 55 and 56 on page 107).

Table 36: Coefficient of determination $\mathfrak{R}_c^2$ in % — Equation (35), one-day time horizon

	Balanced	Bond	Equity	Money market
Institutional	0.3	0.8	1.6	1.9
Insurance	0.1	0.1	0.6	0.8
Retail	0.5	3.1	1.4	0.6
Third-party distributor	0.7	1.5	1.3	4.4

Remark 17 *The previous results suggest that redemption rates do not depend on market risk factors on a short-term basis. However, fund managers generally have the feeling that redemption rates increase when there is a stress on market returns. Nevertheless, we know that returns are more or less independent from one day to another. Therefore, we consider another approach using market sentiment. For that, we compute the average redemption rate when the VIX index is above 30, and calculate its relative variation with respect to the entire period. Results are given in Table 37. We observe an impact in particular for bond/equity funds and institutional/third-party distributor investors.*

Table 37: Relative variation of the redemption rate $\mathcal{R}(t)$ when VIX ≥ 30

	Balanced	Bond	Equity	Money market
Institutional	+17.3%	+54.7%	+74.3%	+64.7%
Insurance	−63.4%	−1.1%	−14.2%	+75.7%
Retail	+6.1%	+21.5%	+13.8%	−4.5%
Third-party distributor	+37.6%	+43.6%	+49.5%	+22.7%

---

[44]Nevertheless, we verify that β_2 is negative for equity funds, even though the relationship between redemption rate and stock returns is not convincing as shown in Figure 53 on page 108.

6 Conclusion

Liquidity stress testing is a recent topic in asset management, which has given rise to numerous publications from regulators (AMF, 2017; BaFin, 2017; ESMA, 2019; FSB, 2017; IOSCO, 2015, 2018), investment management associations (AFG, 2015; EFAMA, 2020) and affiliated researchers from central banks and international bodies (Arora *et al.*, 2019; Baranova *et al.*, 2017; Bouveret, 2017; Fricke and Fricke, 2017; Gourdel *et al.*, 2018). On the academic side, few studies specifically concern liquidity stress testing in asset management[45]. Therefore, we observe a gap between general concepts and specific measurement models. As such, the purpose of our study is to propose several analytical approaches in order to implement LST practical programs.

Besides the historical approach that considers non-parametric risk measures, we have developed a frequency-severity model that is useful when building parametric risk measures of liquidity stress testing. This statistical approach can be seen as a reduced-form model based on three parameters: the redemption frequency, the expected redemption severity and the redemption uncertainty. Like the historical approach, the frequency-severity model requires some expert judgements to correct some data biases. Nevertheless, both historical and analytical approaches are simple enough to verify properties of risk ordering coherency between fund and investor categories.

We have also developed an individual-based behavioral model, which is an extension of the frequency-severity model. We have shown that redemption risk depends on the fund liability structure, and is related to the Herfindahl index of assets under management held by unitholders. Even if this model is hard to implement because it requires knowing the comprehensive liability structure, it allows us to justify liquidity stress testing based on the largest fund holders. Moreover, this model shows the importance of cross-correlation between unitholders of a same investor category, but also of several investor categories. Nevertheless, the individual-based behavioral model is flexible enough that it can easily take into account dependencies between investors by incorporating a copula model. Again, the issue with this extended individual-based behavioral model lies in the knowledge of the liability structure.

The production of stress scenarios can be obtained by considering a risk measure applied to the redemption rate. For the historical approach, we can use a value-at-risk or a conditional value-at-risk figure, which is estimated with non-parametric statistical methods. For the frequency-severity and individual-based behavioral models, the estimation of the VaR or CVaR is based on analytical formulas. Moreover, these models may produce parametric stress scenarios for a given return time. Another issue concerns the choice of data between gross or net redemption rates for calibrating these stress scenarios. For some categories, net redemption rates may be used to proxy gross redemption rates, because they are very close in stress periods. However, we also demonstrate that it is better to use gross redemption rates for some investor or fund categories (e.g. retail investors or money market funds).

The design of macro stress testing programs is more complicated than expected. Since the flow-performance relationship is extensively documented by academic research, it is valid at low frequencies, typically on a quarterly or annual basis. In this case, we may observe inflows towards the best fund managers. However, this relationship mainly concerns relative performance, whereas macro stress testing programs deal with absolute performance. Indeed, relative performance is a key parameter when we want to analyze the idiosyncratic liability liquidity risk at the fund level. Nevertheless, the liquidity risk in asset management

---

[45]Because data on liabilities are not publicly available. However, we can cite Christoffersen and Xu (2017) and Darolles *et al.* (2018), who specifically study asset management flows with respect to the liability structure of the investment fund.

primarily involves systemic periods of liquidity shortage that impact a given asset class. Our empirical results are mixed since drawing a relationship between redemption rates and market risk factors in stress periods is not obvious because there are lead/lag effects and liquidity stress periods never look the same. For instance, the redemption stress scenario on money market funds during the covid-19 crisis and the first quarter of 2020 is very different from the redemption stress scenario during the Lehman Brothers' bankruptcy in September and October 2008. Indeed, we observe a significant lag of one/two months in the case of the covid-19 crisis. In a similar way, the liquidity stress transmission to equity funds has not been immediate and has been delayed by several weeks.

The current interest in liquidity stress testing is related to the Financial Stability Board's tasks on systemic risk (FSB, 2010, 2015) and shadow banking supervision (FSB, 2017, 2018). As explained by Blanqué and Mortier (2019b), "*regulation of asset managers has been lagging behind that of banks since the global financial crisis*". The implementation of the liquidity coverage ratio (LCR) and the net stable funding ratio (NSFR), the use of liquidity and high-quality liquid assets (HQLA) buffers and the definition of regulatory monitoring tools date back to 2010 for the banking industry[46] (BCBS, 2010, 2013). The regulatory framework on liquidity stress testing proposed by ESMA (2019) is an important step for the development of liquidity measurement in the asset management industry. In this paper, we develop an analytical framework and give some answers. However, it is still early days and much remains to be done.

---

[46]The LCR became a minimum requirement for BCBS member countries in January 2015.

References

ARORA, R., BÉDARD-PAGÉ, G., LEBLANC, G.O., and SHOTLANDER, R. (2019), Bond Funds and Fixed-Income Market Liquidity: A Stress-Testing Approach, *Bank of Canada Technical Report*, 115.

Association Française de la Gestion Financière (2015), Code of Conduct on the Use of Stress Tests, *AFG Report*, April.

Autorité des Marchés Financiers (2017), The Use of Stress Tests as Part of Risk Management, *AMF Guide*, February.

BARANOVA, Y., COEN, J., NOSS, J., and LOWE, P. (2017), Simulating Stress Across the Financial System: The Resilience of Corporate Bond Markets and the Role of Investment Funds, *Financial Stability Paper*, 42, Bank of England.

BARBER, B.M., HUANG, X., and ODEAN, T. (2016), Which Factors Matter to Investors? Evidence from Mutual Fund Flows, *Review of Financial Studies*, 29(10), pp. 2600-2642.

Basel Committee on Banking Supervision (1996), *Amendment to the Capital Accord to Incorporate Market Risks*, January 1996.

Basel Committee on Banking Supervision (1999), *A New Capital Adequacy Framework*, First Consultative Paper on Basel II, June 1999.

Basel Committee on Banking Supervision (2001), *The New Basel Capital Accord*, Second Consultative Paper on Basel II, January 2001.

Basel Committee on Banking Supervision (2010), *Basel III: A Global Regulatory Framework for More Resilient Banks and Banking Systems*, December 2010.

Basel Committee on Banking Supervision (2013), *Basel III: The Liquidity Coverage Ratio and Liquidity Risk Monitoring Tools*, January 2013.

Basel Committee on Banking Supervision (2016), *Interest Rate Risk in the Banking Book*, April 2016.

Basel Committee on Banking Supervision (2017), *Stress Testing Principles*, Consultative Document, December 2017.

BELLANDO, R., and TRAN-DIEU, L. (20111), Fund Flow/Performance Relationship — A Case Study of French Mutual Funds, *Revue Economique*, 62(2), pp. 225-276.

BLANQUÉ, P., and MORTIER, V. (2019a), How Investors Should Deal with the Liquidity Dilemna, *Amundi CIO Insights*, February.

BLANQUÉ, P., and MORTIER, V. (2019b), Liquidity Dilemna Needs A Regulatory Response, *Amundi Investment Talks*, October.

Board of Governors of the Federal Reserve System (2017), Supervisory Scenarios for Annual Stress Tests Required under the Dodd-Frank Act Stress Testing Rules and the Capital Plan Rule, www.federalreserve.gov/supervisionreg/dfast-archive.htm.

BOUVERET, A. (2017), Liquidity Stress Tests for Investment Funds: A Practical Guide, *IMF Working Paper*, 17/226.

BRINSON, G.P., SINGER, B.D., and BEEBOWER, G.L. (1991), Determinants of Portfolio Performance II: An Update, *Financial Analysts Journal*, 47(3), pp. 40-48.

BRUNNERMEIER, M.K., and PEDERSEN, L.H. (2009), Market Liquidity and Funding Liquidity, *Review of Financial Studies*, 22(6), pp. 2201-2238.

Bundesanstalt für Finanzdienstleistungsaufsicht (2017), Liquidity Stress Testing by German Asset Management Companies, December 2017.

CAI, F., HAN, S., LI, D., and LI, Y. (2019), Institutional Herding and its Price Impact: Evidence from the Corporate Bond Market, *Journal of Financial Economics*, 131(1), pp. 139-167.

CASHMAN, G.D., DELI, D., NARDARI, F., and VILLUPURAM, S.V. (2014), Investor Behavior in the Mutual Fund Industry: Evidence from Gross Flows, *Journal of Economics and Finance*, 38(4), pp. 541-567.

CHEN, Y., and QIN, N. (2017), The Behavior of Investor Flows in Corporate Bond Mutual Funds, *Management Science*, 63(5), pp. 1365-1381.

CHOI, J., HOSEINZADE, S., SHIN, S.S., and TEHRANIAN, H. (2019), Corporate Bond Mutual Funds and Asset Fire Sales, *SSRN*, www.ssrn.com/abstract=2731844.

CHRISTOFFERSEN, S.K., and Xu, H. (2015), Investor Attrition and Fund Flows in Mutual Funds, *Journal of Financial and Quantitative Analysis*, 52(3), pp. 867-893.

COVAL, J.D., and STAFFORD, E. (2007), Asset Fire Sales (and Purchases) in Equity Markets, *Journal of Financial Economics*, 86(2), pp. 479-512.

DAROLLES, S., LE FOL, G., LU, Y., and SUN, T. (2018), A Self-Exciting Model for Mutual Fund Flows: Investor Behaviour and Liability Risk, *Paris December 2018 Finance Meeting EUROFIDAI-AFFI*.

DÖTZ, N., and WETH, M.A. (2019), Redemptions and Asset Liquidations in Corporate Bond Funds, *Discussion Paper*, 11, Deutsche Bundesbank.

DUARTE, F., and EISENBACH, T.M. (2013), Fire-sale Spillovers and Systemic Risk (Revised December 2019), *Staff Report*, 645, Federal Reserve Bank of New York.

European Banking Authority (2020a), 2020 EU-wide Stress Testing, *Methodological Note*, January.

European Banking Authority (2020b), Market Risk Shocks, *Methodological Note*, January.

European Central Bank (2019), Sensitivity Analysis of Liquidity Risk – Stress Test 2019, *Final Report*, September.

European Fund and Asset Management Association (2020), Managing Fund Liquidity Risk in Europe — Recent Regulatory Enhancements & Proposals for Further Improvements, *AMIC/EFAMA Report*, January.

European Securities and Markets Authority (2019), Guidelines on Liquidity Stress Testing in UCITS and AIFs, *Final Report*, September.

FERREIRA, M.A., KESWANI, A., MIGUEL, A.F., and RAMOS, S.B. (2012), The Flow-Performance Relationship Around The World, *Journal of Banking & Finance*, 36(6), pp. 1759-1780.

Financial Stability Board (2010), *Reducing the Moral Hazard Posed by Systemically Important Financial Institutions*, Consultation Document, October 2010.

Financial Stability Board (2015), *Assessment Methodologies for Identifying Non-bank Non-insurer Global Systemically Important Financial Institutions*, Second Consultation Document, March 2015.

Financial Stability Board (2017), *Policy Recommendations to Address Structural Vulnerabilities from Asset Management Activities*, January 2017.

Financial Stability Board (2020), *Global Monitoring Report on Non-Bank Financial Intermediation 2019*, January 2020.

FRICKE, C., and FRICKE, D. (2017), Vulnerable Asset Management? The Case of Mutual Funds, *Discussion Paper*, 32, Deutsche Bundesbank.

GOLDSTEIN, I., JIANG, H., and NG, D.T. (2017), Investor Flows and Fragility in Corporate Bond Funds, *Journal of Financial Economics*, 126(3), pp. 592-613.

GOURDEL, R., MAQUI, E., and SYDOW, M. (2018), Investments Funds Under Stress, *ECB Working Paper*, 2323.

GRILLET-AUBERT, L. (2018), Macro Stress Tests: What do they mean for the Markets and for the Asset Management Industry?, *Risk and Trend Mapping*, Autorité des Marchés Financiers, June.

GRINBLATT, M., TITMAN, S., and WERMERS, R. (1995), Momentum Investment Strategies, Portfolio Performance, and Herding: A Study of Mutual Fund Behavior, *American Economic Review*, 85(5), pp. 1088-1105.

HUANG, J., WEI, K.D. and YAN, H. (2007), Participation Costs and the Sensitivity of Fund Flows to Past Performance, *Journal of Finance*, 62(3), pp. 1273-1311.

International Organization of Securities Commissions (2015), Liquidity Management Tools in Collective Investment Schemes, *Final Report*, 28, December.

International Organization of Securities Commissions (2018), Recommendations for Liquidity Risk Management for Collective Investment Schemes, *Final Report*, 01, February.

IVKOVIĆ, Z., and WEISBENNER, S. (2009), Individual Investor Mutual Fund Flows, *Journal of Financial Economics*, 92(2), pp. 223-237.

KACPERCZYK, M., and SCHNABL, P. (2013), How Safe are Money Market Funds?, *Quarterly Journal of Economics*, 128(3), pp. 1073-1122.

LAKONISHOK, J., SHLEIFER, A., and VISHNY, R.W. (1992) The Impact of Institutional Trading on Stock Prices, *Journal of Financial Economics*, 32(1), pp. 23-43.

LOU, D. (2012), A Flow-based Explanation for Return Predictability, *Review of Financial Studies*, 25(12), pp. 3457-3489.

MIN, Y., and AGRESTI, A. (2002), Modeling Nonnegative Data with Clumping at Zero: A Survey, *Journal of the Iranian Statistical Society*, 1(1-2), pp. 7-33

NELSEN, R.B. (2006), *An Introduction to Copulas*, Second edition, Springer.

O'NEAL, E.S. (2004), Purchase and Redemption Patterns of US Equity Mutual Funds, *Financial Management*, 33(1), pp. 63-90.

ONG, L.L. (2014), *A Guide to IMF Stress Testing: Methods and Models*, International Monetary Fund.

OSPINA, R., and FERRARI, S.L. (2010), Inflated Beta Distributions, *Statistical papers*, 51(1), pp. 111-126.

PERSAUD, A.D. (2003), *Liquidity Black Holes: Understanding, Quantifying and Managing Financial Liquidity Risk*, Risk Books.

RONCALLI, T. (2020), *Handbook of Financial Risk Management*, Chapman & Hall/CRC Financial Mathematics Series.

RONCALLI, T., and WEISANG, G. (2015a), Asset Management and Systemic Risk, *SSRN*, www.ssrn.com/abstract=2610174.

RONCALLI, T., and WEISANG, G. (2015b), *Response to FSB-IOSCO Second Consultative Document, Assessment Methodologies for Identifying Non-Bank Non-Insurer Global Systemically Important Financial Institutions*, May 28, https://www.fsb.org/wp-content/uploads/Thierry-Roncalli-and-Guillaume-Weisang.pdf.

SCHMIDT, L., TIMMERMANN, A., and WERMERS, R. (2016), Runs on Money Market Mutual Funds, *American Economic Review*, 106(9), pp. 2625-2657.

Securities and Exchange Commission (2015), Open-End Fund Liquidity Risk Management Programs; Swing Pricing; Re-Opening of Comment Period for Investment Company Reporting Modernization Release, *Proposed Rule*, 33-9922, September.

Securities and Exchange Commission (2016), Investment Company Liquidity Risk Management Programs, *Final Rule*, 33-10233, October.

Securities and Exchange Commission (2018a), Investment Company Liquidity Disclosure, *Proposed Rule*, IC-33046, March.

Securities and Exchange Commission (2018b), Investment Company Liquidity Disclosure, *Final Rule*, IC-33142, June.

SHLEIFER, A., and VISHNY, R. (2011), Fire Sales in Finance and Macroeconomics, *Journal of Economic Perspectives*, 25(1), pp. 29-48.

SIAS, R.W. (2004), Institutional Herding, *Review of Financial Studies*, 17(1), pp. 165-206.

SIRRI, E.R., and TUFANO, P. (1998), Costly Search and Mutual Fund Flows, *Journal of Finance*, 53(5), pp. 1589-1622.

THOMPSON, J. (2019), H2O, Woodford and GAM Crises Highlight Liquidity Risk, *Financial Times*, 29 June 2019.

WERMERS, R. (1999), Mutual Fund Herding and the Impact on Stock Prices, *Journal of Finance*, 54(2), pp. 581-622.

WYLIE, S. (2005), Fund Manager Herding: A Test of the Accuracy of Empirical Results using UK Data, *Journal of Business*, 78(1), pp. 381-403.

Appendix

A   Mathematical results

A.1   Granularity and the $\mathbb{X}$-statistic

We consider n funds whose redemption rate is equal to p. The assets under management of each fund are set to \$1. The maximum redemption rate of n funds is equal to the mathematical expectation of n Bernoulli random variables:

$$
\begin{aligned}
p\,(\mathrm{max}) &= \mathbb{E}\left[\max\left(\mathcal{B}_1\left(p\right),\ldots,\mathcal{B}_n\left(p\right)\right)\right] \\
&= 1-\left(1-p\right)^n
\end{aligned}
$$

whereas the redemption rate of the sum of n funds is equal to the expected frequency of a Binomial random variable:

$$
p\,(\mathrm{sum}) = \frac{\mathbb{E}\left[\mathcal{B}\left(n,p\right)\right]}{n} = p
$$

In Table 38, we report the value taken by the ratio $p\,(\mathrm{max})\,/p\,(\mathrm{sum})$. For example, this ratio is equal to 3.71 if $p=5\%$ and $n=4$. To understand this ratio, we can consider a large fund whose redemption probability is p. This fund is split into n funds of the same size. The ratio indicates the multiplication factor to obtain the maximum of the redemption rates among the n funds.

Table 38: Value of the ratio $p\,(\mathrm{max})\,/p\,(\mathrm{sum})$

n	Probability p						
	1 bp	10 bps	1%	5%	10%	20%	50%
1	1.00	1.00	1.00	1.00	1.00	1.00	1.00
2	2.00	2.00	1.99	1.95	1.90	1.80	1.50
3	3.00	3.00	2.97	2.85	2.71	2.44	1.75
4	4.00	3.99	3.94	3.71	3.44	2.95	1.88
5	5.00	4.99	4.90	4.52	4.10	3.36	1.94
10	10.00	9.96	9.56	8.03	6.51	4.46	2.00
50	49.88	48.79	39.50	18.46	9.95	5.00	2.00
100	99.51	95.21	63.40	19.88	10.00	5.00	2.00

A.2   Statistical moments of zero-inflated probability distribution

A.2.1   General formulas

A zero-inflated random variable Z can be written as the product of a Bernoulli random variables $X \sim \mathcal{B}\left(p\right)$ and a positive random variable Y:

$$
Z = XY
$$

Let $\mu'_m\left(Z\right)$ for the m-th moment of Z. Using the previous relationship, we deduce that:

$$
\begin{aligned}
\mu'_m\left(Z\right) &= \mathbb{E}\left[Z^m\right] \\
&= \mathbb{E}\left[X^m Y^m\right] \\
&= \mathbb{E}\left[X^m\right]\mathbb{E}\left[Y^m\right] \\
&= p\mu'_m\left(Y\right)
\end{aligned}
\tag{36}
$$

because X and Y are independent by definition, and $X^m = X$, implying that X^m follows a Bernoulli distribution $\mathcal{B}(p)$. From Equation (36), we can compute the m-th centered moment $\mu_m(Z)$. For that, we recall that:

$$
\begin{aligned}
\mu_1 &= \mu_1' \\
\mu_2 &= \mu_2' - \mu_1^2 \\
\mu_3 &= \mu_3' - 3\mu_2'\mu_1 + 2\mu_1^3 \\
\mu_4 &= \mu_4' - 4\mu_3'\mu_1 + 6\mu_2'\mu_1^2 - 3\mu_1^4
\end{aligned}
$$

We deduce the expression of the second moment:

$$
\mu_2' = \mu_2 + \mu_1^2
$$

For the third moment, we have:

$$
\begin{aligned}
\mu_3' &= \mu_3 + 3\mu_2'\mu_1 - 2\mu_1^3 \\
&= \mu_3 + 3\left(\mu_2 + \mu_1^2\right)\mu_1 - 2\mu_1^3 \\
&= \mu_3 + 3\mu_2\mu_1 + \mu_1^3 \\
&= \gamma_1\mu_2^{3/2} + 3\mu_2\mu_1 + \mu_1^3
\end{aligned}
$$

where γ_1 is the skewness coefficient. For the fourth moment, it follows that:

$$
\begin{aligned}
\mu_4' &= \mu_4 + 4\mu_3'\mu_1 - 6\mu_2'\mu_1^2 + 3\mu_1^4 \\
&= \mu_4 + 4\left(\gamma_1\mu_2^{3/2} + 3\mu_2\mu_1 + \mu_1^3\right)\mu_1 - 6\left(\mu_2 + \mu_1^2\right)\mu_1^2 + 3\mu_1^4 \\
&= \mu_4 + 4\gamma_1\mu_2^{3/2}\mu_1 + 12\mu_2\mu_1^2 + 4\mu_1^4 - 6\mu_2\mu_1^2 - 6\mu_1^4 + 3\mu_1^4 \\
&= \mu_4 + 4\gamma_1\mu_2^{3/2}\mu_1 + 6\mu_2\mu_1^2 + \mu_1^4 \\
&= (\gamma_2 + 3)\mu_2^2 + 4\gamma_1\mu_2^{3/2}\mu_1 + 6\mu_2\mu_1^2 + \mu_1^4
\end{aligned}
$$

where γ_2 is the excess kurtosis coefficient. We can then compute the moments of Z. For the mean, we have:

$$
\begin{aligned}
\mu_1(Z) &= \mu_1'(Z) \\
&= p\mu_1(Y) \tag{37}
\end{aligned}
$$

We deduce that the variance of Z is equal to:

$$
\begin{aligned}
\mu_2(Z) &= \mu_2'(Z) - \mu_1^2(Z) \\
&= p\mu_2'(Y) - p^2\mu_1^2(Y) \\
&= p\mu_2(Y) + p(1-p)\mu_1^2(Y) \tag{38}
\end{aligned}
$$

For the third moment, we have:

$$
\begin{aligned}
\mu_3(Z) &= \mu_3'(Z) - 3\mu_2'(Z)\mu_1(Z) + 2\mu_1^3(Z) \\
&= p\mu_3'(Y) - 3p^2\mu_2'(Y)\mu_1(Y) + 2p^3\mu_1^3(Y) \\
&= p\left(\gamma_1(Y)\mu_2^{3/2}(Y) + 3\mu_2(Y)\mu_1(Y) + \mu_1^3(Y)\right) - \\
&\quad\ 3p^2\left(\mu_2(Y) + \mu_1^2(Y)\right)\mu_1(Y) + 2p^3\mu_1^3(Y) \\
&= p\gamma_1(Y)\mu_2^{3/2}(Y) + 3p(1-p)\mu_2(Y)\mu_1(Y) + p(1-p)(1-2p)\mu_1^3(Y)
\end{aligned}
$$

It follows that the skewness coefficient is equal to:

$$
\begin{aligned}
\gamma_1 (Z) &= \frac{\mu_3 (Z)}{\mu_2^{3/2} (Z)} \\
&= \frac{\vartheta_1 (Z)}{(p\mu_2 (Y) + p(1-p)\mu_1^2 (Y))^{3/2}}
\end{aligned}
\tag{39}
$$

where:

$$
\vartheta_1 (Z) = p\gamma_1 (Y) \mu_2^{3/2} (Y) + 3p(1-p)\mu_2 (Y)\mu_1 (Y) + p(1-p)(1-2p)\mu_1^3 (Y)
$$

For the fourth moment, we have:

$$
\begin{aligned}
\mu_4 (Z) &= \mu_4' (Z) - 4\mu_3' (Z)\mu_1 (Z) + 6\mu_2' (Z)\mu_1^2 (Z) - 3\mu_1^4 (Z) \\
&= p\mu_4' (Y) - 4p^2\mu_3' (Y)\mu_1 (Y) + 6p^3\mu_2' (Y)\mu_1^2 (Y) - 3p^4\mu_1^4 (Y) \\
&= p(\gamma_2 (Y) + 3)\mu_2^2 (Y) + 4p\gamma_1 (Y)\mu_2^{3/2} (Y)\mu_1 (Y) + 6p\mu_2 (Y)\mu_1^2 (Y) + p\mu_1^4 (Y) - \\
&\quad 4p^2\gamma_1 (Y)\mu_2^{3/2} (Y)\mu_1 (Y) - 12p^2\mu_2 (Y)\mu_1^2 (Y) - 4p^2\mu_1^4 (Y) + \\
&\quad 6p^3\mu_2 (Y)\mu_1^2 (Y) + 6p^3\mu_1^4 (Y) - 3p^4\mu_1^4 (Y) \\
&= p(\gamma_2 (Y) + 3)\mu_2^2 (Y) + 4p(1-p)\gamma_1 (Y)\mu_2^{3/2} (Y)\mu_1 (Y) + \\
&\quad 6p(1-p)^2\mu_2 (Y)\mu_1^2 (Y) + p(1-p)(1-3p+3p^2)\mu_1^4 (Y)
\end{aligned}
\tag{40}
$$

We deduce that the excess kurtosis coefficient is equal to:

$$
\begin{aligned}
\gamma_2 (Z) &= \frac{\mu_4 (Z)}{\mu_2^2 (Z)} - 3 \\
&= \frac{\vartheta_2 (Z)}{(p\mu_2 (Y) + p(1-p)\mu_1^2 (Y))^2}
\end{aligned}
\tag{41}
$$

where:

$$
\begin{aligned}
\vartheta_2 (Z) &= p(\gamma_2 (Y) + 3)\mu_2^2 (Y) + 4p(1-p)\gamma_1 (Y)\mu_2^{3/2} (Y)\mu_1 (Y) + \\
&\quad 6p(1-p)^2\mu_2 (Y)\mu_1^2 (Y) + p(1-p)(1-3p+3p^2)\mu_1^4 (Y) - \\
&\quad 3p^2\mu_2^2 (Y) - 6p^2(1-p)\mu_2 (Y)\mu_1^2 (Y) - 3p^2(1-p)^2\mu_1^4 (Y) \\
&= (p\gamma_2 (Y) + 3p(1-p))\mu_2^2 (Y) + 4p(1-p)\gamma_1 (Y)\mu_2^{3/2} (Y)\mu_1 (Y) + \\
&\quad 6p(1-p)(1-2p)\mu_2 (Y)\mu_1^2 (Y) + p(1-p)(1-6p+6p^2)\mu_1^4 (Y)
\end{aligned}
$$

We can deduce the following properties:

1. The skewness of Z is equal to zero if and only if:

   (a) the skewness of Y is equal to zero and the frequency probability p is equal to one;

   (b) the frequency probability p is equal to zero, meaning that Z is always equal to zero.

2. The excess kurtosis of Z is equal to zero if and only if:

   (a) the kurtosis of Y is equal to 3 and the frequency probability p is equal to one;

(b) the frequency probability p is equal to zero, meaning that Z is always equal to zero.

In other cases, the skewness and excess kurtosis coefficients of Z are different from zero even if the random variable Y is not skewed and has not fat tails.

Remark 18 *The previous results seem to be contradictory with the properties given in Equation (17) on page 26. In fact, the limit case $p \to 0^+$ is not equal to $p = 0$, because there is a singularity at the point $p = 0$.*

A.2.2 Application to the beta distribution

We assume that $Y \sim \mathcal{B}(a, b)$. Since we have:

$$\mu_1(Y) = \frac{a}{a + b}$$

we deduce that:

$$\mu_1(Z) = p \frac{a}{a + b}$$

For the second moment, we have:

$$\mu_2(Y) = \frac{ab}{(a + b)^2 (a + b + 1)}$$

and:

$$
\begin{aligned}
\mu_2(Z) &= p \frac{ab}{(a + b)^2 (a + b + 1)} + p(1 - p) \left(\frac{a}{a + b} \right)^2 \\
&= p \frac{ab + (1 - p) a^2 (a + b + 1)}{(a + b)^2 (a + b + 1)}
\end{aligned}
$$

This formula has been already found by Ospina and Ferrari (2010). The skewness and excess kurtosis coefficients of the beta distribution are equal to:

$$\gamma_1(Y) = \frac{2(b - a)\sqrt{a + b + 1}}{(a + b + 2)\sqrt{ab}}$$

and:

$$\gamma_2(Y) = \frac{6(a - b)^2 (a + b + 1)}{ab(a + b + 2)(a + b + 3)} - \frac{6}{(a + b + 3)}$$

We plug these different expressions into the general formulas[47] to obtain $\gamma_1(Z)$ and $\gamma_2(Z)$.

A.3 Maximum likelihood of the zero-inflated model

We consider a sample $\{x_1, \ldots, x_n\}$ of n observations, and we assume that X follows a zero-inflated model, whose frequency and probability distributions are p and $\mathbf{G}(x; \theta)$. The log-likelihood of the ith observation is equal to:

$$
\begin{aligned}
\ell_i(p, \theta) &= \ln \Pr\{X = x_i\} \\
&= \ln f(x_i) \\
&= \mathbb{1}\{x_i = 0\} \cdot \ln(1 - p) + \mathbb{1}\{x_i > 0\} \cdot \ln(pg(x_i; \theta)) \\
&= \mathbb{1}\{x_i = 0\} \cdot \ln(1 - p) + \mathbb{1}\{x_i > 0\} \cdot \ln p + \mathbb{1}\{x_i > 0\} \cdot \ln g(x_i; \theta)
\end{aligned}
$$

---

[47]The formulas are not reported here because they don't have a lot of interest.

We deduce that the log-likelihood function is equal to:

$$
\begin{aligned}
\ell\left(p,\theta\right) &= \sum_{i=1}^{n} \ell_i\left(p,\theta\right) \\
&= n_0 \ln\left(1-p\right) + \left(n-n_0\right)\ln p + \sum_{x_i>0} \ln g\left(x_i\right)
\end{aligned}
$$

where n_0 is the number of observations x_i that are equal to zero. The maximum likelihood estimator $\left(\hat{p},\hat{\theta}\right)$ is defined as follows:

$$
\left\{\hat{p},\hat{\theta}\right\} = \arg\max \ell\left(p,\theta\right)
$$

and satisfies the first-order conditions:

$$
\begin{cases}
\partial_p \ell\left(\hat{p};\hat{\theta}\right) = 0 \\
\partial_\theta \ell\left(\hat{p};\hat{\theta}\right) = \mathbf{0}
\end{cases}
$$

We deduce that:

$$
\begin{aligned}
\partial_p \ell\left(\hat{p};\hat{\theta}\right) &= 0 \Leftrightarrow -\frac{n_0}{1-\hat{p}} + \frac{n-n_0}{\hat{p}} = 0 \\
&\Leftrightarrow \hat{p} = \frac{n-n_0}{n}
\end{aligned}
\tag{42}
$$

The concentrated log-likelihood function becomes:

$$
\ell\left(\hat{p},\theta\right) = n_0 \ln n_0 + \left(n-n_0\right)\ln\left(n-n_0\right) - n\ln n + \sum_{x_i>0} \ln g\left(x_i\right)
$$

Therefore, the ML estimator $\hat{\theta}$ corresponds to the ML estimator of θ when considering only the observations x_i that are strictly positive:

$$
\begin{aligned}
\hat{\theta} &= \arg\max \ell\left(\hat{p},\theta\right) \\
&= \arg\max \sum_{x_i>0} \ln g\left(x_i\right)
\end{aligned}
\tag{43}
$$

Remark 19 *In the case of the zero-inflated beta model, we have $\theta=(a,b)$ and:*

$$
\left\{\hat{a},\hat{b}\right\} = \arg\max \sum_{x_i>0}\left(\left(a-1\right)\ln x_i + \left(b-1\right)\ln\left(1-x_i\right) - \ln \mathcal{B}\left(a,b\right)\right)
\tag{44}
$$

A.4 Statistical properties of the individual-based model

We define the random variable $\tilde{Z}$ as the sum of products of two random variables:

$$
\tilde{Z} = \sum_{i=1}^{n} \omega_i \tilde{X}_i \tilde{Y}_i
$$

where $\tilde{X}_i \sim \mathcal{B}\left(\tilde{p}\right)$ and $\tilde{Y}_i$ are *iid* random variables. Moreover, we assume that $\omega_i > 0$ and $\sum_{i=1}^{n} \omega_i = 1$.

A.4.1 Computation of $\Pr\left\{\tilde{Z} = 0\right\}$

This case corresponds to the situation where no client redeems:

$$
\begin{aligned}
\Pr\left\{\tilde{Z} = 0\right\} &= \Pr\left\{\sum_{i=1}^{n} \omega_i \tilde{X}_i \tilde{Y}_i = 0\right\} \\
&= \Pr\left\{\tilde{X}_1 = 0, \ldots, \tilde{X}_n = 0\right\} \\
&= \prod_{i=1}^{n} \Pr\left\{\tilde{X}_i = 0\right\} \\
&= (1 - \tilde{p})^n
\end{aligned}
\tag{45}
$$

A.4.2 Statistical moments

First moment For the mean, we have:

$$
\begin{aligned}
\mathbb{E}\left[\tilde{Z}\right] &= \mathbb{E}\left[\sum_{i=1}^{n} \omega_i \tilde{X}_i \tilde{Y}_i\right] \\
&= \sum_{i=1}^{n} \omega_i \mathbb{E}\left[\tilde{X}_i\right] \mathbb{E}\left[\tilde{Y}_i\right]
\end{aligned}
$$

We deduce that:

$$
\mu_1\left(\tilde{Z}\right) = \tilde{p}\mu_1\left(\tilde{Y}\right)
\tag{46}
$$

Second moment Since we have $\mathbb{E}\left[\tilde{X}_i^2\right] = \tilde{p}$ and $\mathbb{E}\left[\tilde{Y}_i^2\right] = \mu_2'\left(\tilde{Y}\right)$, it follows that:

$$
\begin{aligned}
\mathbb{E}\left[\tilde{Z}^2\right] &= \mathbb{E}\left[\left(\sum_{i=1}^{n} \omega_i \tilde{X}_i \tilde{Y}_i\right)^2\right] \\
&= \mathbb{E}\left[\sum_{i=1}^{n} \omega_i^2 \tilde{X}_i^2 \tilde{Y}_i^2 + 2\sum_{j>i} \omega_i \omega_j \tilde{X}_i \tilde{X}_j \tilde{Y}_i \tilde{Y}_j\right] \\
&= \tilde{p}\mu_2'\left(\tilde{Y}\right)\sum_{i=1}^{n} \omega_i^2 + 2\tilde{p}^2\mu_1^2\left(\tilde{Y}\right)\sum_{j>i} \omega_i \omega_j
\end{aligned}
$$

We notice that:

$$
\begin{aligned}
1 &= \sum_{i=1}^{n} \omega_i \\
&= \left(\sum_{i=1}^{n} \omega_i\right)^2 \\
&= \sum_{i=1}^{n} \omega_i^2 + 2\sum_{j>i} \omega_i \omega_j
\end{aligned}
$$

We deduce that:

$$
\begin{aligned}
\mu_2\left(\tilde{Z}\right) &= \mathbb{E}\left[\tilde{Z}^2\right] - \mathbb{E}^2\left[\tilde{Z}\right] \\
&= \tilde{p}\mu_2'\left(\tilde{Y}\right)\sum_{i=1}^{n}\omega_i^2 + 2\tilde{p}^2\mu_1^2\left(\tilde{Y}\right)\sum_{j>i}\omega_i\omega_j - \tilde{p}^2\mu_1^2\left(\tilde{Y}\right) \\
&= \tilde{p}\mu_2'\left(\tilde{Y}\right)\sum_{i=1}^{n}\omega_i^2 + 2\tilde{p}^2\mu_1^2\left(\tilde{Y}\right)\sum_{j>i}\omega_i\omega_j - \\
&\qquad \tilde{p}^2\mu_1^2\left(\tilde{Y}\right)\left(\sum_{i=1}^{n}\omega_i^2 + 2\sum_{j>i}\omega_i\omega_j\right)
\end{aligned}
$$

Therefore, the variance of $\tilde{Z}$ is equal to:

$$
\begin{aligned}
\mu_2\left(\tilde{Z}\right) &= \left(\tilde{p}\mu_2'\left(\tilde{Y}\right) - \tilde{p}^2\mu_1^2\left(\tilde{Y}\right)\right)\sum_{i=1}^{n}\omega_i^2 \\
&= \tilde{p}\left(\mu_2\left(\tilde{Y}\right) + (1-\tilde{p})\mu_1^2\left(\tilde{Y}\right)\right)\sum_{i=1}^{n}\omega_i^2 \qquad (47)
\end{aligned}
$$

Remark 20 *In the equally-weighted case, we obtain:*

$$
\mu_2\left(\tilde{Z}\right) = \frac{\tilde{p}\left(\mu_2\left(\tilde{Y}\right) + (1-\tilde{p})\mu_1^2\left(\tilde{Y}\right)\right)}{n}
$$

Application to the beta severity distribution If we assume that $\tilde{Y}_i \sim \mathcal{B}\left(\tilde{a}, \tilde{b}\right)$, we have:

$$
\mu_1\left(\tilde{Y}\right) = \frac{\tilde{a}}{\tilde{a}+\tilde{b}}
$$

and:

$$
\mu_2\left(\tilde{Y}\right) = \frac{\tilde{a}\tilde{b}}{\left(\tilde{a}+\tilde{b}\right)^2\left(\tilde{a}+\tilde{b}+1\right)}
$$

We deduce that:

$$
\mu_1\left(\tilde{Z}\right) = \tilde{p}\frac{\tilde{a}}{\tilde{a}+\tilde{b}}
$$

and:

$$
\begin{aligned}
\mu_2\left(\tilde{Z}\right) &= \frac{\tilde{p}}{n}\left(\frac{\tilde{a}\tilde{b}}{\left(\tilde{a}+\tilde{b}\right)^2\left(\tilde{a}+\tilde{b}+1\right)} + (1-\tilde{p})\frac{\tilde{a}^2}{\left(\tilde{a}+\tilde{b}\right)^2}\right) \\
&= \tilde{p}\frac{\tilde{a}}{n}\left(\frac{\tilde{b} + (1-\tilde{p})\tilde{a}\left(\tilde{a}+\tilde{b}+1\right)}{\left(\tilde{a}+\tilde{b}\right)^2\left(\tilde{a}+\tilde{b}+1\right)}\right)
\end{aligned}
$$

A.5 Moment matching between the zero-inflated model and the individual-based model

In order to calibrate the probability p, we match the redemption probability $\Pr\{\mathcal{R} > 0\}$. Using the results in Appendix A.4.1 on page 83, we obtain:

$$
\begin{aligned}
p &= 1 - \Pr\{\mathcal{R} = 0\} \\
&= 1 - (1 - \tilde{p})^n
\end{aligned}
$$

For the first moment, we have:

$$\mathbb{E}[\mathcal{R}] = p\mu = \tilde{p}\tilde{\mu}$$

We deduce that:

$$\mu = \frac{\tilde{p}}{1 - (1 - \tilde{p})^n}\tilde{\mu}$$

For the second moment, we have:

$$\sigma^2(\mathcal{R}) = p\sigma^2 + p(1 - p)\mu^2 = \tilde{p}\left(\tilde{\sigma}^2 + (1 - \tilde{p})\tilde{\mu}^2\right)\sum_{i=1}^{n}\omega_i^2$$

It follows that:

$$
\begin{aligned}
\sigma^2 &= \frac{\tilde{p}\left(\tilde{\sigma}^2 + (1 - \tilde{p})\tilde{\mu}^2\right)\sum_{i=1}^{n}\omega_i^2 - p(1 - p)\mu^2}{p} \\
&= \frac{\tilde{p}\left(\tilde{\sigma}^2 + (1 - \tilde{p})\tilde{\mu}^2\right)\sum_{i=1}^{n}\omega_i^2}{1 - (1 - \tilde{p})^n} - \frac{(1 - \tilde{p})^n\tilde{p}^2}{\left(1 - (1 - \tilde{p})^n\right)^2}\tilde{\mu}^2 \\
&= \left(\frac{\tilde{p}\mathcal{H}(\omega)}{1 - (1 - \tilde{p})^n}\right)\tilde{\sigma}^2 + \\
&\qquad \left(\frac{\tilde{p}\left((1 - \tilde{p}) - (1 - \tilde{p})^n\right)\mathcal{H}(\omega) - \tilde{p}^2(1 - \tilde{p})^n(1 - \mathcal{H}(\omega))}{\left(1 - (1 - \tilde{p})^n\right)^2}\right)\tilde{\mu}^2
\end{aligned}
$$

where $\mathcal{H}(\omega) = \sum_{i=1}^{n}\omega_i^2$ is the Herfindahl index.

Remark 21 *If we consider the equally-weighted case $\omega_i = n^{-1}$, we have $\mathcal{H}(\omega) = n^{-1}$ and:*

$$\sigma^2 = \frac{1}{n}\left(\frac{\tilde{p}}{1 - (1 - \tilde{p})^n}\right)\tilde{\sigma}^2 + \frac{1}{n}\left(\frac{\tilde{p}\left((1 - \tilde{p}) - (1 - \tilde{p})^n\right) - \tilde{p}^2(1 - \tilde{p})^n(n - 1)}{\left(1 - (1 - \tilde{p})^n\right)^2}\right)\tilde{\mu}^2$$

When $\tilde{p} \neq 0$, the limit cases are:

$$\lim_{n\to\infty} p = 1$$

and:

$$\lim_{n\to\infty} \mu = \tilde{p}\tilde{\mu}$$

For the parameter σ, we obtain:

$$\lim_{n\to\infty} \sigma^2 = \tilde{p}\left(\tilde{\sigma}^2 + (1 - \tilde{p})\tilde{\mu}^2\right)\mathcal{H}(\omega)$$

For an infinitely fine-grained liability structure, we have:

$$\lim_{n\to\infty} \sigma^2 = 0$$

A.6 Upper bound of the Herfindahl index under partial information

Let π_k be a probability distribution, meaning that $\pi_k \geq 0$ and $\sum_{k=1}^{n} \pi_k = 1$. The Herfindahl index is equal to:

$$
\begin{aligned}
\mathcal{H} &= \sum_{k=1}^{n} \pi_k^2 \\
&= \sum_{k=1}^{n} \pi_{k:n}^2 \\
&= \sum_{k=1}^{n} \pi_{n-k+1:n}^2
\end{aligned}
$$

where:

$$
0 \leq \min \pi_k = \pi_{1:n} \leq \pi_{2:n} \leq \cdots \leq \pi_{k:n} \leq \pi_{k+1:n} \leq \cdots \leq \pi_{n:n} = \max \pi_k
$$

We have:

$$
\mathcal{H} = \sum_{k=1}^{m} \pi_{n-k+1:n}^2 + \sum_{k=m+1}^{n} \pi_{n-k+1:n}^2
$$

where $k = 1 : m$ denotes the largest contributions that are known, meaning that we don't know the values taken by $\{\pi_{1:n}, \ldots, \pi_{n-m:n}\}$. Since we have $\pi_{n-k:n} \leq \pi_{n-k+1:n}$, we deduce that:

$$
\begin{aligned}
\sum_{k=m+1}^{n} \pi_{n-k+1:n}^2 &\leq \left(\frac{1 - \sum_{k=1}^{m} \pi_{n-k+1:n}}{\pi_{n-m+1:n}} \right) \pi_{n-m+1:n}^2 \\
&= \left(1 - \sum_{k=1}^{m} \pi_{n-k+1:n} \right) \pi_{n-m+1:n}
\end{aligned}
$$

and[48]:

$$
\mathcal{H} \leq \mathcal{H}_m^+ = \sum_{k=1}^{m} \pi_{n-k+1:n}^2 + \left(1 - \sum_{k=1}^{m} \pi_{n-k+1:n} \right) \pi_{n-m+1:n} \tag{48}
$$

An example is given in Table 39. The Herfindahl index is equal to 17.96%. Using the first three largest values, we obtain an estimate of 20.50%.

Table 39: Example of partial Herfindahl index computation

m	1	2	3	4	5	6	7	8
π_m (in %)	30.00	20.00	15.00	10.00	9.00	7.00	5.00	4.00
$\mathcal{H}_m^+$ (in %)	30.00	23.00	20.50	18.75	18.50	18.18	18.00	17.96

A.7 Correlated redemptions with copula functions

We define the random variable $\tilde{Z}$ as previously:

$$
\tilde{Z} = \sum_{i=1}^{n} \omega_i \tilde{X}_i \tilde{Y}_i
$$

---

[48] We verify that $\mathcal{H}_n^+ = \mathcal{H}$.

where $\tilde{Y}_i$ are *iid* random variables. We assume that $\tilde{X}_i \sim \mathcal{B}(\tilde{p})$ are identically distributed, but not independent. We note $\mathbf{C}(u_1, \dots, u_n)$ the copula function of the random vector $\left(\tilde{X}_1, \dots, \tilde{X}_n\right)$ and $\mathbf{B}(x)$ the cumulative distribution function of the Bernoulli random variable $\mathcal{B}(\tilde{p})$. This means that $\mathbf{B}(0) = 1 - \tilde{p}$ and $\mathbf{B}(1) = 1$.

In practice we use the Clayton copula:

$$\mathbf{C}_{(\theta_c)}(u_1, \dots, u_n) = \left(u_1^{-\theta_c} + \dots + u_n^{-\theta_c} - n + 1\right)^{-1/\theta_c}$$

or the Normal copula[49]:

$$\mathbf{C}_{(\theta_c)}(u_1, \dots, u_n) = \Phi\left(\Phi^{-1}(u_1) + \dots + \Phi^{-1}(u_n); \mathcal{C}_n(\theta_c)\right)$$

The Clayton parameter satisfies $\theta_c \geq 0$ whereas the Normal parameter θ_c lies in the range $[-1, 1]$. Moreover, we notice that the expressions of the bivariate copula functions are:

$$\mathbf{C}_{(\theta_c)}(u_1, u_2) = \mathbf{C}_{(\theta_c)}(u_1, u_2, 1, \dots, 1) = \left(u_1^{-\theta_c} + u_2^{-\theta_c} - 1\right)^{-1/\theta_c}$$

and:

$$\mathbf{C}_{(\theta_c)}(u_1, u_2) = \mathbf{C}_{(\theta_c)}(u_1, u_2, 1, \dots, 1) = \Phi\left(\Phi^{-1}(u_1) + \Phi^{-1}(u_2); \mathcal{C}_2(\theta_c)\right)$$

A.7.1 Joint probability of two $\tilde{X}_i$'s

We consider the bivariate case. The probability mass function is described by the following contingency table:

$$
\begin{array}{c|cc|c}
 & \tilde{X}_2 = 0 & \tilde{X}_1 = 1 & \\
\hline
\tilde{X}_1 = 0 & \pi_{0,0} & \pi_{0,1} & \pi_0 = 1 - \tilde{p} \\
\tilde{X}_1 = 1 & \pi_{1,0} & \pi_{1,1} & \pi_1 = \tilde{p} \\
\hline
 & \pi_0 = 1 - \tilde{p} & \pi_1 = \tilde{p} & 1
\end{array}
\tag{49}
$$

Since we have $\Pr\left\{\tilde{X}_1 \leq u_1, \tilde{X}_2 \leq u_2\right\} = \mathbf{C}_{(\theta_c)}(\mathbf{B}(u_1), \mathbf{B}(u_2))$, we deduce that:

$$
\begin{aligned}
\mathbf{C}_{(\theta_c)}(\mathbf{B}(0), \mathbf{B}(0)) &= \mathbf{C}_{(\theta_c)}(1 - \tilde{p}, 1 - \tilde{p}) \\
\mathbf{C}_{(\theta_c)}(\mathbf{B}(0), \mathbf{B}(1)) &= \mathbf{C}_{(\theta_c)}(1 - \tilde{p}, 1) = 1 - \tilde{p} \\
\mathbf{C}_{(\theta_c)}(\mathbf{B}(1), \mathbf{B}(0)) &= \mathbf{C}_{(\theta_c)}(1, 1 - \tilde{p}) = 1 - \tilde{p} \\
\mathbf{C}_{(\theta_c)}(\mathbf{B}(1), \mathbf{B}(1)) &= \mathbf{C}_{(\theta_c)}(1, 1) = 1
\end{aligned}
$$

and:

$$
\begin{array}{c|cc|c}
 & \tilde{X}_2 = 0 & \tilde{X}_1 = 1 & \\
\hline
\tilde{X}_1 = 0 & \mathbf{C}_{(\theta_c)}(1 - \tilde{p}, 1 - \tilde{p}) & 1 - \tilde{p} - \mathbf{C}_{(\theta_c)}(1 - \tilde{p}, 1 - \tilde{p}) & 1 - \tilde{p} \\
\tilde{X}_1 = 1 & 1 - \tilde{p} - \mathbf{C}_{(\theta_c)}(1 - \tilde{p}, 1 - \tilde{p}) & \mathbf{C}_{(\theta_c)}(1 - \tilde{p}, 1 - \tilde{p}) + 2\tilde{p} - 1 & \tilde{p} \\
\hline
 & 1 - \tilde{p} & \tilde{p} & 1
\end{array}
\tag{50}
$$

In the case where $\mathbf{C}_{(\theta_c)} = \mathbf{C}^{\perp}$, $\tilde{X}_1$ and $\tilde{X}_2$ are independent, we retrieve the results obtained for the individual-based model:

$$
\begin{array}{c|cc|c}
 & \tilde{X}_2 = 0 & \tilde{X}_1 = 1 & \\
\hline
\tilde{X}_1 = 0 & (1 - \tilde{p})^2 & (1 - \tilde{p})\tilde{p} & 1 - \tilde{p} \\
\tilde{X}_1 = 1 & (1 - \tilde{p})\tilde{p} & \tilde{p}^2 & \tilde{p} \\
\hline
 & 1 - \tilde{p} & \tilde{p} & 1
\end{array}
\tag{51}
$$

---

[49]The Normal copula depends on the correlation matrix Σ. Here, we assume a uniform redemption correlation, implying that Σ is the constant correlation matrix $\mathcal{C}_n(\theta_c)$ where θ_c is the pairwise correlation.

because $\mathbf{C}^{\perp}(u_1, u_2) = u_1 u_2$. In the case where $\mathbf{C}_{(\theta_c)} = \mathbf{C}^{+}$, $\tilde{X}_1$ and $\tilde{X}_2$ are perfectly dependent and we obtain the following contingency table:

$$
\begin{array}{c|cc|c}
 & \tilde{X}_2 = 0 & \tilde{X}_1 = 1 & \\
\hline
\tilde{X}_1 = 0 & 1 - \tilde{p} & 0 & 1 - \tilde{p} \\
\tilde{X}_1 = 1 & 0 & \tilde{p} & \tilde{p} \\
\hline
 & 1 - \tilde{p} & \tilde{p} & 1
\end{array}
\tag{52}
$$

because $\mathbf{C}^{+}(u_1, u_2) = \min(u_1, u_2)$. The contingency tables (51) and (52) represent the two extremes cases.

Remark 22 *If we use a radially symmetric copula (Nelsen, 2006) such that:*

$$
\mathbf{C}_{(\theta_c)}(u_1, u_2) = u_1 + u_2 - 1 + \mathbf{C}_{(\theta_c)}(1 - u_1, 1 - u_2)
$$

the contingency table (50) becomes:

$$
\begin{array}{c|cc|c}
 & \tilde{X}_2 = 0 & \tilde{X}_1 = 1 & \\
\hline
\tilde{X}_1 = 0 & 1 - 2\tilde{p} + \mathbf{C}_{(\theta_c)}(\tilde{p}, \tilde{p}) & \tilde{p} - \mathbf{C}_{(\theta_c)}(\tilde{p}, \tilde{p}) & 1 - \tilde{p} \\
\tilde{X}_1 = 1 & p - \mathbf{C}_{(\theta_c)}(\tilde{p}, \tilde{p}) & \mathbf{C}_{(\theta_c)}(\tilde{p}, \tilde{p}) & \tilde{p} \\
\hline
 & 1 - \tilde{p} & \tilde{p} & 1
\end{array}
$$

In the general case, we obtain a similar contingency table by replacing the copula function $\mathbf{C}_{(\theta_c)}(u_1, u_2)$ by its corresponding survival function $\breve{\mathbf{C}}_{(\theta_c)}(u_1, u_2)$ because we have (Nelsen, 2006):

$$
\breve{\mathbf{C}}_{(\theta_c)}(u_1, u_2) = u_1 + u_2 - 1 + \mathbf{C}_{(\theta_c)}(1 - u_1, 1 - u_2)
$$

A.7.2 Computation of $\Pr\left\{\tilde{Z} = 0\right\}$

This case corresponds to the situation where no client redeems:

$$
\begin{aligned}
\Pr\left\{\tilde{Z} = 0\right\} &= \Pr\left\{\sum_{i=1}^{n} \omega_i \tilde{X}_i \tilde{Y}_i = 0\right\} \\
&= \Pr\left\{\tilde{X}_1 = 0, \ldots, \tilde{X}_n = 0\right\} \\
&= \mathbf{C}_{(\theta_c)}(1 - \tilde{p}, \ldots, 1 - \tilde{p})
\end{aligned}
\tag{53}
$$

In the case where $\mathbf{C}_{(\theta_c)} = \mathbf{C}^{\perp}$, we retrieve the result $\Pr\left\{\tilde{Z} = 0\right\} = (1 - \tilde{p})^n$. In the case where $\mathbf{C}_{(\theta_c)} = \mathbf{C}^{+}$, we obtain $\Pr\left\{\tilde{Z} = 0\right\} = 1 - \tilde{p}$.

A.7.3 Statistical moments

First moment For the mean, we have:

$$
\begin{aligned}
\mathbb{E}\left[\tilde{Z}\right] &= \mathbb{E}\left[\sum_{i=1}^{n} \omega_i \tilde{X}_i \tilde{Y}_i\right] \\
&= \sum_{i=1}^{n} \omega_i \mathbb{E}\left[\tilde{X}_i\right] \mathbb{E}\left[\tilde{Y}_i\right]
\end{aligned}
$$

We deduce that:

$$
\mu_1\left(\tilde{Z}\right) = \tilde{p}\mu_1\left(\tilde{Y}\right)
\tag{54}
$$

Second moment Using the contingency table (50), we have:

$$
\begin{aligned}
\mathbb{E}\left[\tilde{X}_1 \tilde{X}_2\right] &= \mathbf{C}_{(\theta_c)}\left(1-\tilde{p}, 1-\tilde{p}\right) + 2\tilde{p} - 1 \\
&= \check{\mathbf{C}}_{(\theta_c)}\left(\tilde{p}, \tilde{p}\right)
\end{aligned}
$$

It follows that:

$$
\begin{aligned}
\mathbb{E}\left[\tilde{Z}^2\right] &= \mathbb{E}\left[\left(\sum_{i=1}^{n} \omega_i \tilde{X}_i \tilde{Y}_i\right)^2\right] \\
&= \mathbb{E}\left[\sum_{i=1}^{n} \omega_i^2 \tilde{X}_i^2 \tilde{Y}_i^2 + 2\sum_{j>i} \omega_i \omega_j \tilde{X}_i \tilde{X}_j \tilde{Y}_i \tilde{Y}_j\right] \\
&= \tilde{p}\mu_2'\left(\tilde{Y}\right)\sum_{i=1}^{n}\omega_i^2 + 2\check{\mathbf{C}}_{(\theta_c)}\left(\tilde{p}, \tilde{p}\right)\mu_1^2\left(\tilde{Y}\right)\sum_{j>i}\omega_i\omega_j
\end{aligned}
$$

and

$$
\begin{aligned}
\mu_2\left(\tilde{Z}\right) &= \mathbb{E}\left[\tilde{Z}^2\right] - \mathbb{E}^2\left[\tilde{Z}\right] \\
&= \tilde{p}\mu_2'\left(\tilde{Y}\right)\sum_{i=1}^{n}\omega_i^2 + 2\check{\mathbf{C}}_{(\theta_c)}\left(\tilde{p}, \tilde{p}\right)\mu_1^2\left(\tilde{Y}\right)\sum_{j>i}\omega_i\omega_j - \tilde{p}^2\mu_1^2\left(\tilde{Y}\right) \\
&= \tilde{p}\left(\mu_2\left(\tilde{Y}\right) + \mu_1^2\left(\tilde{Y}\right)\right)\mathcal{H}\left(\omega\right) + \check{\mathbf{C}}_{(\theta_c)}\left(\tilde{p}, \tilde{p}\right)\mu_1^2\left(\tilde{Y}\right)\left(1 - \mathcal{H}\left(\omega\right)\right) - \tilde{p}^2\mu_1^2\left(\tilde{Y}\right) \\
&= \tilde{p}\mu_2\left(\tilde{Y}\right)\mathcal{H}\left(\omega\right) + \left(\tilde{p}\mathcal{H}\left(\omega\right) + \check{\mathbf{C}}_{(\theta_c)}\left(\tilde{p}, \tilde{p}\right)\left(1 - \mathcal{H}\left(\omega\right)\right) - \tilde{p}^2\right)\mu_1^2\left(\tilde{Y}\right) \\
&= \left(\tilde{p}\mu_2\left(\tilde{Y}\right) + \left(\tilde{p} - \check{\mathbf{C}}_{(\theta_c)}\left(\tilde{p}, \tilde{p}\right)\right)\mu_1^2\left(\tilde{Y}\right)\right)\mathcal{H}\left(\omega\right) + \left(\check{\mathbf{C}}_{(\theta_c)}\left(\tilde{p}, \tilde{p}\right) - \tilde{p}^2\right)\mu_1^2\left(\tilde{Y}\right)
\end{aligned}
$$

$$(55)$$

In the case where $\mathbf{C}_{(\theta_c)} = \mathbf{C}^{\perp}$, we have $\check{\mathbf{C}}_{(\theta_c)}\left(\tilde{p}, \tilde{p}\right) = \tilde{p}^2$. Therefore, we retrieve the result found in Equation (47) on page 84:

$$
\mu_2\left(\tilde{Z}\right) = \tilde{p}\left(\mu_2\left(\tilde{Y}\right) + \left(1 - \tilde{p}\right)\mu_1^2\left(\tilde{Y}\right)\right)\mathcal{H}\left(\omega\right)
$$

In the case where $\mathbf{C}_{(\theta_c)} = \mathbf{C}^{+}$, we have $\check{\mathbf{C}}_{(\theta_c)}\left(\tilde{p}, \tilde{p}\right) = \tilde{p}$ and we obtain:

$$
\mu_2\left(\tilde{Z}\right) = \tilde{p}\mu_2\left(\tilde{Y}\right)\mathcal{H}\left(\omega\right) + \tilde{p}\left(1 - \tilde{p}\right)\mu_1^2\left(\tilde{Y}\right)
$$

A.8 Statistical moments of the redemption frequency

We recall that $\tilde{X}_i \sim \mathcal{B}\left(\tilde{p}\right)$, meaning that $\mathbb{E}\left[\tilde{X}_i\right] = \mathbb{E}\left[\tilde{X}_i^2\right] = \tilde{p}$. The weighted redemption frequency is defined as follows:

$$
\mathcal{F} = \sum_{i=1}^{n} \omega_i \tilde{X}_i
$$

We have:

$$
\begin{aligned}
\mathbb{E}\left[\mathcal{F}\right] &= \mathbb{E}\left[\sum_{i=1}^{n} \omega_i \tilde{X}_i\right] \\
&= \tilde{p}
\end{aligned}
$$

and:

$$\begin{aligned}
\mathbb{E}\left[\mathcal{F}^2\right] &= \mathbb{E}\left[\left(\sum_{i=1}^{n}\omega_i\tilde{X}_i\right)^2\right]\\
&= \mathbb{E}\left[\sum_{i=1}^{n}\omega_i^2\tilde{X}_i^2 + 2\sum_{j>i}\omega_i\omega_j\tilde{X}_i\tilde{X}_j\right]\\
&= \tilde{p}\mathcal{H}\left(\omega\right) + \check{\mathbf{C}}_{(\theta_c)}\left(\tilde{p},\tilde{p}\right)\left(1-\mathcal{H}\left(\omega\right)\right)
\end{aligned}$$

We deduce that:

$$\mu_2\left(\mathcal{F}\right) = \tilde{p}\mathcal{H}\left(\omega\right) + \check{\mathbf{C}}_{(\theta_c)}\left(\tilde{p},\tilde{p}\right)\left(1-\mathcal{H}\left(\omega\right)\right) - \tilde{p}^2$$

Remark 23 *We notice that the expected value and the volatility of the redemption frequency are related in the following way:*

$$\mu_2\left(\mathcal{F}\right) = \mathbb{E}\left[\mathcal{F}\right]\left(\mathcal{H}\left(\omega\right) - \mathbb{E}\left[\mathcal{F}\right]\right) + \check{\mathbf{C}}\left(\mathbb{E}\left[\mathcal{F}\right],\mathbb{E}\left[\mathcal{F}\right]\right)\left(1-\mathcal{H}\left(\omega\right)\right) \tag{56}$$

A.9 Pearson correlation between two redemption frequencies

We consider two redemption frequencies $\mathcal{F}_1$ and $\mathcal{F}_2$. The redemption frequency $\mathcal{F}_k$ is associated to the liability structure $(\omega_{k,1},\ldots,\omega_{k,n_k})$ and corresponds to an investor category, whose redemption probability is $\tilde{p}_k$ and frequency correlation is characterized by the copula function $\mathbf{C}_{(\theta_k)}$ $(k=1,2)$. We also assume that the redemption correlation between the two investor categories is defined by the copula function $\mathbf{C}_{(\theta_{12})}$. It follows that we have three copula functions:

- $\mathbf{C}_{(\theta_1)}$ is the copula function that defines the frequency correlation between the investors of the first category;

- $\mathbf{C}_{(\theta_2)}$ is the copula function that defines the frequency correlation between the investors of the second category;

- $\mathbf{C}_{(\theta_{12})}$ is the copula function that defines the frequency correlation between the investors of the first category and those of the second category.

In the case where the two categories are the same, we have $\mathbf{C}_{(\theta_1)} = \mathbf{C}_{(\theta_2)} = \mathbf{C}_{(\theta_{12})} = \mathbf{C}_{(\theta_c)}$.

To compute the covariance between $\mathcal{F}_1$ and $\mathcal{F}_2$, we calculate the mathematical expectation of the cross product:

$$\begin{aligned}
\mathbb{E}\left[\mathcal{F}_1\mathcal{F}_2\right] &= \mathbb{E}\left[\left(\sum_{i=1}^{n_1}\omega_{1,i}\tilde{X}_{1,i}\right)\left(\sum_{j=1}^{n_2}\omega_{2,j}\tilde{X}_{2,j}\right)\right]\\
&= \mathbb{E}\left[\sum_{i=1}^{n_1}\sum_{j=1}^{n_2}\omega_{1,i}\omega_{2,j}\tilde{X}_{1,i}\tilde{X}_{2,j}\right]\\
&= \mathbb{E}\left[\tilde{X}_{1,i}\tilde{X}_{2,j}\right]\left(\sum_{i=1}^{n_1}\sum_{j=1}^{n_2}\omega_{1,i}\omega_{2,j}\right)\\
&= \check{\mathbf{C}}_{(\theta_{12})}\left(\tilde{p}_1,\tilde{p}_2\right)
\end{aligned}$$

because $\sum_{i=1}^{n_1} \sum_{j=1}^{n_2} \omega_{1,i} \omega_{2,j} = 1$. We deduce the expression of the Pearson correlation:

$$\rho\left(\mathcal{F}_1, \mathcal{F}_2\right) = \frac{\check{\mathbf{C}}_{(\theta_{12})}\left(\tilde{p}_1, \tilde{p}_2\right) - \tilde{p}_1 \tilde{p}_2}{\sqrt{\mu_2\left(\mathcal{F}_1\right) \mu_2\left(\mathcal{F}_2\right)}} \tag{57}$$

where:

$$\mu_2\left(\mathcal{F}_k\right) = \tilde{p}_k\left(\mathcal{H}\left(\omega_k\right) - \tilde{p}_k\right) + \check{\mathbf{C}}_{(\theta_k)}\left(\tilde{p}_k, \tilde{p}_k\right)\left(1 - \mathcal{H}\left(\omega_k\right)\right) \qquad k = 1, 2$$

Remark 24 *The Pearson correlation $\rho\left(\mathcal{F}_1, \mathcal{F}_2\right)$ is equal to zero if only if[50] $\mathbf{C}_{(\theta_k)}$ is the product copula $\mathbf{C}^{\perp}$.*

Remark 25 *In the case where the two investor categories are the same and the liability structures are equally-weighted, we have $\tilde{p}_1 = \tilde{p}_2 = \tilde{p}$ and $\mathbf{C}_{(\theta_1)} = \mathbf{C}_{(\theta_2)} = \mathbf{C}_{(\theta_{12})} = \mathbf{C}_{(\theta_c)}$, and we obtain:*

$$\rho\left(\mathcal{F}_1, \mathcal{F}_2\right) = \frac{\check{\mathbf{C}}_{(\theta_c)}\left(\tilde{p}, \tilde{p}\right) - \tilde{p}^2}{\sqrt{\mu_2\left(\mathcal{F}_1\right) \mu_2\left(\mathcal{F}_2\right)}} \tag{58}$$

where:

$$\mu_2\left(\mathcal{F}_k\right) = \check{\mathbf{C}}_{(\theta_c)}\left(\tilde{p}, \tilde{p}\right) - \tilde{p}^2 + \frac{\tilde{p} - \check{\mathbf{C}}_{(\theta_c)}\left(\tilde{p}, \tilde{p}\right)}{n_k} \qquad k = 1, 2$$

The limiting case $n_k \to \infty$ is equal to $\rho\left(\mathcal{F}_1, \mathcal{F}_2\right) = 1$. This is normal since $\mathcal{F}_1$ and $\mathcal{F}_2$ converges to $\tilde{p}$ when the liability structure is infinitely fine-grained.

B   Data

---

[50]We recall that $\mathbf{C}_{(\theta_k)}$ is the Clayton or the Normal copula. In the general case, this property does not hold.

Table 40: Breakdown of the liability dataset by investor and fund categories

Total number n of observations	Balanced	Bond	Enhanced Treasury	Equity	Money Market	Other	Structured	Total
Auto-consumption	22 762	46 651	3 784	46 678	6 175	34 064	0	160 114
Central bank	2 791	7 400	0	4 730	602	0	0	15 523
Corporate	10 780	13 457	2 305	6 962	7 812	6 164	0	47 480
Corporate pension fund	14 827	24 429	427	17 975	3 029	5 474	427	66 588
Employee savings plan	9 894	4 240	1 349	19 145	3 232	0	5 279	43 139
Institutional	50 813	95 013	3 961	76 057	9 542	31 973	241	267 600
Insurance	10 577	45 494	3 303	23 145	12 633	6 528	0	101 680
Other	27 938	29 817	5 816	4 898	9 347	18 717	0	96 533
Retail	140 023	86 937	7 531	99 624	15 418	31 370	83 496	464 399
Sovereign	7 291	12 788	854	14 183	3 471	5 308	0	43 895
Third-party distributor	63 792	86 716	5 247	123 004	11 160	15 407	5 126	310 452
Total	361 488	452 942	34 577	436 401	82 421	155 005	94 569	1 617 403

Total number n_1 of redemptions	Balanced	Bond	Enhanced Treasury	Equity	Money Market	Other	Structured	Total
Auto-consumption	3 744	8 796	1 135	11 871	3 040	883	0	29 469
Central bank	4	16	0	38	18	0	0	76
Corporate	324	484	144	159	3 110	20	0	4 241
Corporate pension fund	460	513	17	447	213	17	2	1 669
Employee savings plan	264	120	40	519	74	0	145	1 162
Institutional	1 973	3 098	74	3 422	2 754	229	0	11 550
Insurance	568	1 562	114	1 596	2 409	61	0	6 310
Other	1 145	926	219	805	2 009	278	0	5 382
Retail	54 095	36 018	3 932	67 862	6 882	5 030	22 783	196 602
Sovereign	494	118	9	381	521	2	0	1 525
Third-party distributor	19 837	29 140	2 277	54 689	7 127	4 569	334	117 973
Total	82 908	80 791	7 961	141 789	28 157	11 089	23 264	375 959

Source: Amundi Cube Database (2020) and authors' calculation.

Table 41: Breakdown of the liability dataset by investor and fund categories (without mandates and dedicated mutual funds)

Total number n of observations	Balanced	Bond	Enhanced Treasury	Equity	Money Market	Other	Structured	Total
Auto-consumption	16 147	43 189	3 783	43 737	6 008	13 793	0	126 657
Central bank	1 281	580	0	476	0	0	0	2 337
Corporate	1 862	6 542	2 305	5 468	7 812	4 235	0	28 224
Corporate pension fund	2 344	8 650	427	9 031	2 670	1 277	0	24 399
Employee savings plan	9 894	4 240	1 349	19 145	3 232	0	5 279	43 139
Institutional	6 858	36 792	3 716	41 104	8 329	16 029	0	112 828
Insurance	3 436	13 011	3 303	21 832	8 543	5 750	0	55 875
Other	7 577	12 751	5 428	4 155	9 333	11 788	0	51 032
Retail	115 394	77 879	6 692	95 393	14 798	27 834	83 118	421 108
Sovereign	2 969	2 261	854	3 405	2 853	1 746	0	14 088
Third-party distributor	55 696	75 591	4 929	114 171	10 732	13 483	5 126	279 728
Total	223 458	281 486	32 786	357 917	74 310	95 935	93 523	1 159 415

Total number n_1 of redemptions	Balanced	Bond	Enhanced Treasury	Equity	Money Market	Other	Structured	Total
Auto-consumption	3 492	8 385	1 135	11 137	3 040	881	0	28 070
Central bank	2	2	0	7	0	0	0	11
Corporate	280	405	144	157	3 110	9	0	4 105
Corporate pension fund	190	292	17	304	202	0	0	1 005
Employee savings plan	264	120	40	519	74	0	145	1 162
Institutional	1 328	2 312	73	2 677	2 734	166	0	9 290
Insurance	419	874	114	1 576	2 385	60	0	5 428
Other	733	493	200	804	2 008	262	0	4 500
Retail	51 454	35 079	3 932	67 250	6 770	4 875	22 707	192 067
Sovereign	484	72	9	343	520	1	0	1 429
Third-party distributor	18 808	28 242	2 266	52 445	7 077	4 431	334	113 603
Total	77 454	76 276	7 930	137 219	27 920	10 685	23 186	360 670

Source: Amundi Cube Database (2020) and authors' calculation.

C Additional results

Figure 37: Third-party distributor
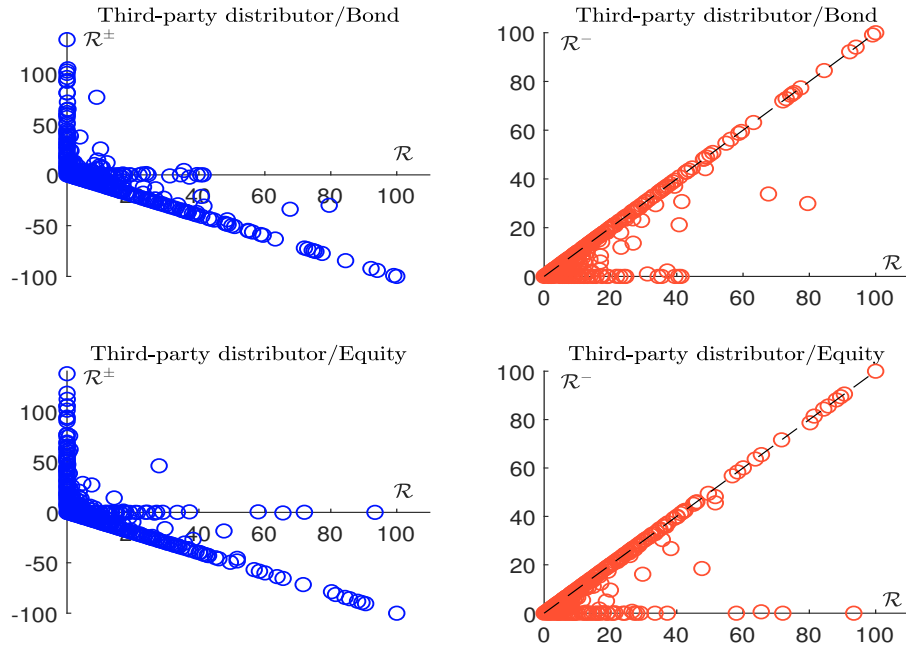
Figure 38: Relationship between the stress scenario of the big fund and the stress scenario of n equivalent small funds
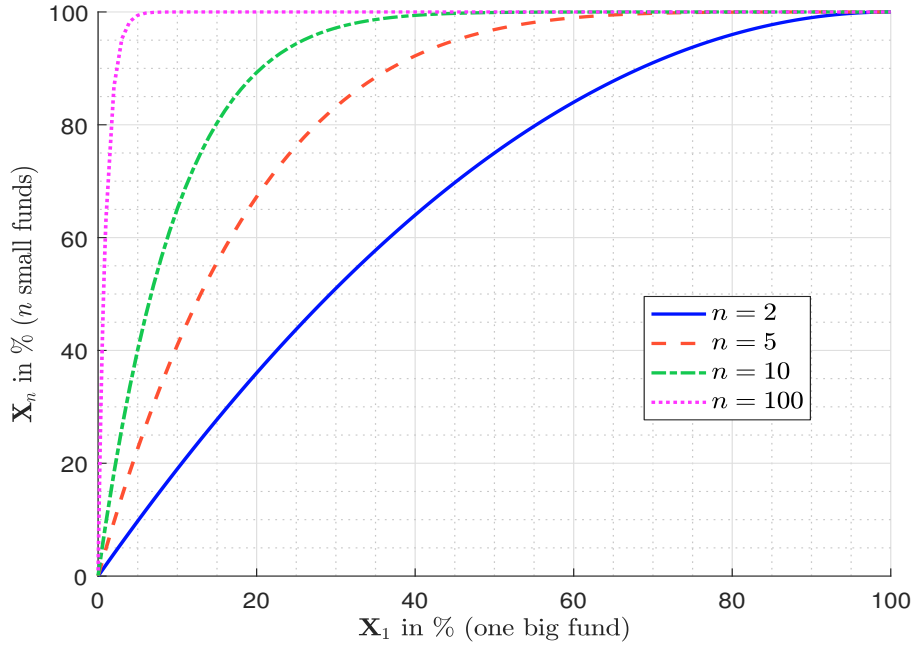
Figure 39: Relationship between the confidence level α of $\mathbf{F}^{-1}(\alpha)$ and the confidence level $\alpha_{\mathbf{G}}$ of $\mathbf{G}^{-1}(\alpha_{\mathbf{G}})$
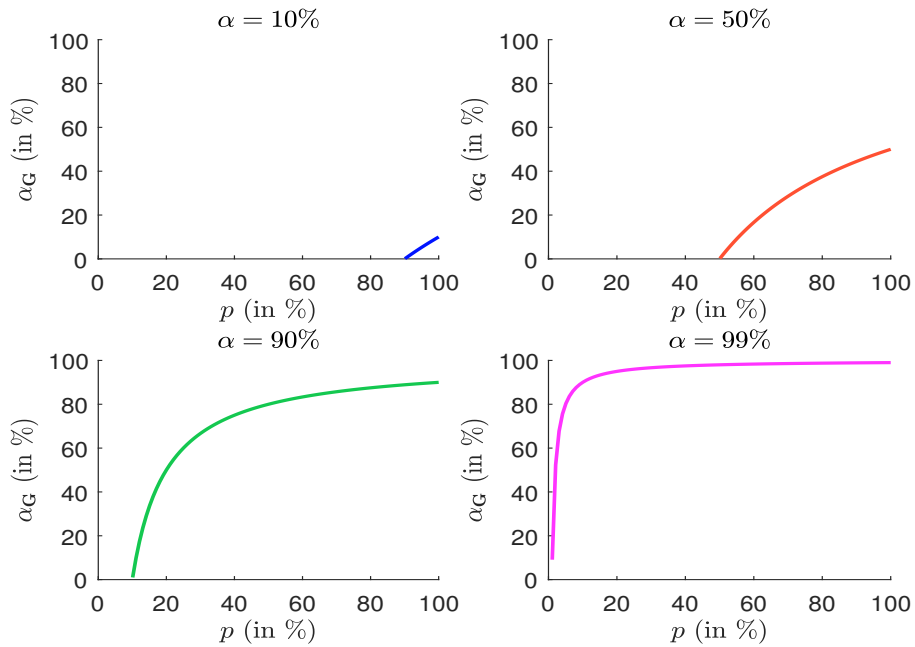
Figure 40: Stress scenario $\mathbb{S}\left(\mathcal{T}\right)$ in % ($p = 5\%$)
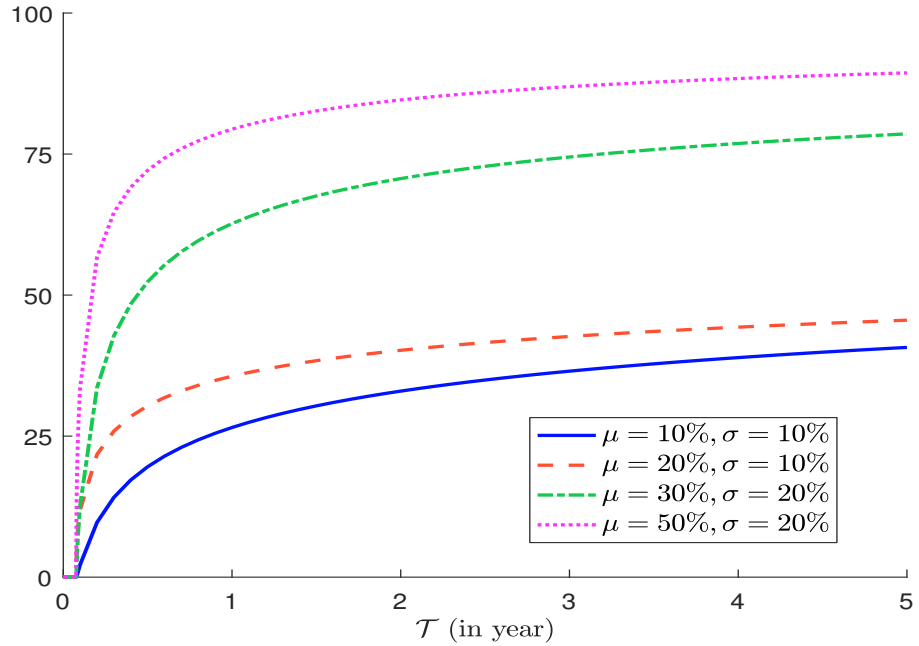
Figure 41: Stress scenario $\mathbb{S}\left(\mathcal{T}\right)$ in % ($p = 50\%$)
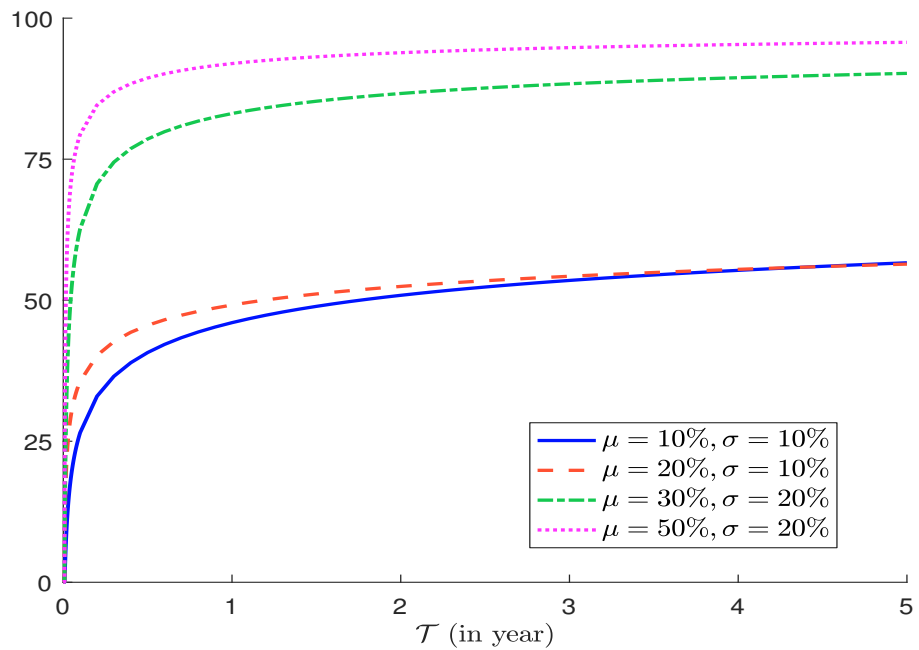
Table 42: Estimated value of a (method of moments)

	(1)	(2)	(3)	(4)	(5)	(6)	(7)	(8)
Auto-consumption	0.02	0.05	0.03	0.03	0.09	0.06		0.04
Central bank								
Corporate	0.00	0.04			0.21			0.14
Corporate pension fund		0.01		0.01	0.21			0.04
Employee savings plan	0.14			0.04				0.04
Institutional	0.01	0.04		0.06	0.10			0.05
Insurance	0.01	0.02		0.02	0.12			0.05
Other	0.05	0.05		0.01	0.05	0.01		0.03
Retail	0.01	0.01	0.01	0.01	0.05	0.01	0.00	0.01
Sovereign	0.05			0.02	0.11			0.04
Third-party distributor	0.01	0.03	0.02	0.02	0.07	0.01	0.02	0.02
Total	0.01	0.02	0.02	0.01	0.07	0.02	0.00	0.02

(1) = balanced, (2) = bond, (3) = enhanced treasury, (4) = equity, (5) = money market, (6) = other, (7) = structured, (8) = total

Table 43: Estimated value of b (method of moments)

	(1)	(2)	(3)	(4)	(5)	(6)	(7)	(8)
Auto-consumption	1.23	2.86	1.20	2.25	2.81	2.23		2.28
Central bank								
Corporate	0.78	1.62			5.34			3.61
Corporate pension fund		0.41		0.50	2.69			1.09
Employee savings plan	10.89			1.84				1.73
Institutional	1.21	1.52		2.13	2.15			1.60
Insurance	0.78	0.91		1.07	3.58			1.91
Other	5.58	1.84		1.04	1.35	1.17		1.23
Retail	3.29	3.56	2.98	4.11	2.39	3.07	1.11	3.00
Sovereign	86.69			0.83	0.90			0.87
Third-party distributor	3.83	4.21	1.44	5.22	5.14	1.48	1.43	3.89
Total	2.68	2.80	1.01	2.89	2.58	1.60	0.97	2.43

(1) = balanced, (2) = bond, (3) = enhanced treasury, (4) = equity, (5) = money market, (6) = other, (7) = structured, (8) = total

Table 44: Estimated value of a (method of maximum likelihood)

	(1)	(2)	(3)	(4)	(5)	(6)	(7)	(8)
Auto-consumption	0.20	0.26	0.26	0.23	0.32	0.25		0.24
Central bank								
Corporate	0.23	0.19			0.39			0.30
Corporate pension fund		0.13		0.13	0.37			0.16
Employee savings plan	1.03			0.52				0.57
Institutional	0.22	0.19		0.21	0.28			0.22
Insurance	0.14	0.15		0.17	0.28			0.19
Other	0.26	0.21		0.27	0.25	0.28		0.23
Retail	0.31	0.30	0.26	0.33	0.27	0.27	0.36	0.29
Sovereign	0.68			0.17	0.31			0.19
Third-party distributor	0.40	0.28	0.24	0.30	0.34	0.27	0.26	0.30
Total	0.29	0.25	0.23	0.27	0.29	0.24	0.32	0.25

(1) = balanced, (2) = bond, (3) = enhanced treasury, (4) = equity, (5) = money market, (6) = other, (7) = structured, (8) = total

Table 45: Estimated value of b (method of maximum likelihood)

	(1)	(2)	(3)	(4)	(5)	(6)	(7)	(8)
Auto-consumption	6.53	11.36	17.89	15.80	7.50	8.40		10.51
Central bank								
Corporate	26.32	6.03			8.96			6.55
Corporate pension fund		1.66		3.12	4.14			2.70
Employee savings plan	74.62			24.41				30.29
Institutional	16.24	4.94		5.65	4.64			5.04
Insurance	3.56	5.42		5.26	7.14			5.46
Other	28.00	7.99		31.90	4.82	43.34		6.72
Retail	56.99	82.20	51.08	116.86	10.51	48.15	309.26	65.57
Sovereign	1225.65			4.84	2.06			2.92
Third-party distributor	111.38	39.19	15.23	64.70	21.61	36.15	12.11	47.77
Total	44.28	26.79	15.16	44.67	7.80	20.02	206.39	26.76

(1) = balanced, (2) = bond, (3) = enhanced treasury, (4) = equity, (5) = money market, (6) = other, (7) = structured, (8) = total

Table 46: Estimated value of μ in % (method of maximum likelihood)

	(1)	(2)	(3)	(4)	(5)	(6)	(7)	(8)
Auto-consumption	2.92	2.23	1.45	1.43	4.08	2.91		2.20
Central bank								
Corporate	0.87	3.10			4.12			4.43
Corporate pension fund		7.47		4.03	8.29			5.58
Employee savings plan	1.36			2.07				1.85
Institutional	1.32	3.78		3.55	5.77			4.11
Insurance	3.78	2.62		3.08	3.80			3.44
Other	0.93	2.56		0.83	4.99	0.64		3.26
Retail	0.54	0.36	0.51	0.28	2.47	0.56	0.12	0.44
Sovereign	0.06			3.47	13.01			6.08
Third-party distributor	0.36	0.72	1.55	0.46	1.55	0.75	2.13	0.62
Total	0.66	0.92	1.46	0.59	3.53	1.16	0.15	0.92

(1) = balanced, (2) = bond, (3) = enhanced treasury, (4) = equity, (5) = money market, (6) = other, (7) = structured, (8) = total

Table 47: Estimated value of σ in % (method of maximum likelihood)

	(1)	(2)	(3)	(4)	(5)	(6)	(7)	(8)
Auto-consumption	6.05	4.16	2.74	2.88	6.66	5.41		4.28
Central bank								
Corporate	1.77	6.45			6.18			7.34
Corporate pension fund		15.74		9.53	11.74			11.68
Employee savings plan	1.32			2.80				2.39
Institutional	2.73	7.70		7.06	9.59			7.94
Insurance	8.80	6.23		6.82	6.58			7.07
Other	1.78	5.21		1.58	8.84	1.20		6.30
Retail	0.96	0.65	0.99	0.48	4.52	1.06	0.19	0.81
Sovereign	0.07			7.46	18.33			11.79
Third-party distributor	0.56	1.33	3.04	0.83	2.58	1.41	3.95	1.12
Total	1.20	1.80	2.97	1.13	6.13	2.33	0.27	1.81

(1) = balanced, (2) = bond, (3) = enhanced treasury, (4) = equity, (5) = money market, (6) = other, (7) = structured, (8) = total

Table 48: Volatility of the redemption rate in %

	(1)	(2)	(3)	(4)	(5)	(6)	(7)	(8)
Auto-consumption	3.47	3.11	5.42	3.06	6.45	2.40		3.41
Central bank	0.33	1.25		2.29				1.23
Corporate	2.16	2.45	3.43	3.07	5.08	2.22		3.57
Corporate pension fund	3.02	1.92	1.03	2.53	4.09	0.00		2.53
Employee savings plan	0.57	0.41	2.75	1.42	0.59		2.65	1.45
Institutional	2.42	2.58	7.07	2.45	6.89	1.87		3.24
Insurance	3.05	2.79	1.49	2.77	4.53	1.89		3.02
Other	1.15	1.90	4.79	3.22	5.70	1.01		3.26
Retail	1.88	1.74	2.55	1.76	5.18	1.36	1.38	1.95
Sovereign	0.10	0.45	1.66	3.19	10.07	2.39		4.94
Third-party distributor	1.57	2.15	5.22	1.76	3.88	3.37	1.80	2.17
Total	1.96	2.29	4.45	2.18	5.48	2.05	1.51	2.56

(1) = balanced, (2) = bond, (3) = enhanced treasury, (4) = equity, (5) = money market, (6) = other, (7) = structured, (8) = total

Figure 42: Liability weights in the case of the geometric liability structure $\omega_i \propto q^i$
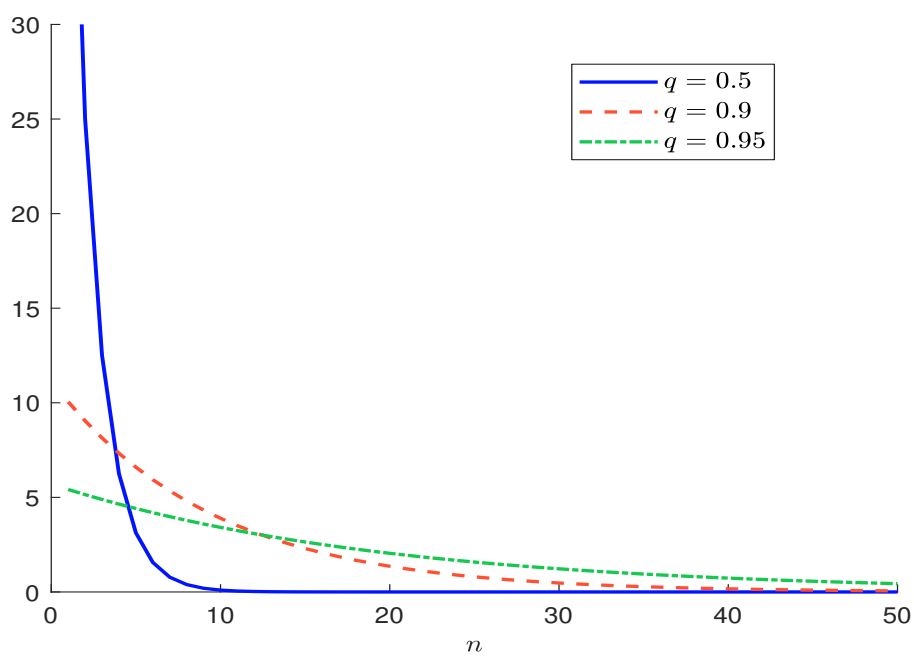
Figure 43: Comparison of $\tilde{\mathbf{F}}\left(x \mid \omega\right)$ and $\tilde{\mathbf{F}}\left(x \mid \mathcal{H}\right)$ ($q = 0.9$ and $\mathcal{H}\left(\omega\right)^{-1} = 18$))
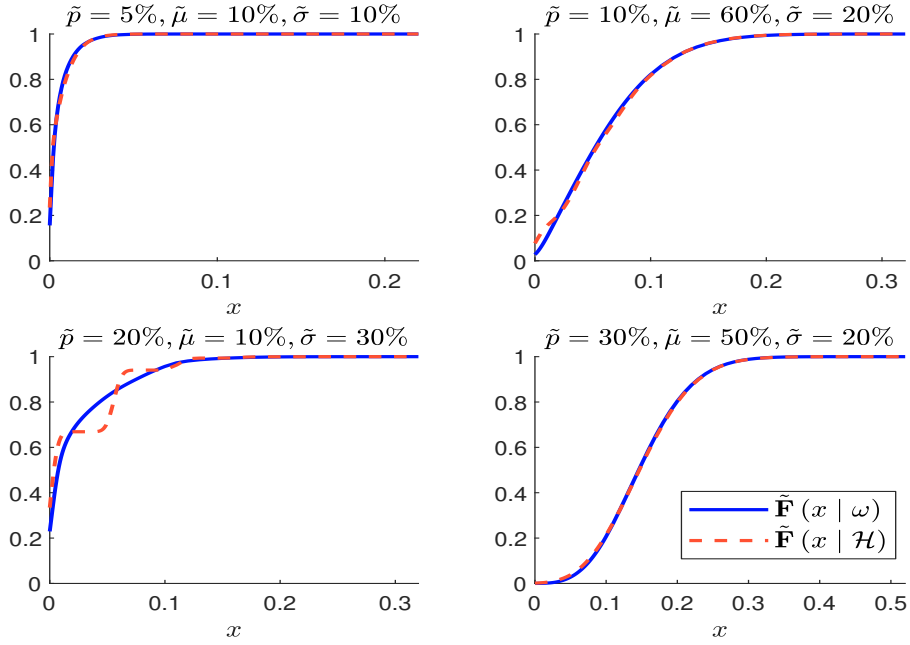
Figure 44: Comparison of $\tilde{\mathbf{F}}\left(x \mid \omega\right)$ and $\tilde{\mathbf{F}}\left(x \mid \mathcal{H}\right)$ ($q = 0.5$ and $\mathcal{H}\left(\omega\right)^{-1} = 3$))
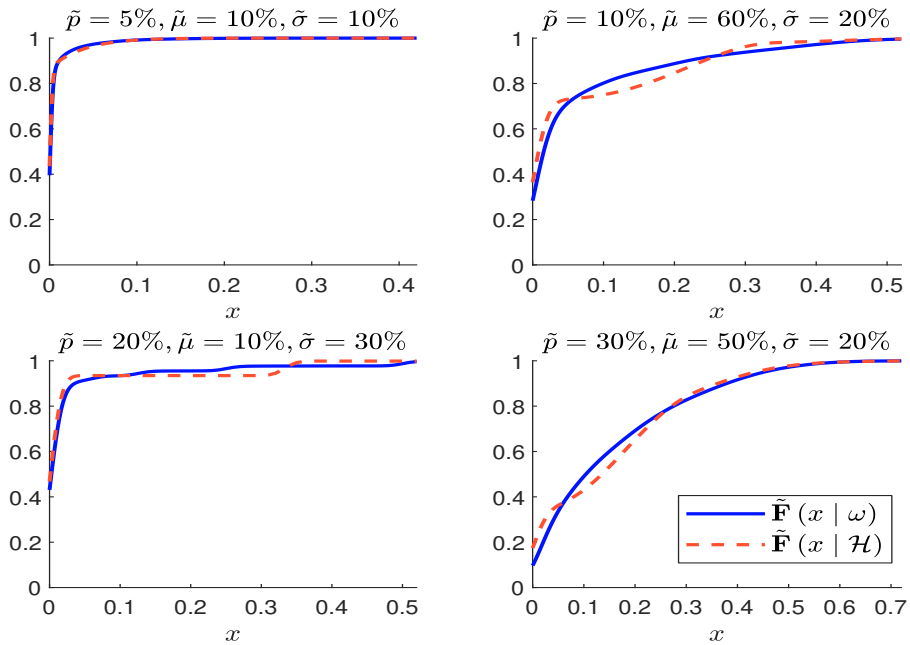
Figure 45: Probability to observe no redemption $\Pr\{\mathcal{R} = 0\}$ in % with respect to the number n of unitholders ($\tilde{p} = 10\%$)
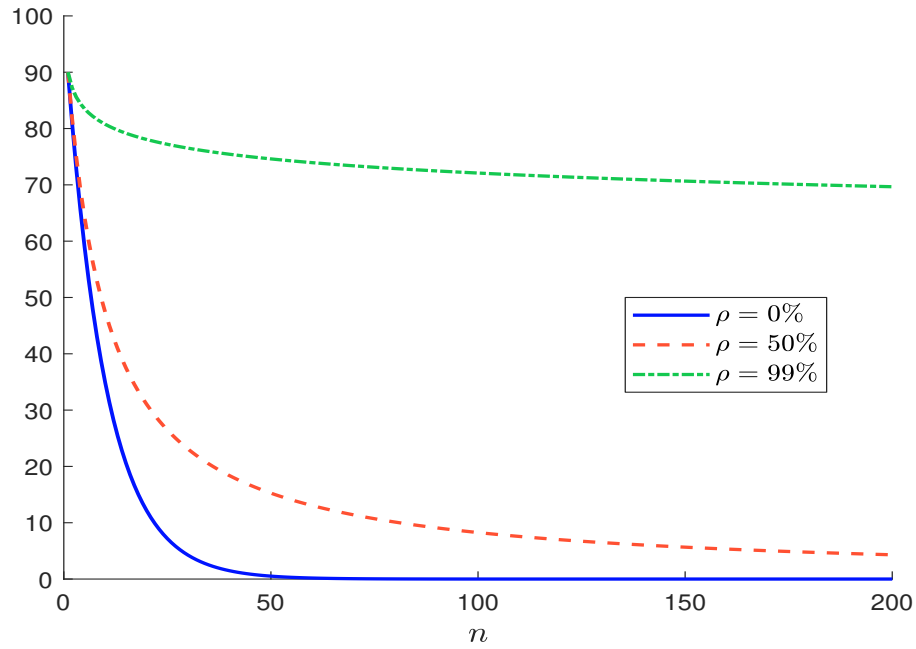
Figure 46: Probability to observe 100% of redemptions $\Pr\{\mathcal{F} = 1\}$ in % ($n = 20$)
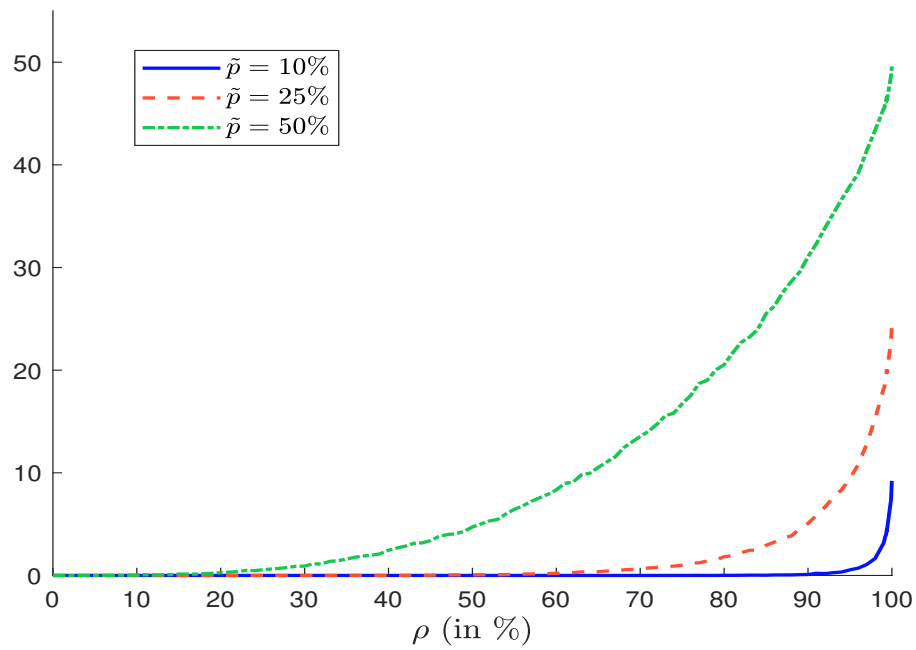
Figure 47: Histogram of the redemption rate in % with respect to the number n of unitholders $(\tilde{p} = 50\%, \tilde{\mu} = 50\%, \tilde{\sigma} = 10\%, \rho = 25\%)$
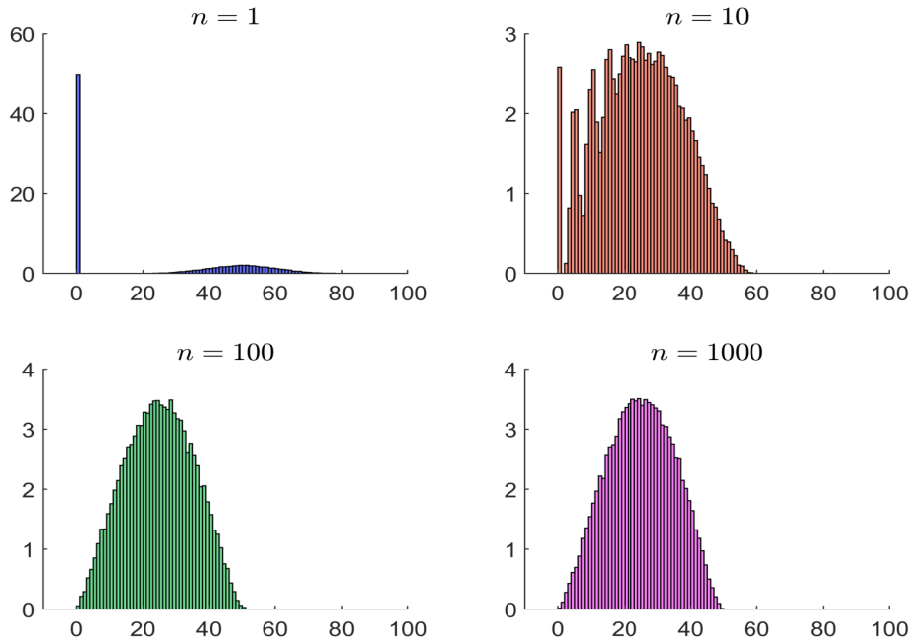
Figure 48: Histogram of the redemption rate in % with respect to the number n of unitholders $(\tilde{p} = 50\%, \tilde{\mu} = 50\%, \tilde{\sigma} = 10\%, \rho = 75\%)$
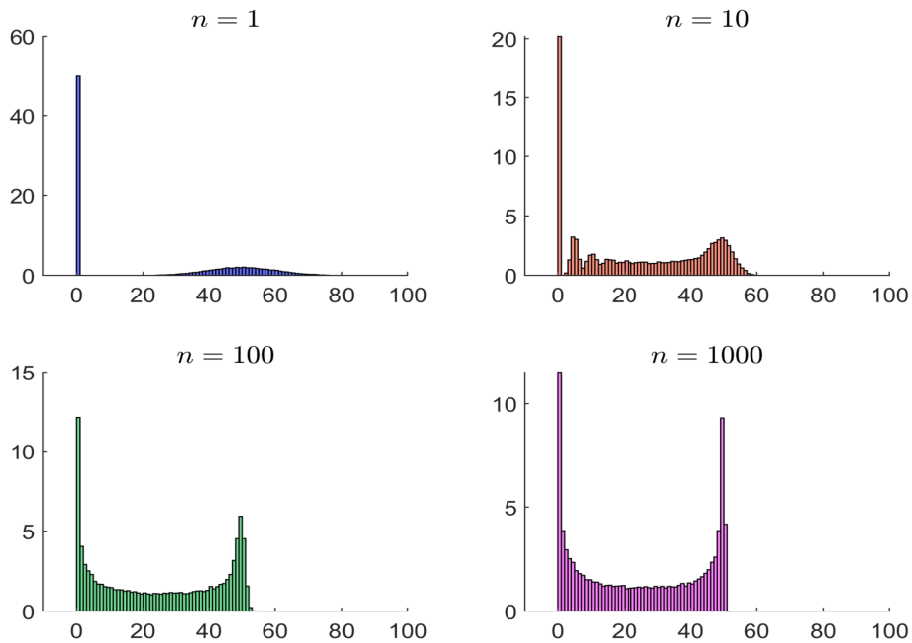
Figure 49: Histogram of the redemption rate in % with respect to the number n of unitholders ($\tilde{p} = 50\%, \tilde{\mu} = 50\%, \tilde{\sigma} = 10\%, \rho = 90\%$)
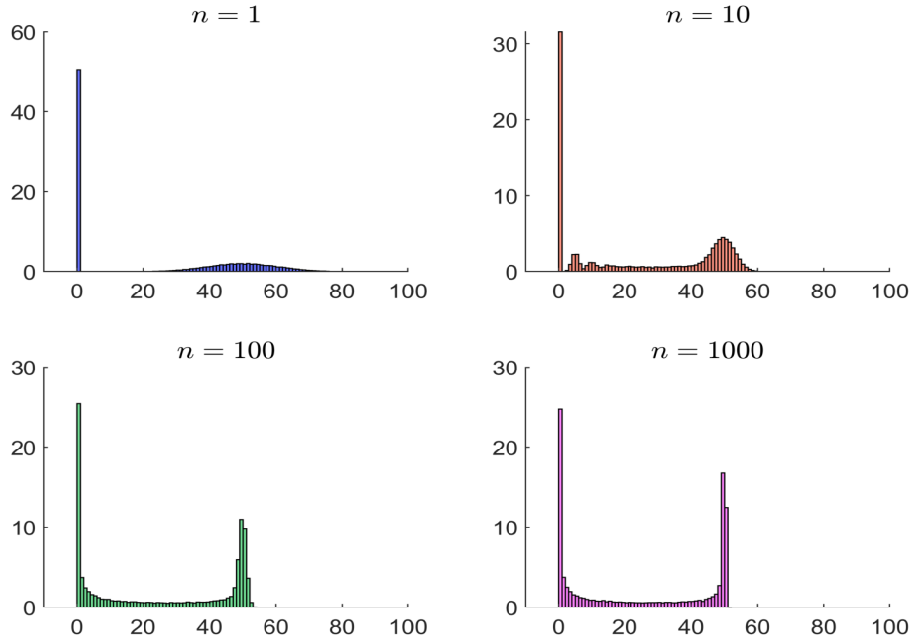
Table 49: Calibrated Pearson correlation (Normal copula, $\mathcal{H}(\omega) = 1/20$)

$\hat{\sigma}(\mathcal{F})$	$\overline{\mathcal{F}}$				
	10.0%	20.0%	25.0%	30.0%	40.0%
10.0%					
20.0%	39.88%	24.58%			
30.0%	50.00%	42.83%	38.88%	35.70%	31.70%
40.0%		50.00%	49.20%	47.77%	45.30%

Figure 50: Dependogram of the bivariate Normal copula
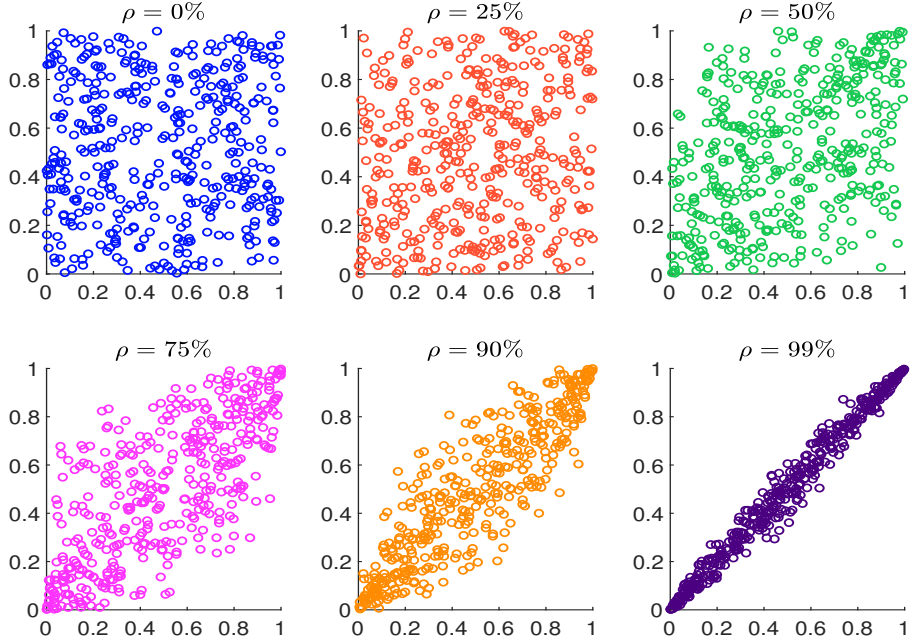
Figure 51: Dependogram of redemption rate frequencies for equity funds
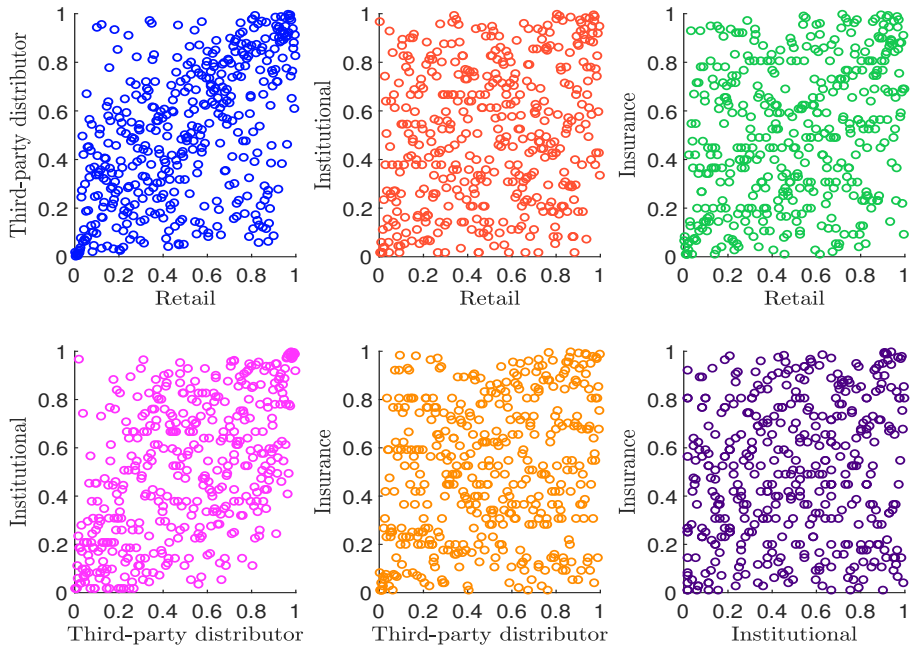
Figure 52: Histogram of the weekly redemption rate in % with respect to the autocorrelation ρ_{time} ($\tilde{p} = 50\%, \tilde{\mu} = 50\%, \tilde{\sigma} = 10\%, \rho = 50\%, n = 10$)
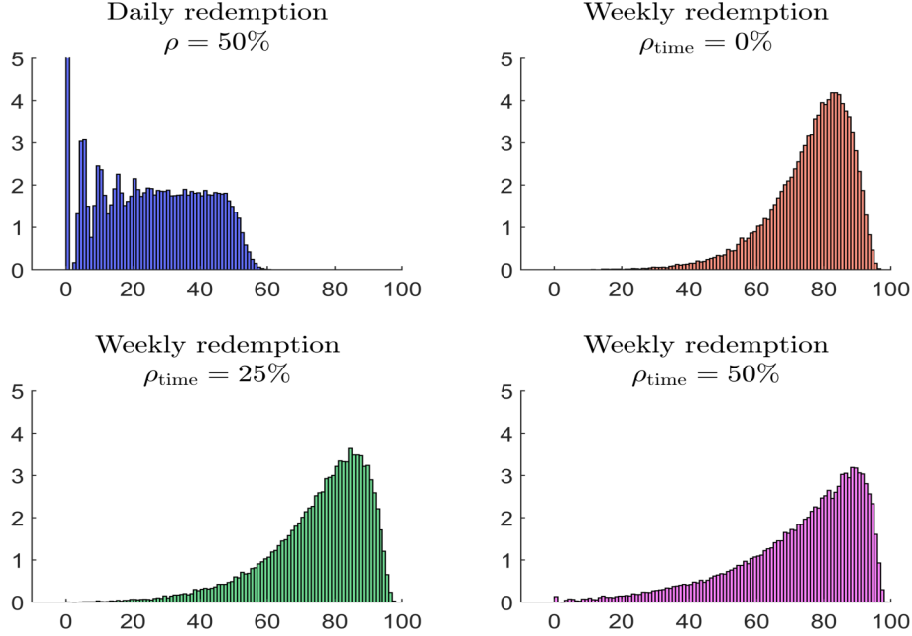
Table 50: Autocorrelation of the redemption frequency in %

	Balanced	Bond	Equity	Money market
Institutional	26.3**	12.9**	3.8	33.9**
Insurance	39.8**	10.5**	1.8	16.9**
Retail	7.9	9.8	25.2**	−0.1
Third-party distributor	15.0**	32.5**	42.4**	13.9**

Table 51: Autocorrelation of the redemption severity in %

	Balanced	Bond	Equity	Money market
Institutional	16.9**	2.0	6.1	21.4**
Insurance	−1.1	8.4	8.5	18.3**
Retail	13.5**	3.1	10.1**	12.5**
Third-party distributor	1.6	13.4**	9.9**	21.3**

Table 52: Coefficient of determination $\mathfrak{R}_c^2$ in % — $\mathcal{R}(t) = \beta_0 + \beta_1 \mathcal{F}(t) + u(t)$

	Balanced	Bond	Equity	Money market
Institutional	9.2	45.2	59.1	55.1
Insurance	2.8	18.4	22.2	53.3
Retail	68.2	61.9	60.1	55.2
Third-party distributor	51.8	66.4	54.2	64.7

Table 53: Coefficient of determination $\mathfrak{R}_c^2$ in % — $\mathcal{R}(t) = \beta_0 + \beta_1 \mathcal{R}^\star(t) + u(t)$

	Balanced	Bond	Equity	Money market
Institutional	88.1	78.3	51.3	93.2
Insurance	99.2	85.3	85.4	94.4
Retail	88.6	93.2	99.1	89.4
Third-party distributor	96.3	95.9	95.6	98.0

Table 54: Coefficient of determination $\mathfrak{R}_c^2$ in % — $\mathcal{R}(t) = \beta_0 + \beta_1 \mathcal{F}(t) + \beta_2 \mathcal{R}^\star(t) + u(t)$

	Balanced	Bond	Equity	Money market
Institutional	89.0	86.8	84.0	96.4
Insurance	99.3	87.2	88.2	97.1
Retail	96.2	97.3	99.7	95.7
Third-party distributor	98.4	98.2	97.6	98.9

Table 55: Coefficient of determination $\mathfrak{R}_c^2$ in % — Equation (35), one-week time horizon

	Balanced	Bond	Equity	Money market
Institutional	0.3	0.7	1.0	1.4
Insurance	0.2	0.5	1.4	2.3
Retail	0.8	2.3	0.6	0.3
Third-party distributor	0.8	0.8	1.2	3.8

Table 56: Coefficient of determination $\mathfrak{R}_c^2$ in % — Equation (35), two-week time horizon

	Balanced	Bond	Equity	Money market
Institutional	1.3	0.7	2.8	2.8
Insurance	0.1	0.3	1.5	5.1
Retail	2.3	2.0	0.8	0.9
Third-party distributor	1.1	2.1	1.5	3.7

Figure 53: Relationship between redemption rate and two-week stock returns (equity category)

Table of Contents